REPORT

Development of high-line differential pressure standards

Mark Hay
David Simpson

September 1999

NPL
National Physical Laboratory

Development of high-line differential pressure standards

Mark Hay
Metrology Limited

David Simpson
National Physical Laboratory

September 1999

ABSTRACT

There has been concern that potential discrepancies exist between different standards used for generating differential pressure at high line pressures. This report details a comparative study, both theoretical and experimental, of three devices: *gas-lubricated 'twin-post' pressure balances*, *oil-lubricated gas-operated 'twin-post' pressure balances* and *pressure 'dividers'*. It shows that agreement between the instruments can be reached when adequate consideration is given to constructing detailed mathematical models associated with instrument performance and the corresponding measurement uncertainty budgets. However, significant measurement discrepancies between the various methods can occur when over-simplistic models are used to describe their characteristics, or over-optimistic estimates of uncertainty are made. Furthermore, and for the same reason, discrepancies are just as likely between devices of similar design.

ISSN 1369-6785

National Physical Laboratory
Queens Road, Teddington, Middlesex, TW11 0LW

Approved on behalf of the Managing Director, NPL
by Dr G R Torr, Head, Centre for Mechanical and Acoustical Metrology

CONTENTS

LIST OF FIGURES

Page

LIST OF TABLES

Page

1 INTRODUCTION

The accurate measurement of differential pressure at high-line pressure is of considerable industrial importance, especially where the measurement and control of fluid flow are concerned. The metering of North Sea gas is an important example, where relatively small differential pressures (typically less than 100 kPa) are measured in the presence of line pressures up to 20 MPa.

Calibration of the large number of measuring instruments involved – typically differential pressure *transmitters* – is a competitive activity which is supported by many manufacturers and calibration laboratories who, for clear commercial reasons, seek the lowest possible measurement uncertainties. There has been a perception that at or above this level of uncertainty measurement discrepancies occur, possibly because the uncertainty budgets have been reduced a little beyond sound metrological justification, perhaps through not taking sufficient factors into account.

The measurement standards used to generate such pressures traceably – and hence calibrate differential pressure transmitters – are commonly of three designs: *gas-lubricated 'twin-post' pressure balances*, *oil-lubricated gas-operated 'twin-post' pressure balances* and *pressure 'dividers'*.

The main aim of the project was to critically evaluate the three devices by developing detailed mathematical models of their operation and the corresponding measurement uncertainty budgets. This report gives details of those uncertainty budgets but avoids suggesting what might be called the very best possible measurement uncertainties – which could be misleading. Instead, emphasis has been placed on suggesting uncertainties that are realistically sustainable in a good environment but subject to normal operating constraints, including time. The practical work was undertaken using just one device of each type; the project did not experiment with apparatus from all manufacturers, nor with systems equivalent to twin-post devices constructed from two separate pressure balances, but provision has been made in the uncertainty budgets where variations between artefacts might be expected to exist.

The project was assisted, particularly in its early stages, by:

- Antech Engineering Ltd
- DH-Budenberg Ltd
- Druck Ltd
- DTI Oil and Gas Office
- Flow Ltd
- Kelton Engineering Ltd
- Magnox Electric
- Metco Services Ltd
- PCD/Beamex
- Ruska Instrument Corporation
- SAE Gauges Ltd
- SIRA Test & Certification Ltd
- Scotia Instrumentation Ltd
- Shell UK Exploration and Production
- Theta Systems Ltd
- UKAS
- Yokogawa (UK) Ltd

– organisations with experience in differential pressure measurements[1], representing manufacturers, end users, UKAS accredited laboratories and consultants. They took part in meetings, held both in London and Aberdeen, and visits were made to six laboratories which were accredited for differential pressure calibration work.

[1] All organisations which took part in the meetings and visits were invited to comment on a draft version of this Report and the final text has been edited as a result. The contents of the Report, however, and are not necessarily representative of all views.

During the discussions, many concerns were expressed about potential discrepancies in high-line differential pressure work. A number of them related to the use of differential pressure transmitters, rather than the calibration standards, whilst others concerned poor environmental conditions and mistakes made by use of inappropriate pressure units. Whilst not strictly within the project's scope, they represent important issues and have been mentioned briefly in Section 15 *Additional sources of measurement discrepancy*, so that they may be taken into account where appropriate.

This report includes sections dealing with principles, ancillary apparatus, environment, calculations, comparisons and sources of discrepancy; some text has been duplicated across sections to assist with readability. Where possible, terminology has been designed to reflect definitions given in official sources, such as the ISO documents *International vocabulary of basic and general terms in metrology*[1], *Guide to the expression of uncertainty in measurement*[2] or the British Standard *Glossary of terms used in metrology*[3], and also the *Guide to the Measurement of Pressure and Vacuum*[4].

2 BASIC PRINCIPLES OF DIFFERENTIAL PRESSURE GENERATORS

2.1 GAS-LUBRICATED TWIN-POST PRESSURE BALANCES

Twin-post pressure balances comprise two nominally identical piston-cylinder units and mass sets, mounted on a common base unit with valves and volume adjusters for controlling pressure.

An *initial equilibrium* is established by *cross-floating*[2] the two pressure balances at a nominated line pressure. An *equalising valve* is closed and the differential pressure generated by applying additional mass to change the *load* on one of the pressure balances.

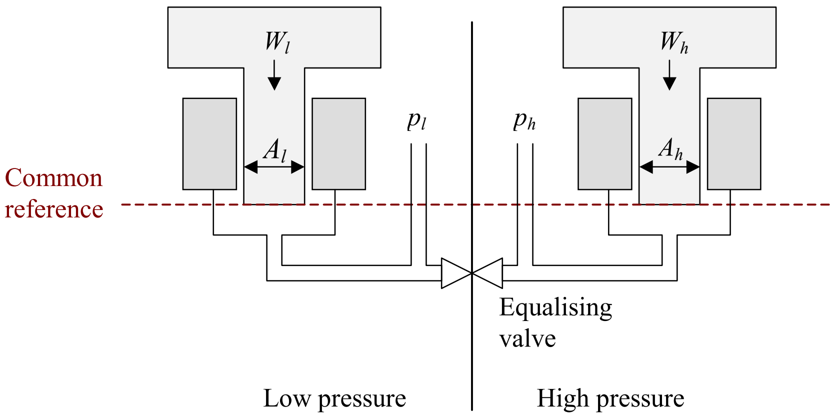

Figure 1 Schematic of gas-lubricated twin-post pressure balance

The terms *low* and *high* are used to identify the two sides of the balance, where *low-pressure* refers to the *line pressure* and *high-pressure* refers to the line pressure *plus* the differential pressure. From Figure 1 it can be seen that with the equalising valve closed and both pistons floating at their correct heights, p_l and p_h, the pressure generated by each pressure balance at the reference level, can be calculated by:

$$p_l = \frac{W_l}{A_l} \quad \text{and} \quad p_h = \frac{W_h}{A_h} \tag{1}$$

where W_l is the total downward force on the *low* piston

A_l is the effective area of the *low* piston-cylinder at the operating pressure and temperature

W_h is the total downward force on the *high* piston

A_h is the effective area of the *high* piston-cylinder at the operating pressure and temperature

[2] *Cross-floating* is the process of adjusting two piston-cylinders until they are in hydrostatic equilibrium.

The differential pressure generated by a gas-lubricated twin-post pressure balance may therefore be expressed as:

$$dp = \frac{W_h}{A_h} - \frac{W_l}{A_l} \qquad (2)$$

Traceability to the SI for the twin-post pressure balances was obtained through effective area and mass comparisons with NPL standards and knowledge of the acceleration due to gravity.

2.2 OIL-LUBRICATED GAS-OPERATED TWIN-POST PRESSURE BALANCES

Generally, oil-lubricated gas-operated twin-post pressure balances use the same principle as gas-lubricated twin-post pressure balances. In this design, however, the pistons are lubricated by a film of oil fed through a hole in each of the cylinders. The oil film is maintained by pressurising the oil reservoirs as shown in Figure 2.

Whilst the presence of the oil influences performance, the basic expression for the differential pressure generated is identical to that for the gas-lubricated twin-post pressure balance.

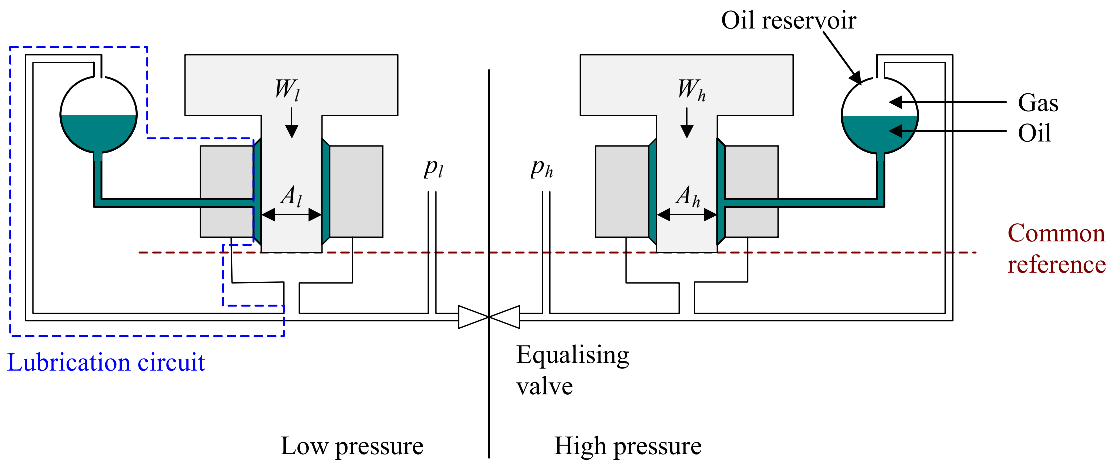

Figure 2 Schematic of an oil-lubricated gas-operated twin-post pressure balance

2.3 PRESSURE DIVIDERS

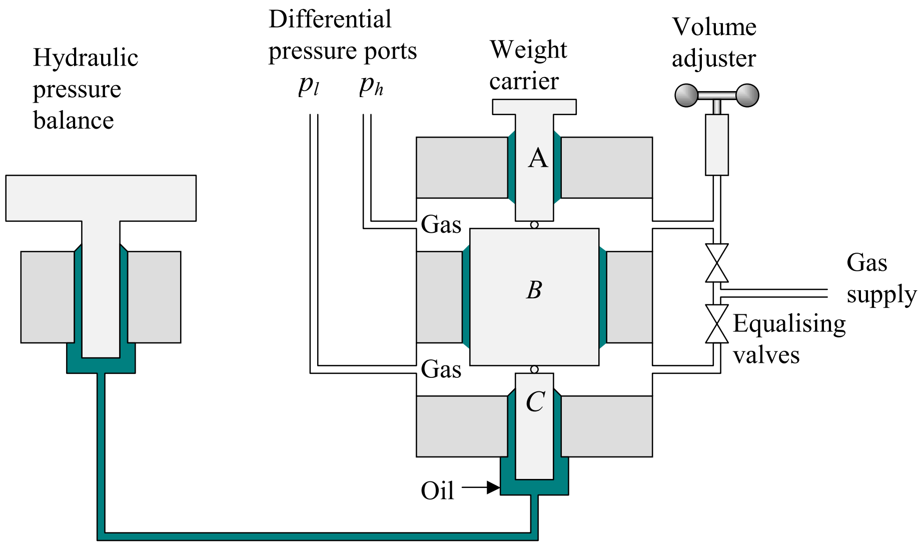

Figure 3 Schematic of a pressure divider

The heart of the *divider* is a rotating assembly comprising three coaxially linked piston-cylinders (identified in Figure 3 as *A*, *B* and *C*). The effective area of piston *B* is nominally 101 times that of pistons *A* and *C*.

A single hydraulic pressure balance is used in conjunction with the divider to generate a pressure which is *divided* by the area ratio of the coaxially linked piston-cylinders. This concept is best explained by describing the operating principle:

When using this system the divider's equalising valves are first opened and line pressure applied to both sides of the middle piston *B*, from a gas supply.

Mass is applied to the hydraulic pressure balance to produce sufficient pressure (approximately 1 MPa) to generate a force at the base of the divider's lower piston *C* which is equal to the downward force generated by the mass of the rotating assembly. This mass includes the three pistons together with their linking mechanisms and the weight carrier above piston *A*. The divider's lower piston-cylinder *C* is effectively cross-floated against the hydraulic piston cylinder. Once equilibrium is achieved, the divider's equalising valves are closed.

To generate a differential pressure, additional mass is added to the hydraulic pressure balance. This increases the pressure at the bottom of piston *C*, generating an upward force on the three-piston assembly. To maintain the divider's *float-position* the pressure at the *high* side of the divider is increased using the volume adjuster; this produces a net downward force on the piston *B* equal to the increased upward force on the base of piston *C*.

The pressure at the *low* port p_l, will remain broadly constant and defines the line pressure, whereas the pressure at the *high* port p_h, will be equal to the line pressure plus the increase in the upper chamber pressure applied to balance the increased upward force on the lower piston *C*. This increase in pressure is the differential pressure, *dp*.

Due to the area ratio of the piston-cylinders, the increase in pressure at the *high* side of the balance required to maintain the float-position is nominally one hundred times less than the increase in pressure at the base of piston *C*.

The upward force due to the increase in hydraulic pressure is equal to:

$$\Delta p_{oil} \; A_C \tag{3}$$

Where Δp_{oil} is the increase in hydraulic pressure

A_C is the area of piston *C*

The downward force due to the increase in high-pressure is equal to:

$$dp(A_B - A_A) \tag{4}$$

Where dp is the increase in gas pressure (differential pressure)

A_B is the area of piston *B*

A_A is the area of piston *A*

As the area of piston *B* is nominally 101 times that of pistons *A* and *C*, the ratio between the hydraulic pressure and the differential pressure (the dividing ratio R_D) is nominally 100 as:

$$R_D = \frac{101 - 1}{1} \tag{5}$$

Traceability to the SI for the pressure divider was through comparison with the twin-post pressure balance, whose traceability was through effective area and mass comparisons with NPL standards and knowledge of the value of acceleration due to gravity.

3 ANCILLARY APPARATUS AND MEASUREMENTS

3.1 GENERAL

Ancillary equipment was used in the evaluation of the three differential pressure generators, to observe the generated differential pressure, and to control and monitor parameters which could potentially affect the output of the generators.

3.2 DIFFERENTIAL PRESSURE TRANSMITTERS

Although the evaluation of differential pressure transmitters was not strictly within the scope of the project, it was necessary to examine their various characteristics to establish a robust method of observing the output of the differential pressure generators. Differential pressure transmitters from three manufacturers were purchased for the project, selected to be representative of those used in applications where the highest degree of accuracy is sought – for example the measurement of natural gas flow. The transmitters used were new and had not been exposed to the environmental conditions normally experienced by transmitters in service. This eliminated the potential for problems related to contamination with process fluids or deterioration in performance after use under harsh environmental conditions.

3.2.1 Electrical output

Like most modern differential pressure transmitters, those selected for this project had the ability to transmit the output digitally or as a 4 mA - 20 mA analogue signal. The differential pressure – an inherently analogue quantity – is sensed either by a capacitive or piezo-resistive device. This information, in digital form, is fed to a microprocessor together with additional data – typically temperature, line pressure and characterisation data – from which differential pressure values are computed. The values are then available directly, or after digital to analogue conversion, as a 4 mA - 20 mA output.

It was decided to use the transmitters in analogue mode as this eliminated problems associated with the incompatible digital protocols used by manufacturers and enabled the fast sample rate necessary to observe the dynamic characteristics of the generators.

3.2.2 Quantization

As mentioned in Section 3.2.1, the 4 mA - 20 mA output of a transmitter is produced via a digital to analogue converter and is therefore not strictly analogue; it has discrete steps which can be significant. Resolution of transmitter output was found to be proportional to the *turndown ratio* and in one case it was in excess of 0.025% of the transmitter's *span* (>25 Pa with the span set at 0 kPa - 100 kPa).

To enable the high resolution required for evaluating the generators dynamic characteristics, transmitters were successively re-ranged to a minimal span, with the low- and high-range value set just either side of the generated differential pressure.

3.2.3 Electrical connections

Power was supplied to the transmitters using a 24 V dc supply with a nominal loop resistance of 350 Ω, comprising a 100 Ω standard resistor in series with an additional 250 Ω resistor. The 4 mA - 20 mA output of the transmitters was calculated by dividing the voltage measured across the standard resistor by the value of the standard resistor.

3.2.4 Physical connections

It is frequently reported, with some designs of differential pressure transmitters, that the action of attaching the *process flanges* to a manifold causes stress on the instrument which alters the output (see 'clamping effects' Section 15.1.5). To reduce the possibility of such clamping errors, *three-valve manifolds* were attached to the transmitters and remained so connected for the duration of the project.

A mounting assembly was constructed to position three transmitters and manifolds at a common reference height (see Figure 9, Section 8.2.4).

3.2.5 Data Capture

At the start of the project it was established that observing the output of differential pressure transmitters using a digital display on a voltmeter did not yield sufficient information to precisely evaluate generated differential pressure. A computer system was therefore designed and constructed to observe simultaneously the output from two differential pressure transmitters graphically, in real-time, and with a database used to save measurements for further review and analysis. Transmitters of more than one type were used to ensure that the generated differential pressure being observed was not influenced by any characteristic associated with one particular type of transmitter.

The computer's display was used to observe the dynamic characteristics of the differential pressure generators. From this the time period required to capture a representative set of data was determined and subtle changes in generated differential pressure, which would otherwise have been lost in an oscillating signal, were recorded.

3.2.6 Influence of differential pressure transmitters

To establish how the differential pressure transmitters influenced the dynamic characteristics observed, tests were conducted using transmitters from different manufacturers. A comparison was made between results obtained by simultaneously recording the output of two transmitters connected to the pressure circuit in parallel and those recorded with the transmitters operating individually – with the other transmitter isolated from the pressure system.

Figure 4, Figure 5 and Figure 6 show the outputs from these tests. The blue traces represent the output from one of the transmitters and the red trace the output from the other transmitter. There is no significant change in either the magnitude or general pattern of the wave-form with either or both transmitters connected to the pressure system.

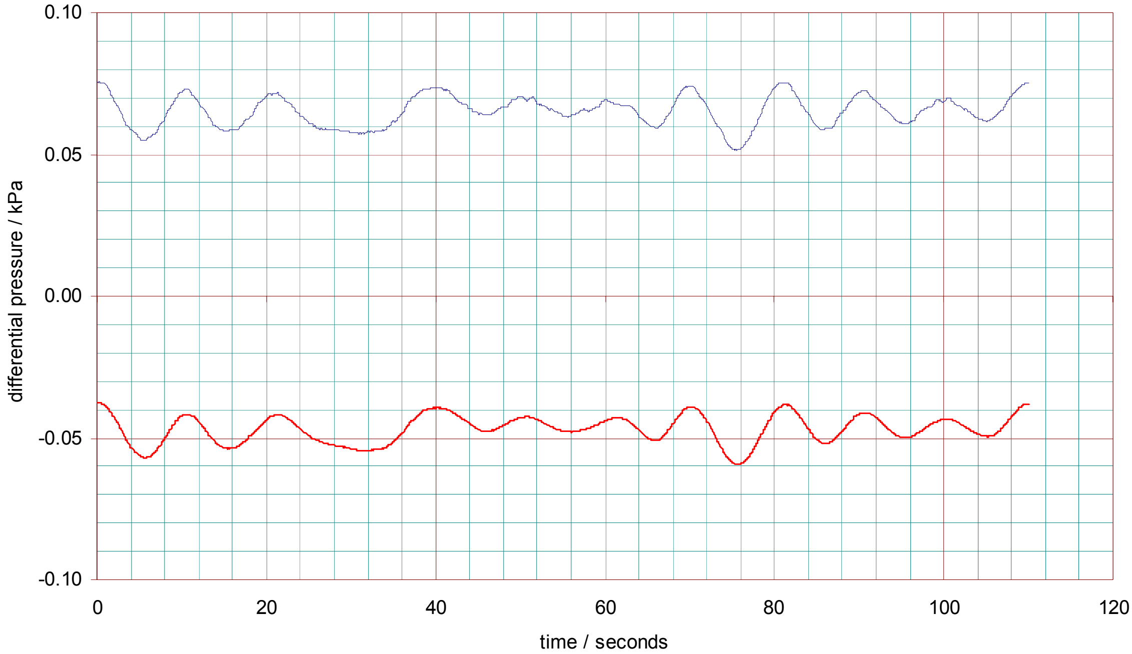

Figure 4 Transmitters from different manufacturers connected in parallel

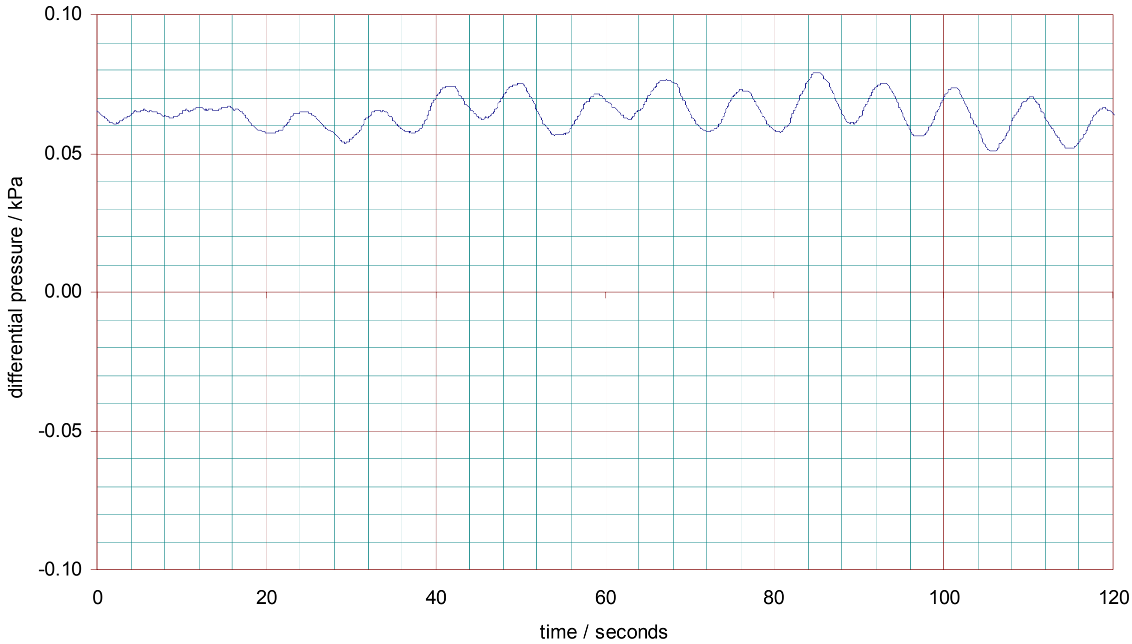

Figure 5 As Figure 4 but with one transmitter isolated

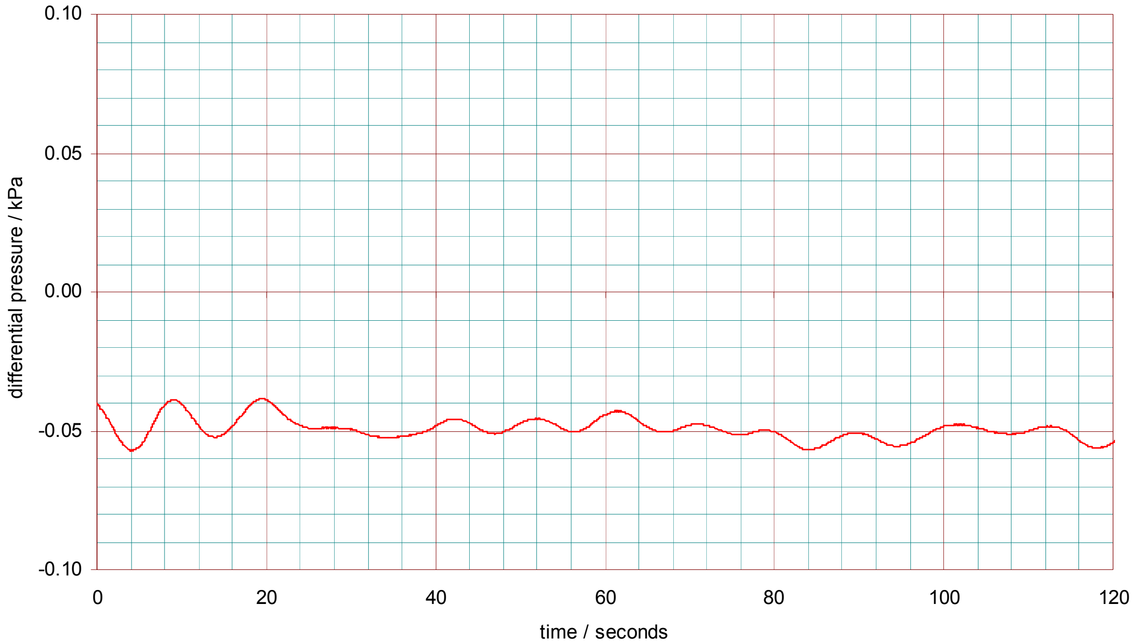

Figure 6 As Figure 5 but with the other transmitter isolated

The traces shown in Figure 4 gave confidence in the suitability of differential pressure transmitters to measure the dynamic characteristics of the generators and, in this case, that there was no significant difference between the responses of either transmitter. The output from a transmitter from the third manufacturer, however, was noticeably ‘noisier’ and was therefore not used to make subsequent measurements.

3.3 PISTON FLOAT-POSITION

Capacitive sensing devices were utilised to measure the *float-position* of the pistons. These devices, used in conjunction with software, gave a real-time graphical representation of piston fall-rate and were used as an aid to achieve equilibrium (see Simpson[5]).

3.4 TEMPERATURE

In order to simulate operation under various thermal conditions a variable temperature enclosure was used to subject apparatus to a range of temperatures.

A 24-probe thermistor temperature-logging device was used to measure the temperatures of component parts of the generators. Software was written to record temperatures in a database and display the recorded temperature graphically in real-time.

3.5 ANGULAR VELOCITY

A non-contact laser tachometer was used to measure the angular velocity of the pistons.

4 LABORATORY ENVIRONMENT

The performance and characteristics of a calibration system may vary considerably from one installation to another depending upon the laboratory environment. The experimental work for this project was conducted in what might be described as a typical environment for a pressure calibration laboratory, using equipment and materials similar to those used in accredited pressure calibration laboratories.

The laboratory was temperature-controlled to nominally 20 °C 24 hours per day; humidity was measured but not controlled. Best endeavours were made to keep the laboratory draft free and free from direct sunlight and radiating heat sources.

All equipment used was permanently located in the laboratory and the differential pressure generators positioned level on firm laboratory benches. Where practicable a three-sided enclosure was placed over the apparatus to shield against potential drafts. No vibration from plant or machinery was apparent.

The calibration gas used was dry oxygen-free nitrogen supplied to the generators via a digital pressure controller to ensure slow and even pressure changes to reduce adiabatic heating effects.

5 DIFFERENTIAL PRESSURE CALCULATION – TWIN-POST

The equations derived under this heading relate to both gas- and oil-lubricated twin-post pressure balances.

Theoretically it is possible to calculate differential pressure generated using a twin-post pressure balance by *independently* calculating the pressure of each of the pressure balances and simply using the equation:

$$dp = p_h - p_l \tag{6}$$

where p_h is the pressure generated by the *high* piston-cylinder

p_l is the pressure generated by the *low* piston-cylinder

The pressure generated by a single pressure balance can at best be estimated with an uncertainty of a few parts in 10^5 (say 30 parts per million[3]). Calculating the differential pressure by *independently* determining the pressure of each pressure balance would therefore result in an uncertainty of around 45 ppm of the line pressure. As the values of differential pressure can be many orders of magnitude less than the line pressure, the corresponding relative uncertainty can easily become unacceptably high.

Cross-floating the pressure balances of the twin-post reduces the problem; this initial state of equilibrium is used as a reference from which differential pressure is subsequently generated.

5.1 THE INITIAL CROSS-FLOAT

To generate the nominated line pressure, mass is applied to both *high* and *low* pistons. An initial cross-floating equilibrium between p_h and p_l is achieved by adjusting the mass applied to the *low* piston until there is no pressure differential.

At this point it can he stated, within a calculated uncertainty, that:

$$p_{ho} = p_{lo} \tag{7}$$

where p_{ho} is the pressure generated by the *high* pressure balance during the initial cross-float

p_{lo} is the pressure generated by the *low* pressure balance during the initial cross-float

[3] 1 part per million (abbreviate to 1 ppm) $\equiv 1 \times 10^{-6}$

5.2 EVALUATION OF FORCE

The downward force on a piston can be calculated using the equation:

$$W = m_t \left(1 - \frac{\rho_a}{\rho_m}\right) g \tag{8}$$

where m_t is the true mass[4] of the load

ρ_a is the calculated density of the ambient air

ρ_m is the density of the components' material

g is the local value of acceleration due to gravity

The floating components of a pressure balance are generally ascribed, through calibration, a *conventional* mass or *weight in air value* with an assumed density of 8000 kg m^{-3}. Using the conventional value for the mass from the calibration certificate, force can be estimated (see Lewis and Peggs[6]) with the equation:

$$W = m\ \phi \left(1 - \frac{\rho_a}{8000}\right) g \tag{9}$$

where m is the *conventional* mass of the floating elements

ϕ is a correction factor to compensate for the differences between the actual density of the material ρ_m and the assumed density of 8000 kg m^{-3}

$$\phi = 1 - (\rho_a - 1.2)\left(\frac{1}{\rho_m} - \frac{1}{8000}\right) \tag{10}$$

5.2.1 The density of air

The density of air may be calculated from measurements of temperature, barometric pressure and relative humidity (see Lewis and Peggs[6]). The density of air is calculated for the period during which the initial cross-float was determined, and is assumed to be constant during the subsequent measurements. The value of uncertainty in air density can be estimated to take account of changes during calibration and appropriate limits set.

5.2.2 The density of the mass material

A number of different materials and construction techniques may be used in the manufacture of the floating components of a pressure balance. The density of each component is often a best estimate based on knowledge of materials and dimensions.

It is assumed that the mass sets used to generate the line pressure are of the same material (ie have the same density) for both *high* and *low* piston-cylinders.

---

[4] The *true* mass is the value which would be determined by weighing in vacuo

5.2.3 Acceleration due to gravity

This is the value of acceleration due to gravity determined for the location of the pressure balance.

5.3 EVALUATION OF PISTON-CYLINDER AREA

Piston-cylinder area at a given pressure and temperature may be expressed as:

$$A_{p,t} = A_o\left(1+\alpha\ p\right)\ \left(1+\lambda\ (t-20)\right) \tag{11}$$

where A_o is the *effective area* of the piston-cylinder at zero pressure

α is a pressure dependent term

p is the given pressure

λ is the sum of the temperature coefficients of the piston and cylinder; $\alpha_p + \alpha_c$.

t is the Celsius temperature of the piston-cylinder

5.4 EVALUATION OF PRESSURE

Pressure generated by a pressure balance may therefore be calculated using the equation:

$$P = \frac{m\ \phi\ \left(1-\dfrac{\rho_a}{8000}\right)\ g}{A_o\ \left(1+\alpha\ P\right)\ \left(1+\lambda\left(t-20\right)\right)} \tag{12}$$

5.5 CALCULATION OF PRESSURE – ‘HIGH’ SIDE

To generate differential pressure, additional mass *dpm* is added to the *high* piston. The increase in pressure thus generated will also cause a small change in the area of the piston-cylinder due to its pressure-dependent nature.

Changes in piston-cylinder temperature between establishing the initial cross-float and making the subsequent differential pressure measurement affects the area of the piston-cylinder and should be taken into consideration when calculating the differential pressure.

The pressure p_h generated by the *high* piston during a differential pressure measurement may be calculated from:

$$p_h = \frac{\left[dpm\ \phi\ \left(1 - \frac{\rho_a}{8000}\right) + m_{ho}\ \phi\ \left(1 - \frac{\rho_a}{8000}\right)\right]\ g}{A_{oh}\ \left(1 + \alpha_h\ p_h\right)\ \left(1 + \lambda\left(t_h - 20\right)\right)} \tag{13}$$

where *dpm* represents the additional mass applied to generate the differential pressure

ϕ is a correction factor to compensate for the differences between the density ρ_m of the material and the assumed density of 8000 kg m^{-3}

ρ_a is the calculated density of the ambient air

g is the value of acceleration due to gravity

m_{ho} is the mass applied to the *high* piston to generate the line pressure

A_{oh} is the effective area of the *high* piston-cylinder

α_h is a pressure-dependent term for the *high* piston-cylinder

λ is the sum of the temperature coefficients of the piston and cylinder

t_h is the Celsius temperature of the *high* piston-cylinder during the generation of differential pressure

The equation may be rearranged to give:

$$p_h = \frac{dpm\ \phi\ \left(1 - \frac{\rho_a}{8000}\right)\ g}{A_{oh}\ \left(1 + \alpha_h\ \left(p_{ho} + dp\right)\right)\ \left(1 + \lambda\ \left(t_h - 20\right)\right)} + \frac{m_{ho}\ \phi\ \left(1 - \frac{\rho_a}{8000}\right)\ g}{A_{oh}\ \left(1 + \alpha_h\ \left(p_{ho} + dp\right)\right)\ \left(1 + \lambda\ \left(t_h - 20\right)\right)} \tag{14}$$

As the pressure p_{ho} during the initial cross-float is calculated from:

$$p_{ho} = \frac{m_{ho}\ \phi\ \left(1 - \frac{\rho_a}{8000}\right)\ g}{A_{oh}\ \left(1 + \alpha_h\ p_{ho}\right)\ \left(1 + \lambda\left(t_{ho} - 20\right)\right)} \tag{15}$$

equation (14) can be rearranged to give:

$$p_h = \frac{dpm\ \phi\ \left(1 - \frac{\rho_a}{8000}\right)\ g}{A_{oh}\ \left(1 + \alpha_h\ \left(p_{ho} + dp\right)\right)\ \left(1 + \lambda\ \left(t_h - 20\right)\right)} + p_{ho}\ \frac{\left(1 + \alpha_h p_{ho}\right)\ \left(1 + \lambda\ \left(t_{ho} - 20\right)\right)}{\left(1 + \alpha_h\ \left(p_{ho} + dp\right)\right)\ \left(1 + \lambda\ \left(t_h - 20\right)\right)} \tag{16}$$

5.6 CALCULATION OF PRESSURE – 'LOW' SIDE

As with the high-pressure side of the equation, a change in the piston-cylinder temperature between the initial cross-float and the measurement will affect the generated differential pressure.

The pressure p_{lo} generated by the *low* piston during the initial cross-float may be calculated from:

$$p_{lo} = \frac{m_{lo}\ \phi \cdot \left(1 - \frac{\rho_a}{8000}\right)\ g}{A_{ol}\left(1 + \alpha_l\ p_{lo}\right)\ \left(1 + \lambda\left(t_{lo} - 20\right)\right)} \tag{17}$$

where m_{lo} is the mass applied to the *low* piston to generate the line pressure

ϕ is a correction factor to compensate for the differences between the actual density ρ_m of the material and the assumed density of 8000 kg m^{-3}

ρ_a is the calculated density of ambient air

g is the value of acceleration due to gravity

A_{ol} is the effective area of the *low* piston-cylinder

α_l is a pressure-dependent term for the *low* piston-cylinder

λ is the sum of the temperature coefficients of the piston and cylinder

t_{lo} is the Celsius temperature of the *low* piston-cylinder during the initial cross-float

The pressure generated by the *low* piston during the measurement can therefore be calculated from:

$$p_l = \frac{m_{lo}\ \phi\ \left(1 - \frac{\rho_a}{8000}\right)\ g}{A_{ol}\ \left(1 + \alpha_l\ p_{lo}\right)\ \left(1 + \lambda\left(t_l - 20\right)\right)} \tag{18}$$

where t_l is the temperature of the *low* piston-cylinder during the generation of differential pressure

Equations (17) and (18) can be combined to express the pressure on the *low* piston in terms of the equilibrium pressure:

$$p_l = p_{lo}\ \frac{\left(1 + \lambda\ \left(t_{lo} - 20\right)\right)}{\left(1 + \lambda\ \left(t_l - 20\right)\right)} \tag{19}$$

5.7 THE DIFFERENTIAL PRESSURE EQUATION

The differential pressure equation:

$$dp = p_h - p_l \tag{20}$$

may be expanded to:

$$\begin{aligned} dp = {} & \frac{dpm\ \phi\ \left(1-\dfrac{\rho_a}{8000}\right)\ g}{A_{oh}\left(1+\alpha_h\ (p_{ho}+dp)\right)\ \left(1+\lambda\ (t_h-20)\right)} \\ & + p_{ho}\frac{(1+\alpha_h p_{ho})\ \left(1+\lambda\ (t_{ho}-20)\right)}{\left(1+\alpha_h\ (p_{ho}+dp)\right)\ \left(1+\lambda\ (t_h-20)\right)} - p_{lo}\frac{\left(1+\lambda\ (t_{lo}-20)\right)}{\left(1+\lambda\ (t_l-20)\right)} \end{aligned} \tag{21}$$

As $p_{lo} = p_{ho}$, p_{lo} can be substituted by p_{ho}:

$$\begin{aligned} dp = {} & \frac{dpm\ \phi\ \left(1-\dfrac{\rho_a}{8000}\right)\ g}{A_{oh}\left(1+\alpha_h\ (p_{ho}+dp)\right)\ \left(1+\lambda\ (t_h-20)\right)} \\ & + p_{ho}\left[\frac{(1+\alpha_h p_{ho})\ \left(1+\lambda\ (t_{ho}-20)\right)}{\left(1+\alpha_h (p_{ho}+dp)\right)\ \left(1+\lambda\ (t_h-20)\right)} - \frac{\left(1+\lambda\ (t_{lo}-20)\right)}{\left(1+\lambda\ (t_l-20)\right)}\right] \end{aligned} \tag{22}$$

Expanding ϕ gives:

$$\begin{aligned} dp = {} & \frac{dpm\ \left[1-(\rho_a-1.2)\ \left(\dfrac{1}{\rho_m}-\dfrac{1}{8000}\right)\right]\ \left(1-\dfrac{\rho_a}{8000}\right)\ g}{A_{oh}\left(1+\alpha_h\ (p_{ho}+dp)\right)\ \left(1+\lambda\ (t_h-20)\right)} \\ & + p_{ho}\left[\frac{(1+\alpha_h p_{ho})\ \left(1+\lambda\ (t_{ho}-20)\right)}{\left(1+\alpha_h (p_{ho}+dp)\right)\ \left(1+\lambda\ (t_h-20)\right)} - \frac{\left(1+\lambda\ (t_{lo}-20)\right)}{\left(1+\lambda\ (t_l-20)\right)}\right] \end{aligned} \tag{23}$$

As t_l and t_h may expressed in terms of the temperature measured during the initial cross-float plus a change in temperature:

$$t_l = t_{lo} + \Delta t_l \qquad \text{and} \qquad t_h = t_{ho} + \Delta t_h \tag{24}$$

The differential pressure equation may be expressed as:

$$dp = \frac{dpm\left[1-(\rho_a-1.2)\left(\frac{1}{\rho_m}-\frac{1}{8000}\right)\right]\left(1-\frac{\rho_a}{8000}\right)g}{A_{oh}\left(1+\alpha_h\ (p_{ho}+dp)\right)\left(1+\lambda\ (t_h-20)\right)} + p_{ho}\left[\frac{(1+\alpha_h p_{ho})\ (1+\lambda\ (t_{ho}-20))}{(1+\alpha_h(p_{ho}+dp))\ (1+\lambda\ (t_{ho}+\Delta t_h-20))}-\frac{(1+\lambda\ (t_{lo}-20))}{(1+\lambda\ (t_{lo}+\Delta t_l-20))}\right] \tag{25}$$

It can be seen that it is not necessary to independently evaluate the pressure at the *low* pressure balance in terms of:

$$p_l = \frac{W_l}{A_l} \tag{26}$$

The pressure generated by the *low* piston-cylinder has effectively been redefined in terms of the pressure generated by the *high* piston-cylinder during the initial cross-float and it is therefore not necessary to calibrate the *low* piston-cylinder.

6 DIFFERENTIAL PRESSURE CALCULATION - DIVIDER

6.1 DIVIDING RATIO

The dividing ratio R_D is the ratio of the additional hydraulic pressure over the generated differential pressure:

$$R_D = \frac{\Delta p_{oil}}{dp} \tag{27}$$

Differential pressure is therefore calculated by dividing the increase in hydraulic pressure by the dividing ratio:

$$dp = \frac{\Delta p_{oil}}{R_D} \tag{28}$$

6.2 CHANGE IN HYDRAULIC PRESSURE

A mass is applied to the hydraulic pressure balance to produce sufficient pressure (approximately 1 MPa) to generate a force at the base of the divider's lower piston C which is equal to the downward force generated by the mass of the rotating assembly (see Figure 3, Section 2.3).

Pressure p_{oil} generated by the hydraulic pressure balance is calculated using the equation:

$$p_{oil} = \frac{m\ \phi \left(1 - \frac{\rho_a}{8000}\right)\ g + \sigma\ c}{A_o\ \left(1 + \alpha\ p_{oil}\right)\ \left(1 + \lambda\ \left(t - 20\right)\right)} + \rho_f\ g\ h \tag{29}$$

where m is the total mass applied to initially balance the divider (including the mass of the piston)

ϕ is the correction factor to compensate for the differences between the density of the material and the assumed density of 8000 kg m^{-3} (see Equation (10))

ρ_a is the measured density of the ambient air

g is the acceleration due to gravity

σ is the surface tension coefficient of the oil

c is the circumference of the floating element of the piston-cylinder assembly at the point where it emerges from the pressure fluid

A_o is the effective area of the piston-cylinder at zero pressure

α is the pressure dependent term of the piston-cylinder

λ is the sum of the temperature coefficients of the piston and cylinder; $\alpha_p + \alpha_c$.

t is the Celsius temperature of the piston-cylinder

ρ_f is the density of the oil

h is the height of the pressure balance above a reference level

Therefore the change in hydraulic pressure Δp_{oil} may be calculated from:

$$\Delta p_{oil} = \frac{(dpm + m)\ \phi \left(1 - \frac{\rho_a}{8000}\right) g + \sigma\ c}{A_o \left(1 + \alpha\ (p_{oil} + \Delta p_{oil})\right) \left(1 + \lambda\ (t - 20)\right)} - \frac{m\ \phi \left(1 - \frac{\rho_a}{8000}\right) g + \sigma\ c}{A_o \left(1 + \alpha\ p_{oil}\right) \left(1 + \lambda\ (t_o - 20)\right)} \tag{30}$$

where dpm is the additional mass applied to generate the differential pressure

p_{oil} is the pressure generated during the initial cross-float

t_o is the piston-cylinder temperature measured during the initial cross-float

t is the piston-cylinder temperature measured during the generation of differential pressure

Equation (30) can be rearranged to give:

$$\Delta p_{oil} = \frac{dpm\ \phi \left(1 - \frac{\rho_a}{8000}\right) g}{A_o \left(1 + \alpha\ (p_{oil} + \Delta p_{oil})\right) \left(1 + \lambda\ (t - 20)\right)} + \frac{m\ \phi \left(1 - \frac{\rho_a}{8000}\right) g + \sigma\ c}{A_o \left(1 + \alpha\ (p_{oil} + \Delta p_{oil})\right) \left(1 + \lambda\ (t - 20)\right)} - \frac{m\ \phi \left(1 - \frac{\rho_a}{8000}\right) g + \sigma\ c}{A_o \left(1 + \alpha\ p_{oil}\right) \left(1 + \lambda\ (t_o - 20)\right)} \tag{31}$$

and simplified to:

$$\Delta p_{oil} = \frac{dpm\ \phi \left(1 - \frac{\rho_a}{8000}\right) g}{A_o \left(1 + \alpha\ (p_{oil} + \Delta p_{oil})\right) \left(1 + \lambda\ (t - 20)\right)} + P_{oil} \left(\frac{\left(1 + \alpha\ p_{oil}\right) \left(1 + \lambda\ (t_o - 20)\right)}{\left(1 + \alpha\ (p_{oil} + \Delta p_{oil})\right) \left(1 + \lambda\ (t - 20)\right)} - 1 \right) \tag{32}$$

Expanding ϕ, gives the formula to calculate the increase in hydraulic pressure:

$$\Delta p_{oil} = \frac{dpm \left[1 - (\rho_a - 1.2) \left(\frac{1}{\rho_m} - \frac{1}{8000}\right)\right] \left(1 - \frac{\rho_a}{8000}\right) g}{A_o \left(1 + \alpha\ (p_{oil} + \Delta p_{oil})\right) \left(1 + \lambda\ (t - 20)\right)} + p_{oil} \left(\frac{\left(1 + \alpha\ p_{oil}\right) \left(1 + \lambda\ (t_o - 20)\right)}{\left(1 + \alpha\ (p_{oil} + \Delta p_{oil})\right) \left(1 + \lambda\ (t - 20)\right)} - 1 \right) \tag{33}$$

Differential pressure generated using the divider may therefore be calculated from:

$$dp = \frac{\frac{dpm \left[1 - (\rho_a - 1.2) \left(\frac{1}{\rho_m} - \frac{1}{8000}\right)\right] \left(1 - \frac{\rho_a}{8000}\right) g}{A_o \left(1 + \alpha\ (p_{oil} + \Delta p_{oil})\right) \left(1 + \lambda\ (t - 20)\right)} + p_{oil} \left(\frac{\left(1 + \alpha\ p_{oil}\right) \left(1 + \lambda\ (t_o - 20)\right)}{\left(1 + \alpha\ (p_{oil} + \Delta p_{oil})\right) \left(1 + \lambda\ (t - 20)\right)} - 1 \right)}{R_D} \tag{34}$$

7 HEIGHT CORRECTION

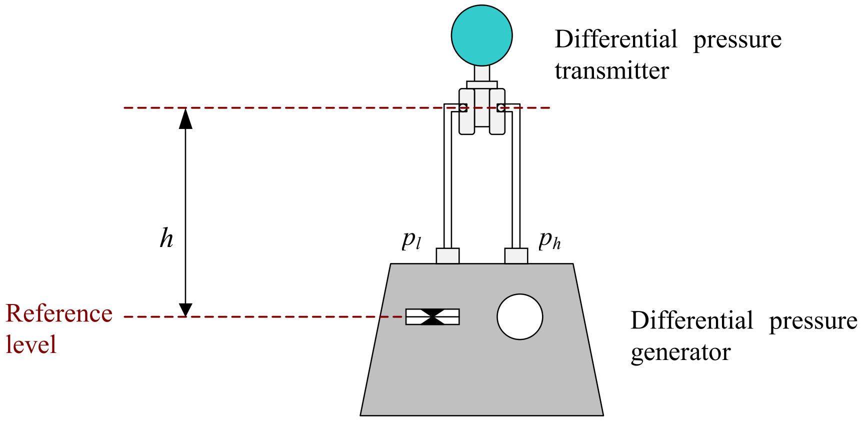

Figure 7 Schematic illustrating height correction

To illustrate changes in differential pressure which will result from differences in height, Figure 7 shows a differential pressure transmitter whose reference level is at a height h above the reference level of the generator.

For each side of the pressure system, the pressure difference between the generator and the transmitter due to the height, may be expressed as:

$$p = \rho \, g \, h \tag{35}$$

where ρ is the density of the pressure medium
g is the acceleration due to gravity
h is the height difference

Assuming that lines through the generator's and the transmitter's ports are both horizontal, h will be equal at each side of the pressure system. The value of g will be the same at both sides and during the initial cross-float both sides of the system are at the same pressure; if the temperature is the same at each side, it is assumed that the density of the fluid is also equal. Changing the pressure at either side of the pressure system will cause a change in density which will result in a pressure differential.

The differential pressure due to the change in density of the fluid can be calculated from:

$$dp = h\ g\ \left[(\rho_{\mathrm{fh}} - \rho_{\mathrm{fho}}) - (\rho_{\mathrm{fl}} - \rho_{\mathrm{flo}})\right] \tag{36}$$

where h is the height difference between the generator and the instrument being calibrated[5]

g is the acceleration due to gravity

ρ_{fh} is the density of the pressure fluid at the *high* port during the generation of differential pressure

ρ_{fho} is the density of the pressure fluid at the *high* port during the initial cross-float

ρ_{fl} is the density of the pressure fluid at the *low* port during the generation of differential pressure

ρ_{flo} is the density of the pressure fluid at the *low* port during the initial cross-float

Nitrogen is generally used as the pressure transmitting fluid and the relationship between pressure, temperature and density is derived from the ideal gas law:

$$P\,V = n\ R\ T \tag{37}$$

where P is the reference absolute pressure of the fluid

V is the volume of the fluid

n is the number of moles of the fluid

R is the universal gas constant

T is the thermodynamic temperature of the fluid

and it can be deduced that

$$\frac{P_1}{T_1\ \rho_1} = \frac{P_2}{T_2\ \rho_2} \tag{38}$$

where P_1 is the reference absolute pressure of the fluid (101.325 kPa)

T_1 is the reference thermodynamic temperature of the fluid (273.15 K)

ρ_1 is the density of the fluid at P_1 and T_1 (1.25046 kg m^{-3})

P_2 is the absolute pressure of the fluid

T_2 is the thermodynamic temperature of the fluid

ρ_2 is the density of the fluid at P_2 and T_2

---

[5]The sign of h is positive if the generator is higher than the instrument being calibrated.

The density of the fluid can therefore be calculated from the equation:

$$\rho_2 = \frac{T_1\ \rho_1\ P_2}{T_2\ P_1} \tag{39}$$

The differential pressure due to the difference in fluid head can therefore be expressed as:

$$dp\ = h\ g\ \frac{T_1\ \rho_1}{P_1}\left[\left(\frac{P_h}{T_h} - \frac{P_{ho}}{T_{ho}}\right) - \left(\frac{P_l}{T_l} - \frac{P_{lo}}{T_{lo}}\right)\right] \tag{40}$$

where P_h is the absolute pressure at the *high* side of the pressure system during the generation of differential pressure

T_h is the thermodynamic temperature at the *high* side of the system during the generation of differential pressure

P_{ho} is the absolute pressure at the *high* side of the system during the initial cross-float

T_{ho} is the thermodynamic temperature at the *high* side of the system during the initial cross-float

P_l is the absolute pressure at the *low* side of the system during the generation of differential pressure

T_1 is the thermodynamic temperature at the *low* side of the system during the generation of differential pressure

P_{lo} is the absolute pressure at the *low* side of the system during the initial cross-float

T_{lo} is the thermodynamic temperature at the *low* side of the system during the initial cross-float

Equation (40) may give the impression that it is possible to accurately correct for differences in height between the generator and the instruments being calibrated. However, the equation cannot take exact account of important factors such as temperature gradients that may be present in the system and oil vapour from piston-lubrication systems that may be suspended in the pressure fluid.

Good practice dictates that, where possible, the instrument being calibrated is mounted close to the generator's reference height, thus minimising the errors in calculating height correction. Although best endeavours may be made to mount the transmitter at the same datum as the generator, it may not always be possible to establish where the correct datum level of the differential pressure transmitter is and this varies between models of transmitter.

The magnitude of the additional differential pressure due to mounting an instrument at a height other than at the datum level is approximately 0.1 ppm of differential pressure per millimetre.

8 EVALUATION OF A GAS-LUBRICATED TWIN-POST PRESSURE BALANCE

8.1 DESIGN

The gas-operated pressure balance, to a certain extent, the least complex of the designs evaluated during this project, essentially comprises two nominally identical gas-lubricated pressure balances.

The instrument evaluated used *re-entrant*[6] tungsten carbide piston-cylinders with effective areas of approximately 8.4 mm^2. The pistons were rotated manually – there was no motor-drive available.

The mass set comprised solid stainless steel ring-weights for the larger values and solid stainless steel platters for the lower denominations. The weights were stacked on an overhanging weight carrier constructed of stainless steel and aluminium. With a mass set made up of dissimilar metals, knowledge of the composition was required in order to determine the density of the load for the calculation of force. The weight carrier pivots on the rounded top of the piston, self-adjusting the centre of gravity to the vertical axis.

The instrument was supplied with mercury in glass thermometers mounted near the base of the piston mounting posts, a few centimetres away from the pistons; they were replaced with thermistor thermometers.

Valves and *volume adjusters* to control the pressure, and a regulator, were housed in the base of the instrument.

8.2 DYNAMIC CHARACTERISTICS

8.2.1 General

Friction between the pistons and cylinders is minimal as the piston-cylinders are lubricated by gas. This low friction enables the pistons to rotate at a relatively constant angular velocity for long periods of time. The low friction also allows relatively free movement of the pistons in the vertical plane with low damping. Although such free movement allows a high degree of sensitivity – very small changes in applied mass produce a detectable change in pressure – the lack of damping increases the time taken to stabilise.

[6] A *re-entrant* piston-cylinder is essentially one which is designed to compensate for the tendency of its cylinder to taper outwards, at its base, as it is pressurised.

8.2.2 Angular velocity

A series of measurements were made at the same nominal differential pressure to investigate the relationship between the generated differential pressure (meaned where it was oscillating) and angular velocity.

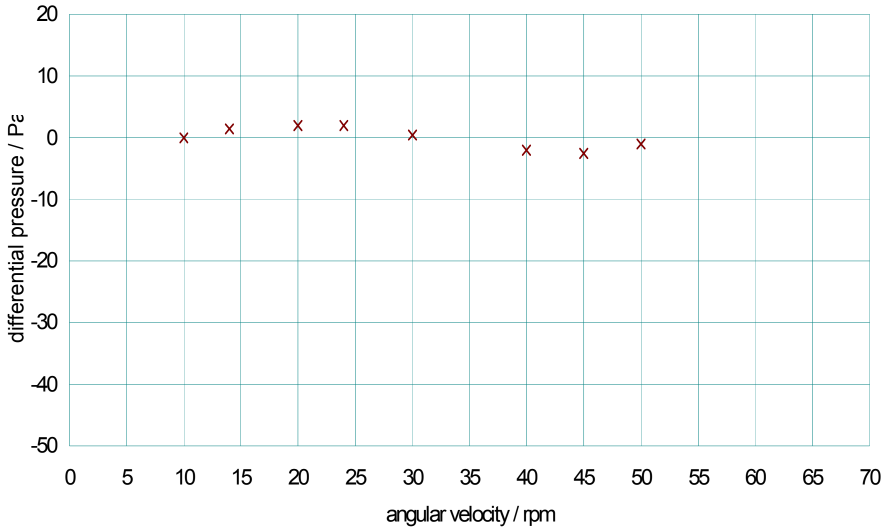

Figure 8 Relationship between angular velocity and generated differential pressure

Figure 8 shows results recorded at a line pressure of 10 MPa. It was found that variations in angular velocity did not cause a significant change in the value of generated differential pressure. It was found, however, that rotating the pistons at a high angular velocity caused instability and therefore increased the time required for piston bounce to subside.

8.2.3 'Piston-bounce'

A dominant characteristic of this type of system is its tendency to exhibit *piston-bounce,* where a disturbance causes the pistons to start oscillating vertically. Disturbance can be caused by the action of; opening or closing a valve, operating a volume-adjuster, adding mass to a piston, vibration or simply by a draft on the weight stack. This results in oscillations in generated differential pressure at the same frequency as the bounce of the pistons (typically between 0.07 Hz and 0.10 Hz). The time period taken for the oscillations to subside is typically between three and five minutes, after such a disturbance.

To illustrate this effect, Figure 11, Figure 12 and Figure 13 show the results of gently adding a 0.5 g weight (equivalent to an increase in differential pressure of approximately 0.5 kPa) to the load on the *high* piston at the mid-range line pressure of 10 MPa.

8.2.4 Pipework configuration

A schematic of the pipework used during this project is shown in Figure 9:

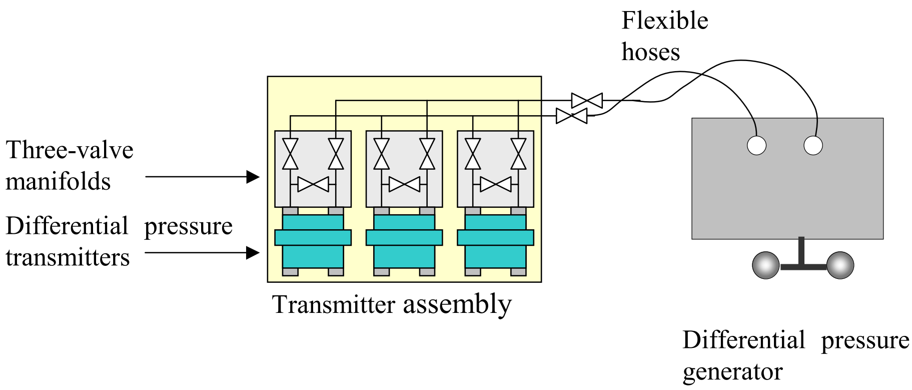

Figure 9 Schematic of pressure circuit – plan view

The *normal* pipework configuration included approximately 1 metre of '¼ inch' pipe (each side of the pressure system) of internal diameter approximately 4.5 mm, to connect together the manifolds of the three differential pressure transmitters mounted on the transmitter assembly. The assembly was connected to the generator via 1 metre flexible hoses with a nominal internal diameter of 6.4 mm.

To examine the potential effect that differences in the dimensions of the pressure system could have on the dynamic characteristics of the generator, additional pipes and tanks were fitted such that they could readily be valved-in or out, thus changing the length and volume of pipework between the generator and the transmitters (see Figure 10).

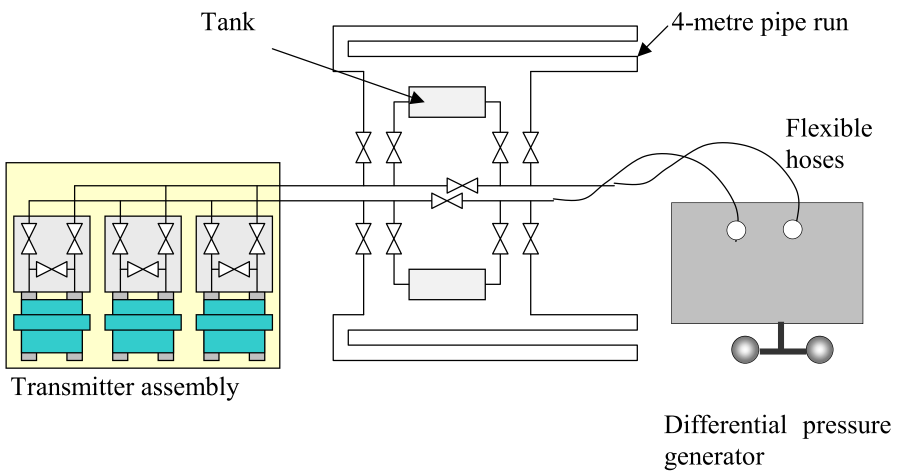

Figure 10 Pressure circuit modified with extra piping and added tanks

A comparison was made between (i) results recorded using the normal pipework configuration, (ii) those recorded after increasing the normal configuration by 4 metres of '¼ inch' pipework (on each side) and (iii) those recorded after increasing the normal pipework by including a 300 ml tank (on each side).

The results in Figure 11, Figure 12 and Figure 13 show that changes in the dimensions and volume of the pressure circuit can have an effect on the dynamic performance of the system. In this case adding extra volume to the circuit has increased the time taken for the system to stabilise after a step increase in pressure generated by placing extra mass on the *high* piston-cylinder. Similar results were obtained at line pressures between 5 MPa and 20 MPa.

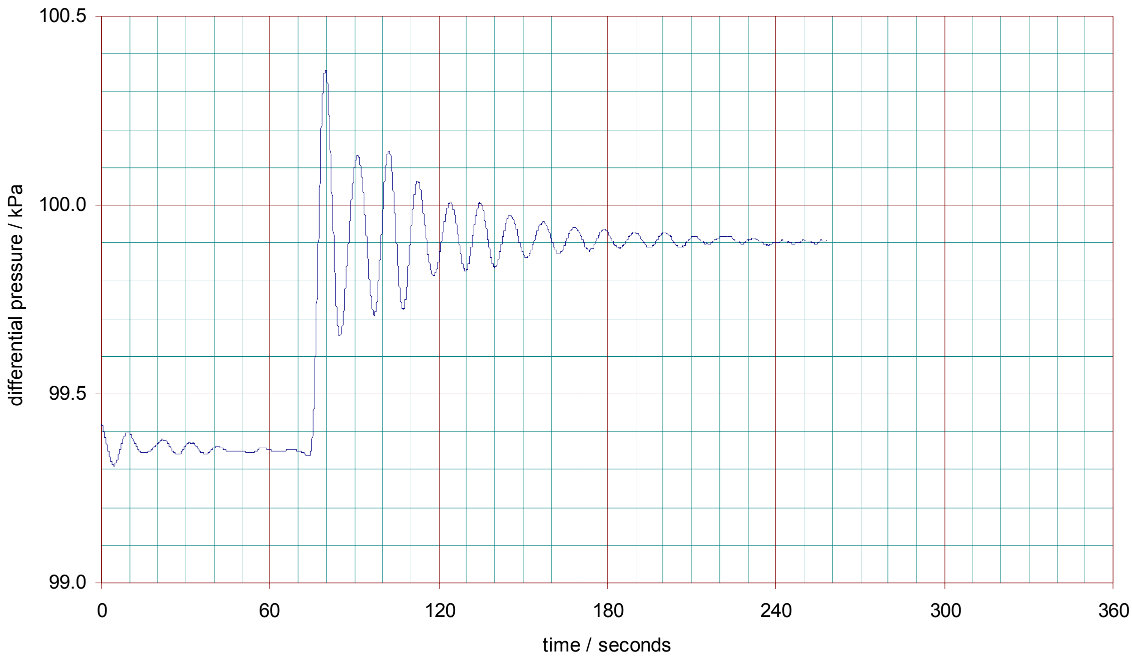

Figure 11 Gas-lubricated twin-post: response to step increase in applied mass – normal pressure circuit

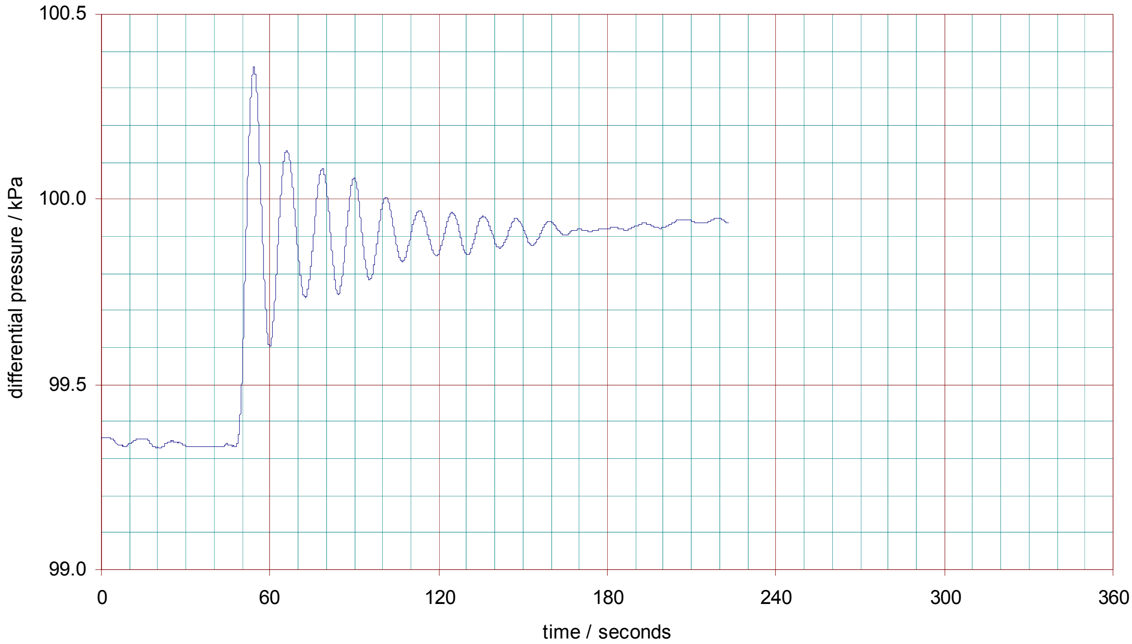

Figure 12 Gas-lubricated twin-post: response to step increase in applied mass – extra pipe.

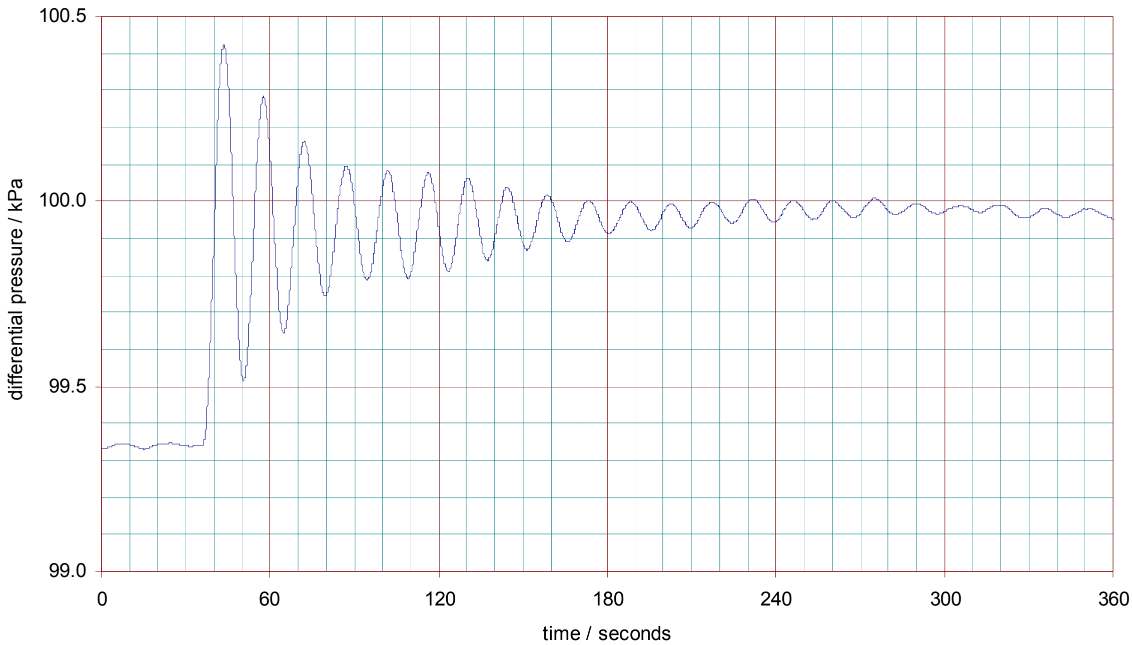

Figure 13 Gas-lubricated twin-post: response to step increase in applied mass – extra tank

8.2.5 Piston 'fall-rate'

Capacitive sensing devices, in conjunction with graphical software, were used to measure the fall-rates of both pistons of the twin-post pressure balance at various line pressures.

The twin-post pressure balance used in this evaluation had valves which could be closed to isolate each piston-cylinder, thus enabling measurement of piston fall-rate without the influence of the pressure circuit. It was found that with pistons isolated the fall-rate was relatively constant, deviating by around 0.2 mm per minute. With the piston isolation valves open the pistons did not fall at such a constant rate, with variations in measured velocity of up to 0.75 mm per minute. The larger value was assumed to be due to variations in temperature of the longer pipework. (Temperature changes cause pressure changes which in turn cause the piston to rise or fall to produce a compensatory change in volume – sometimes called 'barostating').

The fall-rate estimates were made during the time taken for the pistons to fall several millimetres. Typical values recorded for the piston-cylinders in the device under test were between 1 mm to 1.5 mm per minute at 10 MPa and 1.5 mm to 3.0 mm per minute at 20 MPa.

8.2.6 Piston float-position

If the float-position of a piston changes, so too does the pressure at a fixed point beneath it; this happens for two reasons. As a piston moves vertically within its cylinder the fluid head beneath it changes by the same amount and, due to small dimensional variations along the piston and cylinder (eg taper), so does the effective area of the piston-cylinder combination.

The auxiliary capacitive sensors potentially enabled the float-position of the pistons to be determined with a reproducibility of <±0.1 mm but in practice the tolerance in piston height has to be greater, as described in Sections 8.2.8 and 11.3.13.

8.2.7 Piston taper

To quantify the effect of piston taper (see Section 8.2.6), the changes in generated differential pressure caused by individually changing the float-position of each piston were recorded. Figure 14 shows measurements made at a line pressure of 10 MPa (where a change in differential pressure of 10 Pa is approximately equal to a change in area of 1 ppm).

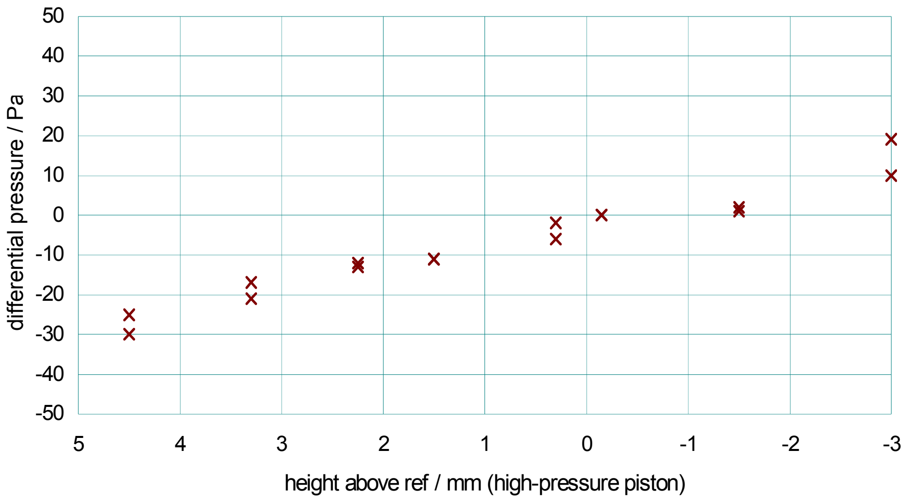

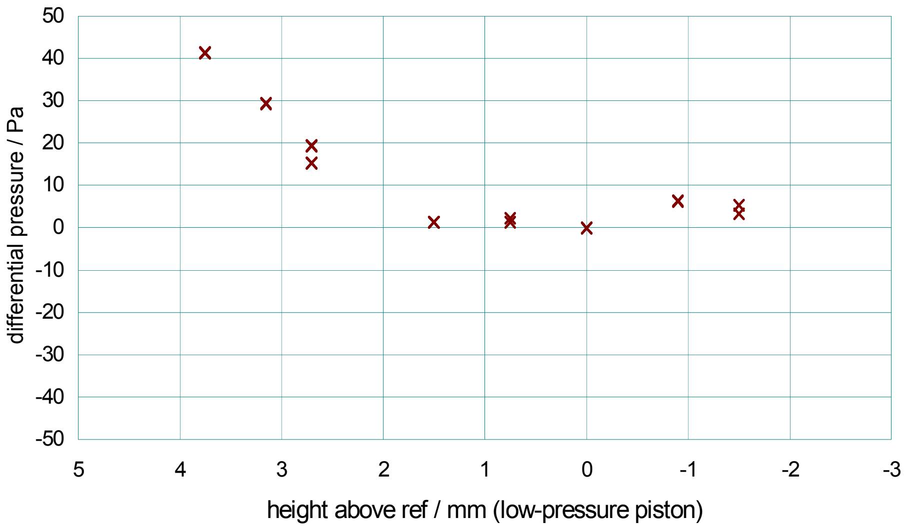

Figure 14 The relationship between piston displacement and generated differential pressure

From Figure 14 it can be seen that as the high-pressure piston falls towards its reference level the differential pressure increases, whereas as the low-pressure piston falls towards its reference level the differential pressure reduces. As the pistons fall the net result is a changing value of differential pressure. Note that the rate at which it changes alters markedly as the low-pressure piston falls below about 2 mm above its reference level.

The empirical proof of this is shown in Figure 15, where a plot of differential pressure vs time essentially combines the effects shown in Figure 13, the turning point at approximately 180 seconds corresponding to the low pressure piston being about 2 mm above its reference level.

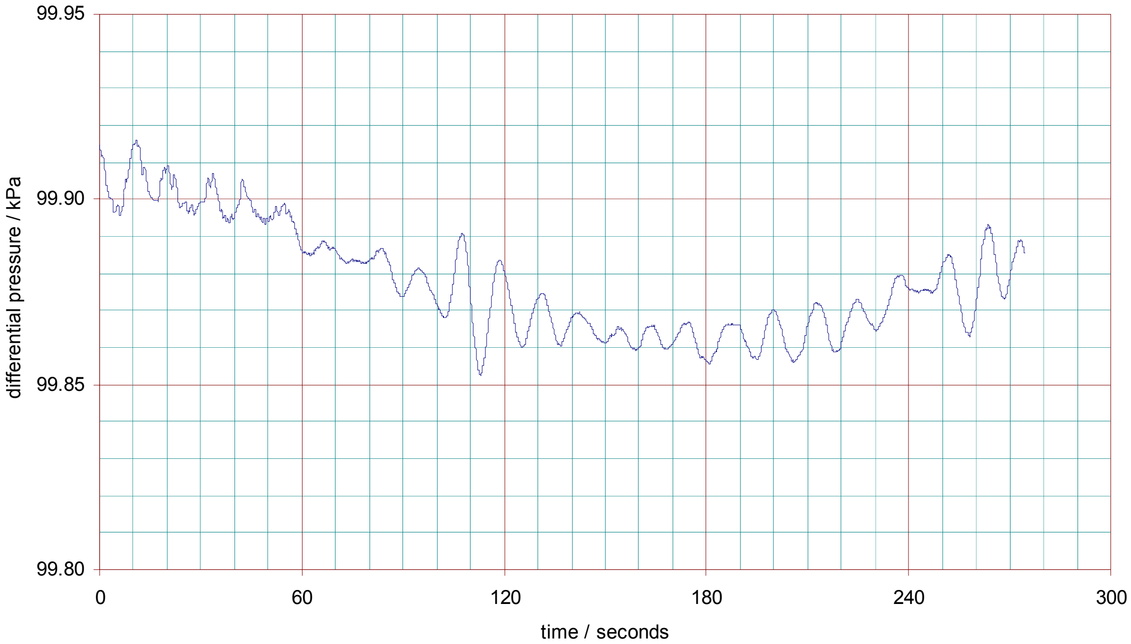

Figure 15 Change in differential pressure caused by piston taper

What may at first appear to be random fluctuations in differential pressure has a pattern, is predictable and can be modelled and controlled.

8.2.8 Combined effects

Achieving a differential pressure, whose value may be properly calculated with low uncertainty, and which is stable for sufficient time to allow practical and meaningful calibrations to be undertaken, relies on a number of conditions being met simultaneously.

Time has to be allowed for the pistons to stop bouncing after any adjustments – this can be in excess of 3 minutes. Given that the pistons are falling during this period, they have to be 'started' at a height considerably above their reference levels. They may fall at different and varying rates and the bouncing tends to prevent accurate determination of the appropriate start-point. Thus it is difficult to estimate in advance the likely degree of simultaneous piston and reference level convergence, and the corresponding effects of dissimilar piston tapers.

As with all measurement systems, it is ultimately impossible to ensure perfect convergence of these effects; realistic tolerances have to be set and corresponding measurement uncertainties calculated.

9 EVALUATION OF AN OIL-LUBRICATED TWIN-POST PRESSURE BALANCE

9.1 DESIGN

Although the principle of operation is the same, there are a number of significant differences in the designs of the gas- and oil-lubricated twin-post pressure balances.

The instrument evaluated used tungsten-carbide piston-cylinders with effective areas of approximately 19 mm^2, more than twice the area of the gas-lubricated device.

The mass set comprised stainless steel ring-weights for the larger values and stainless steel platters for the lower denominations. The weights were stacked on an overhanging weight carrier made of stainless steel with a nickel-plated iron ring at the base for attracting the magnetic level indicator. The weights had cavities filled with small particles of stainless steel, which were used to trim the mass values during the manufacturing process. This resulted in values of the mass very close to nominal, although it increased the uncertainty in estimating the density of the load for the calculation of force.

The instrument was supplied with a platinum resistance thermometer for measuring the temperature of the high piston-cylinder but not the low piston-cylinder. Both piston-cylinder mounting posts contained holes (to enable thermometer probes to be fitted just a few millimetres away from the pistons) and, as it was considered better to measure the temperature of both piston-cylinders (see Section 5.7, The differential pressure equation), thermistor thermometers were inserted into both.

The pistons were rotated by an intermittently-engaging motor-drive mechanism.

A pressure controller was used to apply pressure to the generator at a slow rate (around 20 kPa s^{-1}). This removed the risk of a temperature change due to a rapid change in pressure, also sudden changes in pressure are best avoided in systems containing both oil and gas as rapid flow-rates could propel the oil through the gas pressure circuit resulting in oil contamination. For this reason care was also taken to release gas at a slow rate.

Particular care was taken when levelling the device and the standard practice of placing a spirit level on a slowly rotating weight stack was adopted. The *high* and *low* piston-cylinders could not be levelled separately and the process was undertaken on the high-pressure piston. In practice no difference was found between the level of the two pistons. The ‘bulls eye’ level attached to the base of the instrument was used as a rough guide when repositioning the instrument but as it had no scale it was not used for quantitative measurements.

9.2 PISTON LUBRICATION

9.2.1 Absorption of gas into the lubrication oil

Oil-lubricated twin-post pressure balances contain both gas and oil within the same pressure system and, under pressure, the oil becomes saturated with the gas. The effect of this absorption was observed when attempting to cross-float pistons shortly after pressurisation; an excessive piston fall-rate - of a magnitude consistent with that of a slow gas-leak - was observed. When the system was returned to atmospheric pressure, bubbles of gas floating to the surface of the oil were observed through the window of the oil reservoirs as desorption occurred.

9.2.2 Surface tension

The force due to the surface tension of the oil in a hydraulic pressure balance is generally calculated using the equation:

$$S = \sigma \; c \tag{41}$$

where σ is the surface tension coefficient of the fluid

c is the circumference of the floating element of the assembly at the point where it emerges from the fluid

The device evaluated uses a design in which the pistons emerge from the oil at both ends of the cylinder (see Figure 2), and a first approximation at modelling this design showed the upward force at the bottom of the cylinder as equal to the downward force at the top of the cylinder. A more detailed analysis would reflect differences between the meniscus profiles at the top and bottom of the cylinders due to the effects of gravity and flow etcetera but this was not considered. Whichever model is used to calculate the force due to surface tension the effect on the differential pressure will be negligible providing the forces are constant on both the *high* and the low-pressure pistons for the duration of the calibration. Any initial difference between the forces due to surface tension will be 'balanced out' during the initial cross-float.

9.2.3 The effect of oil lubrication on differential pressure

Lubricating oil escapes from both ends of the cylinders and the potential effect of variations in the mass of oil clinging to the pistons was considered.

During this project the outputs of differential pressure transmitters connected to the system were monitored for a number of several-hour periods but no characteristics consistent with oil build-up or dripping were observed. The pressure balance was operated for several days without significant loss of oil, consistent with a very small oil flow-rate. It is possible however that, had the device been operated for longer, an oil build-up effect might have been eventually detected, either as a sudden, otherwise unexplainable, change in transmitter output or as poor repeatability of the initial cross-float.

9.3 DYNAMIC CHARACTERISTICS

9.3.1 General

The oil-lubrication applied to these instruments produces characteristics which differ from those lubricated by gas. Essentially the oil forms a seal in the piston-cylinder gap which stops the gas escaping. This leads to lower piston fall-rates, a difference that is more apparent at higher pressures, and the oil's viscous drag substantially damps piston-bounce.

The motor-drive mechanism causes periodic pulses in the differential pressure (through intermittently 'nudging' the pistons) and there are two schools of thought about its effect. The first argues that the motor should be used continuously to ensure broadly constant angular velocity, whereas the second says that pulses caused by the motor limit the level of differential pressure stability that may be obtained. Tests were conducted both with and without the motor-drive.

9.3.2 Motor-drive effect

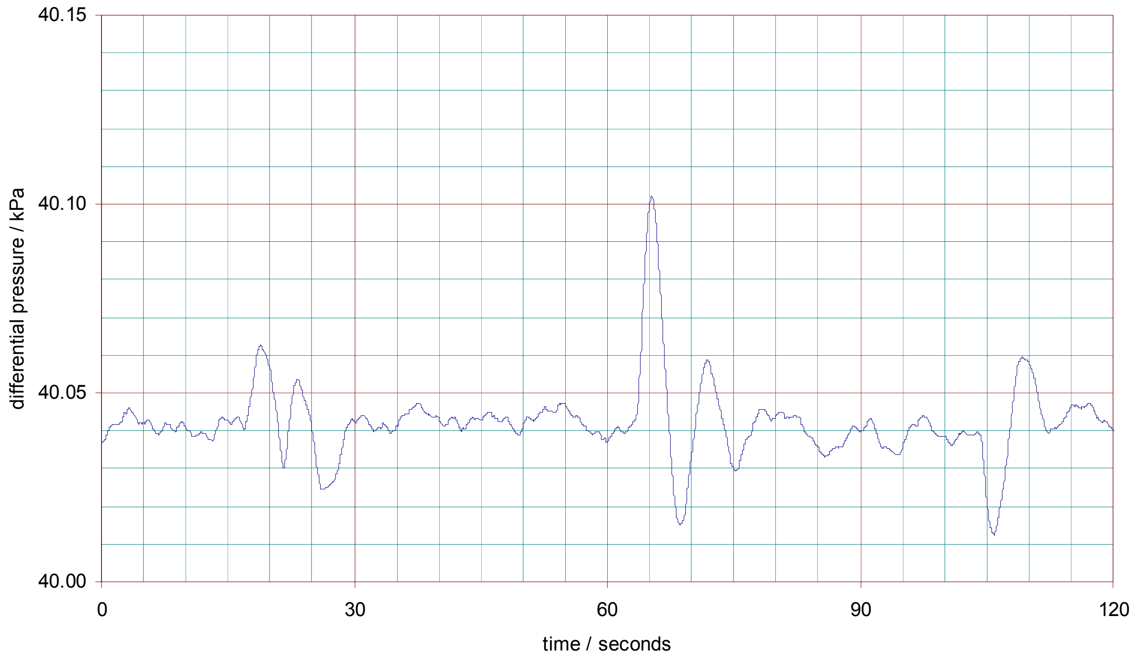

Figure 16 Oil-lubricated twin-post: effects of the motor-drive

Figure 16 shows a typical example of periodic pulses in the differential pressure caused by the motor-drive mechanism (see Section 9.3.1). A trace obtained under similar conditions but without using the motor-drive is shown in Figure 17.

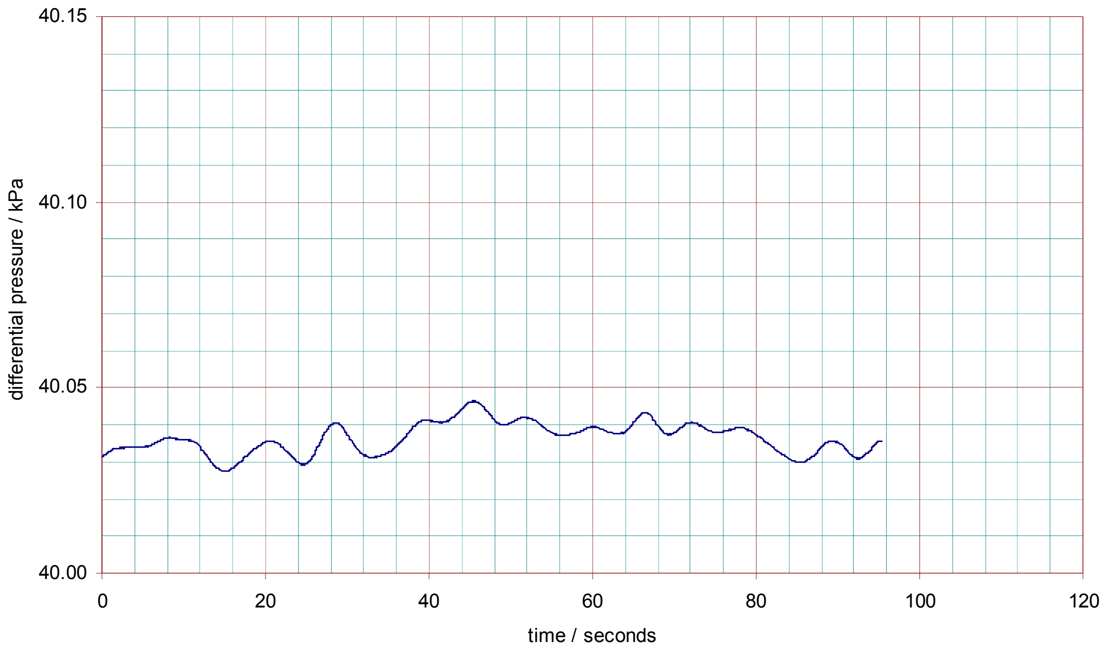

Figure 17 Oil-lubricated twin-post: hand-rotated

9.3.3 Angular velocity

The 'nudging' drive pins were removed from the piston units to enable manual rotation and a series of tests were conducted at various line pressures, observing the output of the generator at different rotational velocities.

As the angular velocities fell below 20 rpm, oscillations in differential pressure, at the same frequency as the piston rotation rates, were observed. Figure 18 shows the differential pressure recorded with the pistons rotating at approximately 19 rpm.

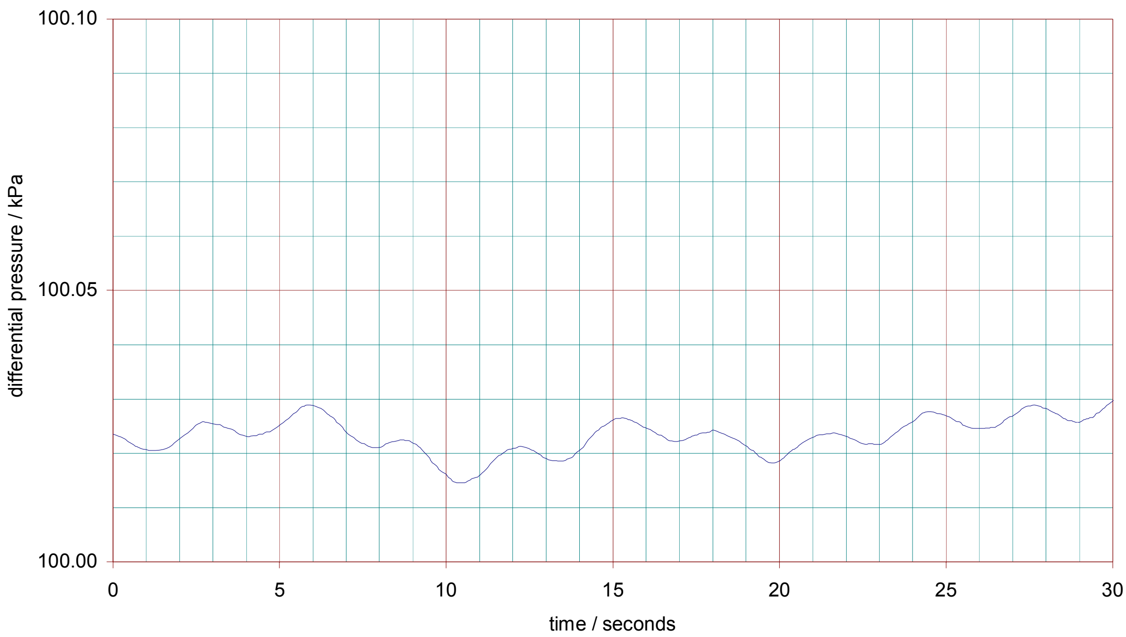

Figure 18 Oil-lubricated twin-post: pistons rotating at 19 rpm (hand-rotated)

An increase in the amplitude of the oscillations was observed at lower rotational velocities, as shown in Figure 19.

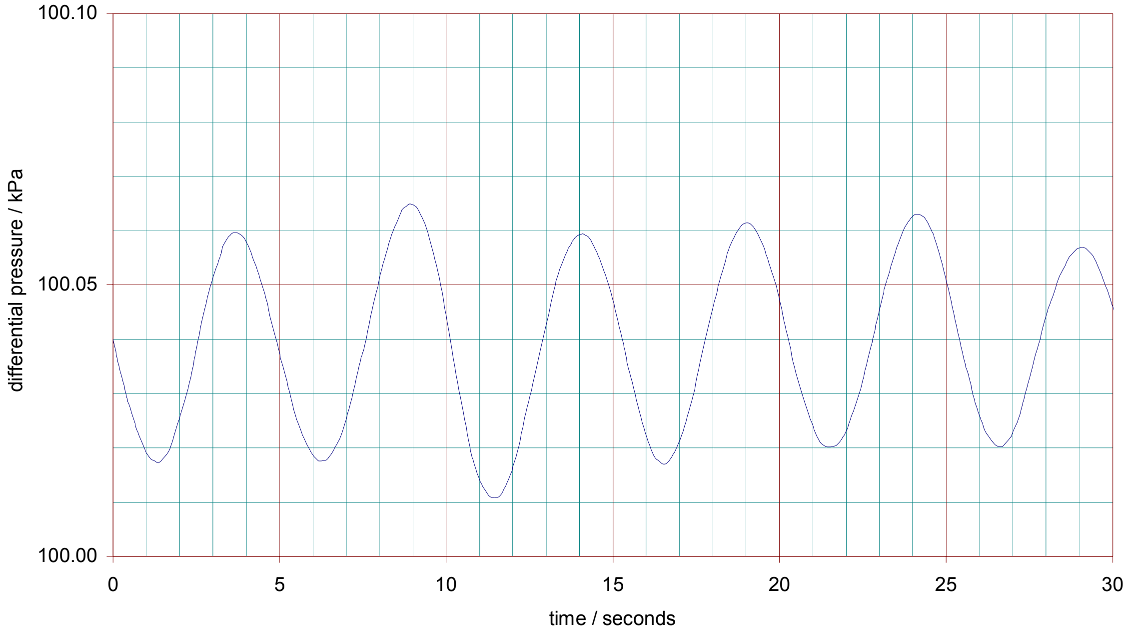

Figure 19 Oil-lubricated twin-post: pistons rotating at 12 rpm (hand-rotated)

A complex waveform was observed when rotating the pistons at different velocities. Figure 20 shows how a 1 rpm difference velocity caused the two pistons to move in and out of phase once every minute – classical *beating*.

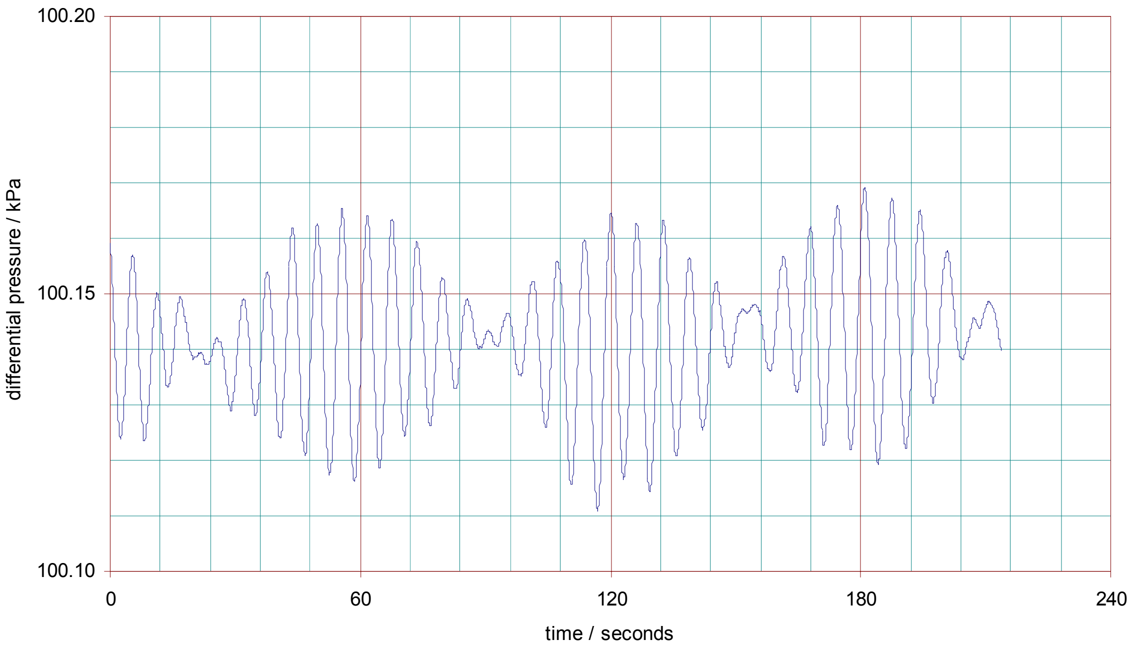

Figure 20 Oil-lubricated twin-post: pistons rotating at 9 rpm and 10 rpm (hand rotated)

From a series of measurements (at the same nominal differential pressure) a relationship was observed between the differential pressure (meaned where it was oscillating) and angular velocity.

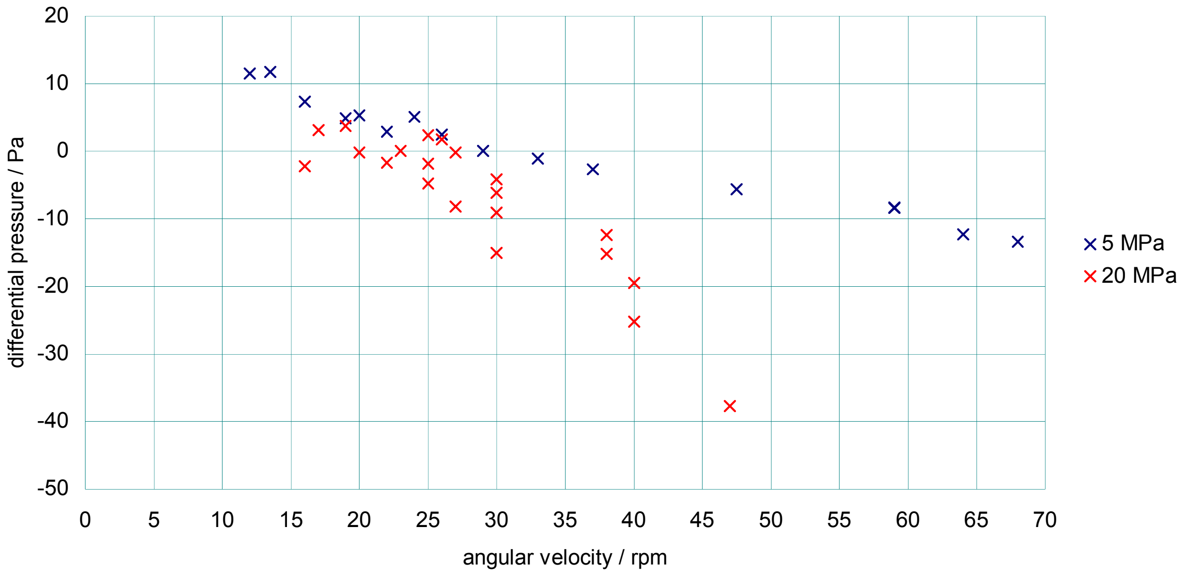

Figure 21 Relationship between angular velocity and generated differential pressure

Figure 21 shows that variations in angular velocity caused the differential pressure to change by very approximately 0.1 ppm of line pressure per rpm. The effect was found to be irrespective of direction of rotation.

9.3.4 Piston 'bounce'

Tests were conducted to observe the response of the oil-lubricated twin-post pressure balance to a step increase in pressure – similar to those in Section 8.2.3 conducted on the gas-lubricated device – which showed the characteristic described as *piston bounce*.

The results showed a marked difference in the damping of the devices which was attributed to the friction of the oil lubricating the piston-cylinders. Figure 22 shows the effect of gently adding a 1 g weight (equivalent to approximately 0.5 kPa) to the load on the *high* piston at the mid-range line pressure of 10 MPa. Note that the scale is the same as that used in the examples shown for the gas-lubricated pressure balance (see Figure 11, Section 8.2.4).

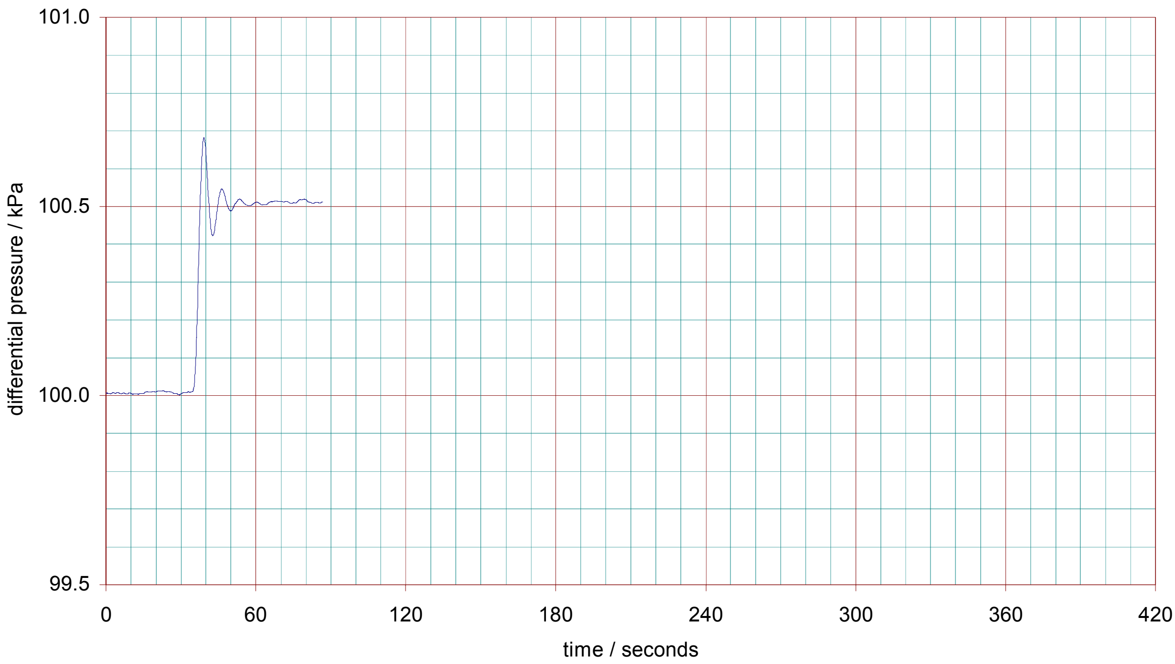

Figure 22 Oil-lubricated twin-post: response to a step increase in applied mass

9.3.5 Pipe-work configuration

The *normal* pipework configuration (see Figure 9) included approximately 1 metre of '¼ inch' pipe (each side of the pressure system) of internal diameter approximately 4.5 mm to connect together the manifolds of the three differential pressure transmitters mounted on the transmitter assembly. The assembly was connected to the generator via 1 metre flexible hoses with a nominal internal diameter of 6.4 mm.

To examine the potential effect that differences in the dimensions of the pressure system could have on the dynamic characteristics of the generator, additional pipes and tanks were fitted such that they could be readily valved-in or out, thus changing the length and volume of pipework between the generator and the transmitters (see Figure 10).

A comparison was made between (i) results recorded using the normal pipework configuration, (ii) those recorded after increasing the normal configuration by 4 metres of '¼ inch' pipework (on each side) and (iii) those recorded after increasing the normal pipework by including a 300 ml tank (on each side).

Figure 23, Figure 24 and Figure 25 – which were made at a line pressure of 10 MPa, show that the changes in pipe configuration did not have a significant effect on the dynamic characteristics. Similar results were obtained at line pressures between 5 MPa and 20 MPa.

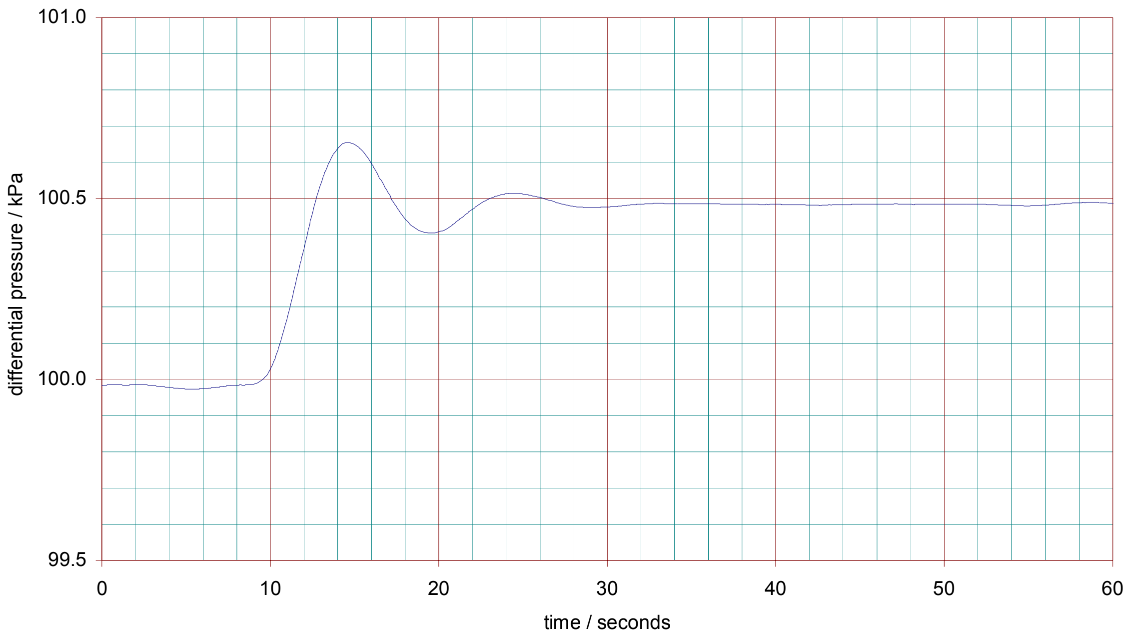

Figure 23 Oil-lubricated twin-post: response to a step increase in applied mass – normal pressure circuit

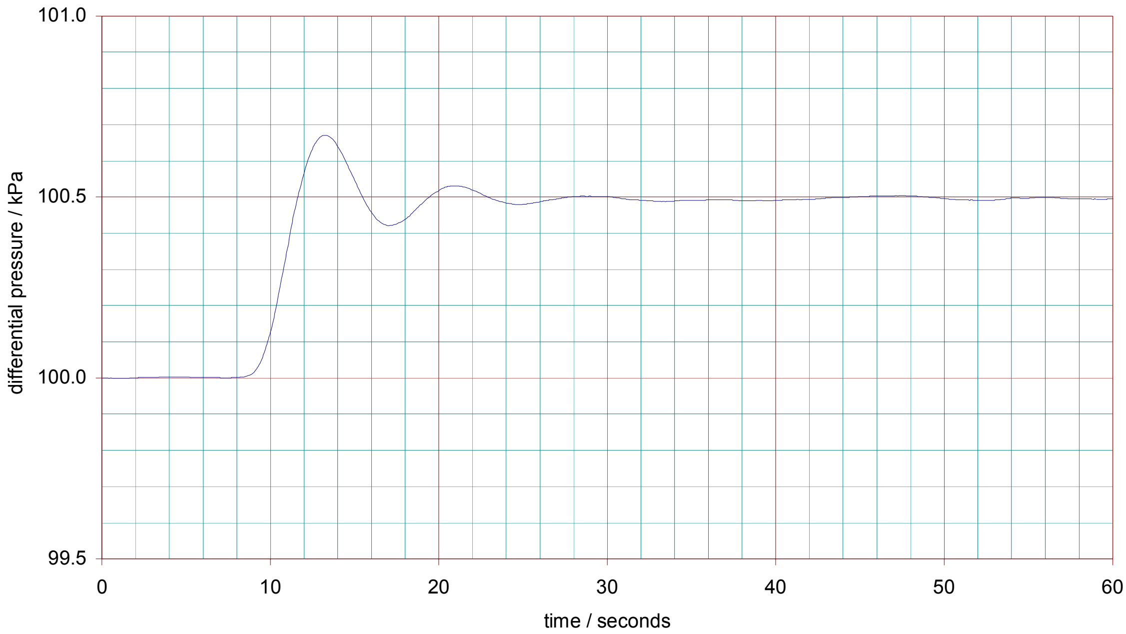

Figure 24 Oil-lubricated twin-post: response to a step increase in applied mass – extra pipe

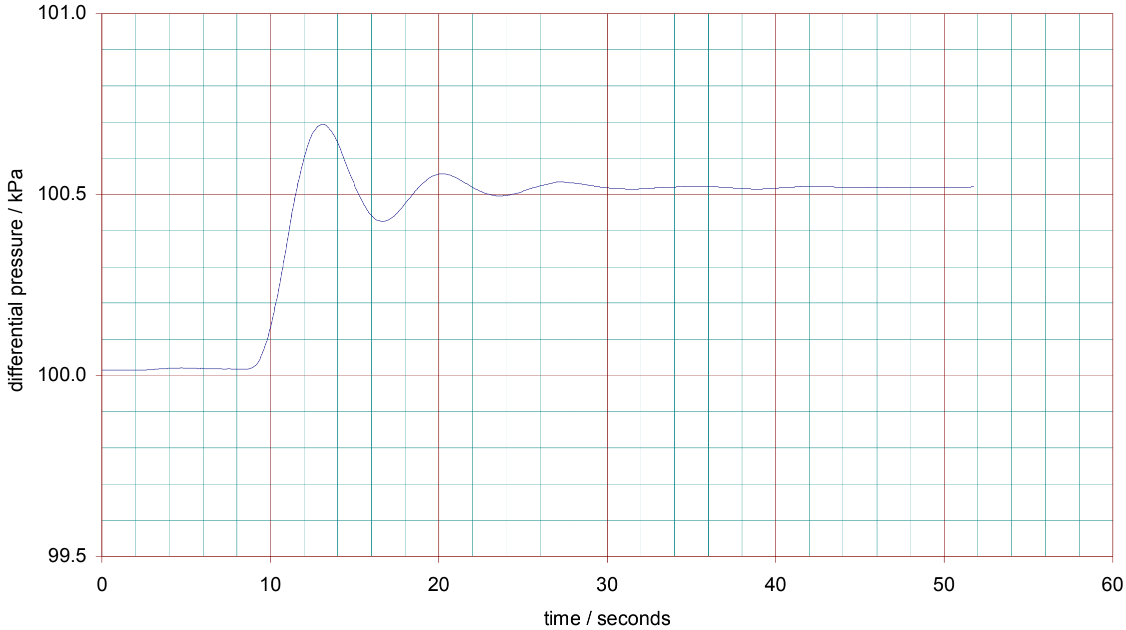

Figure 25 Oil-lubricated twin-post: response to a step increase in applied mass – extra tank

9.3.6 Piston 'fall-rate'

Capacitive sensing devices, in conjunction with graphical software, were used to measure the fall-rates of both pistons of the twin-post pressure balance at various line pressures.

The fall-rates recorded for these piston-cylinders varied up to about 0.5 mm per minute at 20 MPa. At lower pressures the fall-rate was less and frequently small enough to be masked by perturbations to system pressure (eg thermally induced); indeed in some instances pistons would appear to rise rather than fall.

9.3.7 Piston float-position

If the float-position of a piston changes, so too does the pressure at a fixed point beneath it; this happens for two reasons. As a piston moves vertically within its cylinder the fluid head beneath it changes by the same amount and, due to small dimensional variations along the piston and cylinder (eg taper), so does the effective area of the piston-cylinder combination.

The base of the oil-lubricated pressure balances contained piston float-position indicators which were magnetically attracted to the nickel plated iron ring on the weight carriers. Calibrated against a cathetometer, one of the indicators had an error of 0.8 mm. The other indicator was prone to oscillate rapidly as it pivoted, inducing a relatively high-frequency, low-amplitude oscillation in the float-position of the piston.

The auxiliary capacitive sensors enabled the float-position of the pistons to be determined with a reproducibility of <±0.1 mm but in practice the tolerance in piston height had to be greater to allow sufficient time to take readings and avoid spurious pulses caused by the motor-drive.

9.3.8 Piston taper

To quantify the effect of piston taper (see Section 9.3.7), the changes in generated differential pressure caused by individually changing the float-position of each piston were recorded. Figure 26 shows measurements made at a line pressure of 10 MPa (where a change in differential pressure of 10 Pa is approximately equal to a change in area of 1 ppm). The instrument was supplied with a third piston-cylinder and its taper was measured by substituting the low-pressure piston-cylinder.

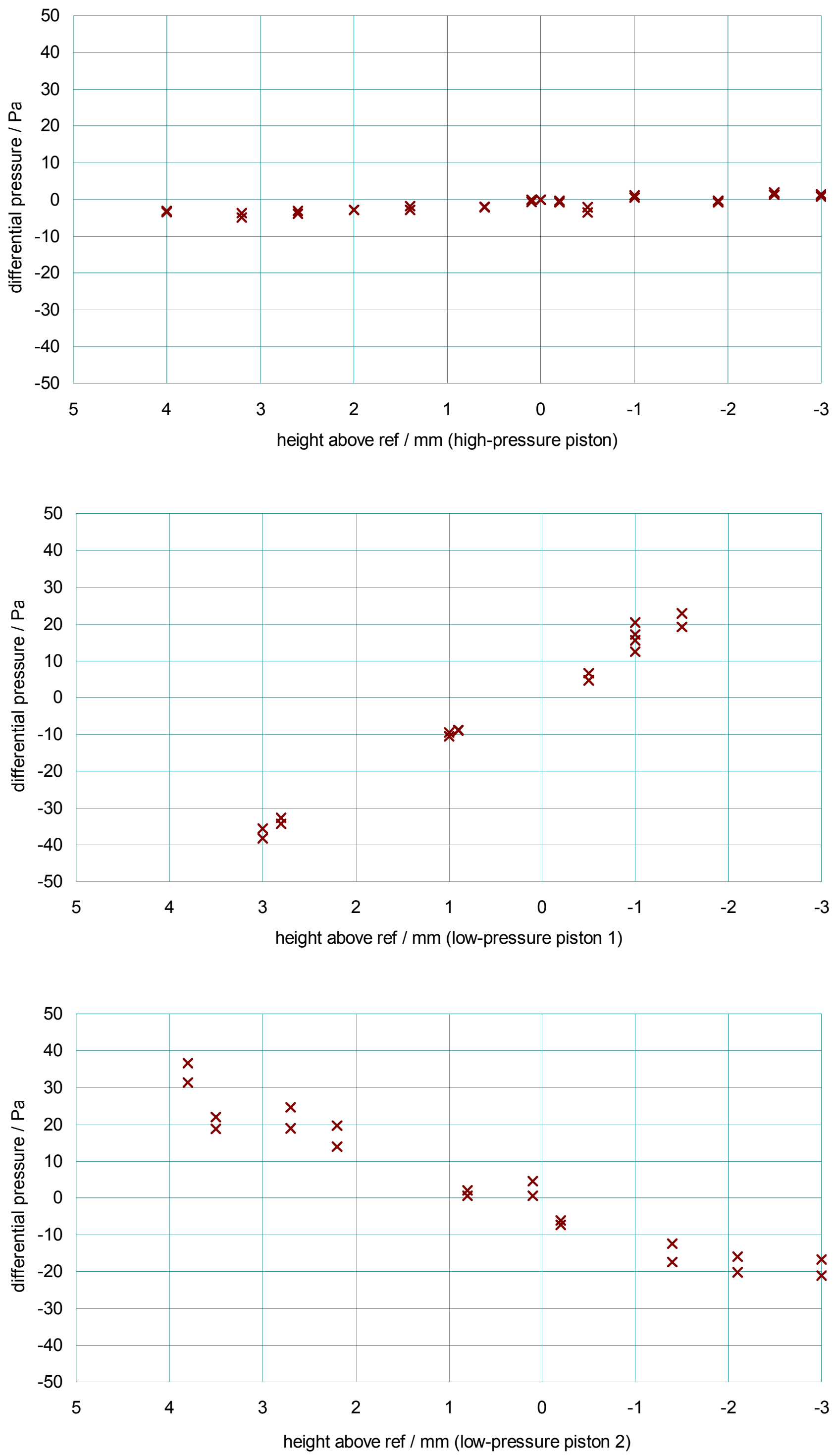

Figure 26 The relationship between piston displacement and generated differential pressure.

From Figure 26 it can be seen that each of the nominally identical piston-cylinders had a significantly different profile; taper in the high-pressure piston caused a change in differential pressure of around 0.1 ppm of the line pressure per millimetre but the two low-pressure pistons caused corresponding changes of approximately 1.3 ppm of the line pressure per millimetre and 0.7 ppm of the line pressure per millimetre.

These differences, in both sign and magnitude, underline that piston position relative to that at the time of the initial cross-float is more significant than the position of the pistons relative to each other. For example, if the third unit was used to replace the high-pressure piston-cylinder instead of the low-pressure piston-cylinder, both pistons falling at the same rate would result in a change in generated differential pressure equivalent to 2 ppm of the line pressure per millimetre.

Again from Figure 26, it can be seen that as the high-pressure piston falls towards its reference level the change in differential pressure is negligible, whereas as the low-pressure piston 1 falls towards its reference level the differential pressure increases.

9.3.9 Combined effects

The net result of piston taper is shown in Figure 27, where the pulses shown are generated by the motor-drive but the main trend is a change in differential pressure by approximately 25 Pa in 7 minutes.

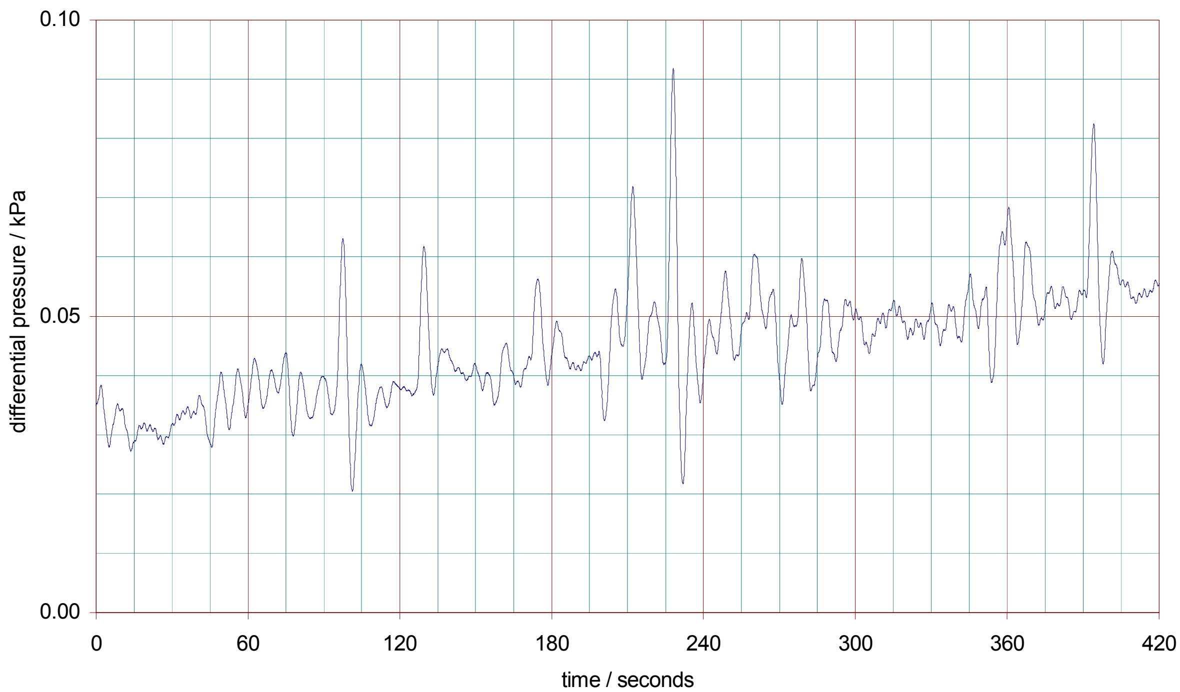

Figure 27 The change in generated differential pressure as pistons fall through the reference level.

Achieving a differential pressure, whose value may be properly calculated with low uncertainty, and which is stable for sufficient time to allow practical and meaningful calibrations to be undertaken, relies on a number of conditions being met simultaneously. The slow piston fall-rate and lack of piston-bounce facilitated simultaneous piston and reference level convergence although, the time-period during which measurements could be made was sometimes limited by an untimely pulse from the motor-drive mechanism.

10 EVALUATION OF A PRESSURE DIVIDER

10.1 GENERAL

Although *divider* characteristics are related to piston-cylinder areas (or at least the ratio of areas), their use, operation and quantification is very different to conventional pressure balances. In many ways easier to operate, the divider is internally more complex, including a number of linking mechanisms and, unlike twin-post pressure balances, it is not realistic to evaluate its performance from analysis of its component parts. Instead it is calibrated as a 'black box', against twin-post pressure balances (see Section 12.1).

10.2 DESIGN

The rotating assembly of the divider was driven by a motor and belt mechanism at a uniform rate (about 24 rpm), and the hydraulic pressure balance was rotated using an intermittently engaging motor-drive mechanism similar to that of the oil-lubricated twin-post device described in Section 9.1.

The divider was not supplied with thermometers and the manufacturer assumed that temperature would affect all three piston-cylinders in a fashion that would not affect the dividing ratio. The hydraulic pressure balance used in conjunction with the divider was supplied with a thermometer for measuring the temperature of its piston-cylinder.

The three pistons of the divider's rotating assembly were lubricated by oil, applied in a similar manner to that used for the oil-lubricated twin-post pressure balance (see Section 2.2).

The vertical displacement of the rotating assembly was indicated by markings below the weight carrier; it was found that using a capacitive height sensor (see Section 3.3) greatly reduced the time taken to achieve the initial balance (see Section 2.3).

Bourdon tube pressure gauges on the front of the divider gave nominal indications of the pressure on the high- and low-pressure sides of the system.

10.3 DYNAMIC CHARACTERISTICS

10.3.1 General

There are significant differences between balancing a twin-post pressure balance and establishing the initial equilibrium with a divider and it can be easy to get the impression that the divider has a slower response time and poorer sensitivity. This is illusory to some degree, however; increasing the differential pressure by 10 Pa requires an additional 1 g mass to be added to the divider's hydraulic piston-cylinder but only 10 mg - 20 mg on a twin-post devices. In practice the resolution of all three devices was broadly similar (< 5 Pa).

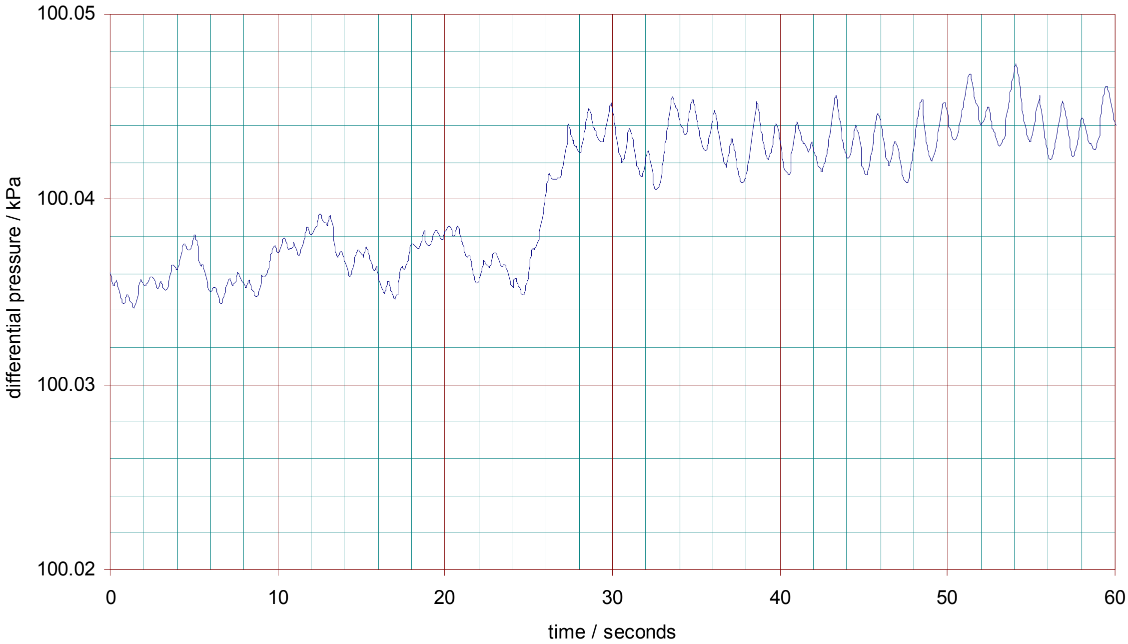

Figure 28 Divider: response to a step increase in applied mass – equivalent to 5 Pa differential pressure

Figure 28 shows the result of adding 0.5 g to the mass of the hydraulic pressure balance to generate a step increase in differential pressure of approximately 5 Pa – this test was conducted at a line pressure of 10 MPa and a differential pressure of 100 kPa.

Analysis of the generated differential pressure showed a complex waveform at the same frequency as that of the dividers rotating assembly. Although the frequency remained constant, variations in the wave-form were observed between measurements recorded at different line and differential pressures. The differences recorded were consistent with what would have been expected when combining a number of waveforms of the same frequency but not necessarily with the same phase or amplitude. It was not possible to operate the divider without the rotating assembly's motor engaged. Alternative examples of divider pressure wave-forms are shown in Figure 29 and Figure 30.

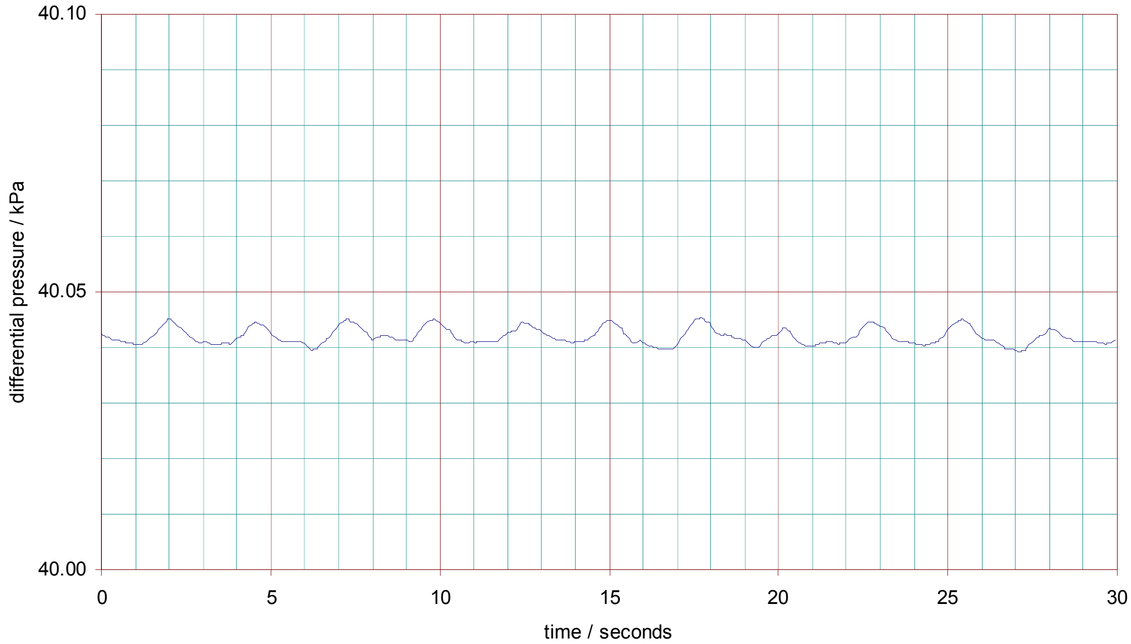

Figure 29 Divider: typical example of generated differential pressure

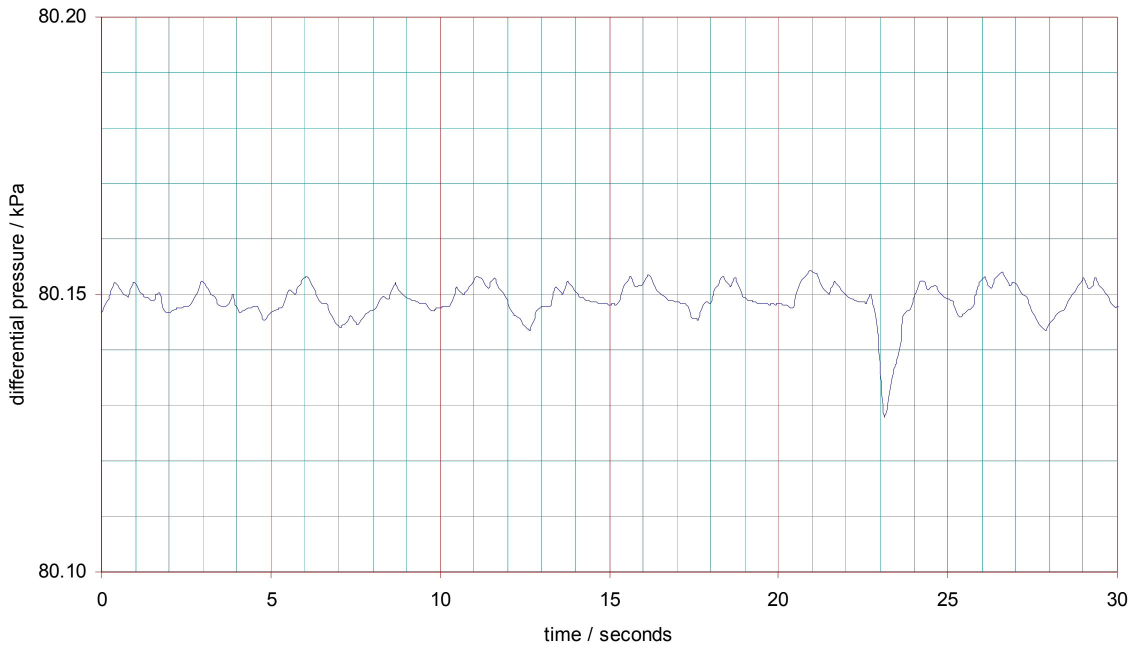

Figure 30 Divider: alternative example of generated differential pressure

Very occasionally (occurring once per several calibration runs) a slight ‘glitch’ was observed where a relatively sudden and spurious change in the generated differential pressure was followed by a ‘recovery’ period of two to three minutes, during which the generated differential pressure returned closely to its original value. Examples are shown in Figure 31 and Figure 32.

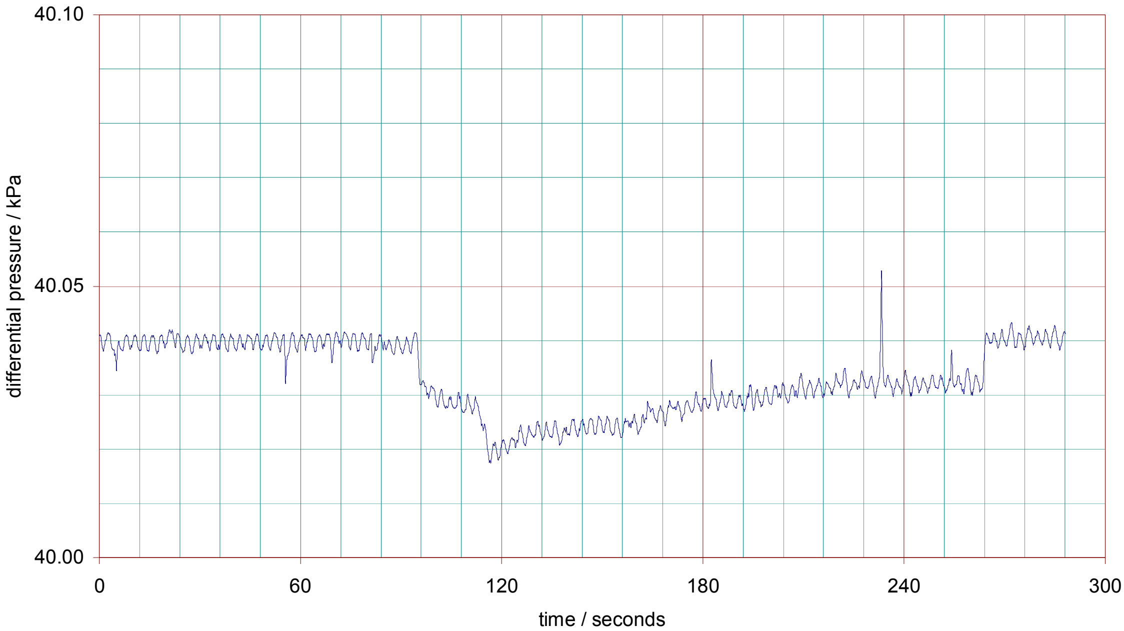

Figure 31 Divider: output showing ‘glitch’ lasting nearly three minutes

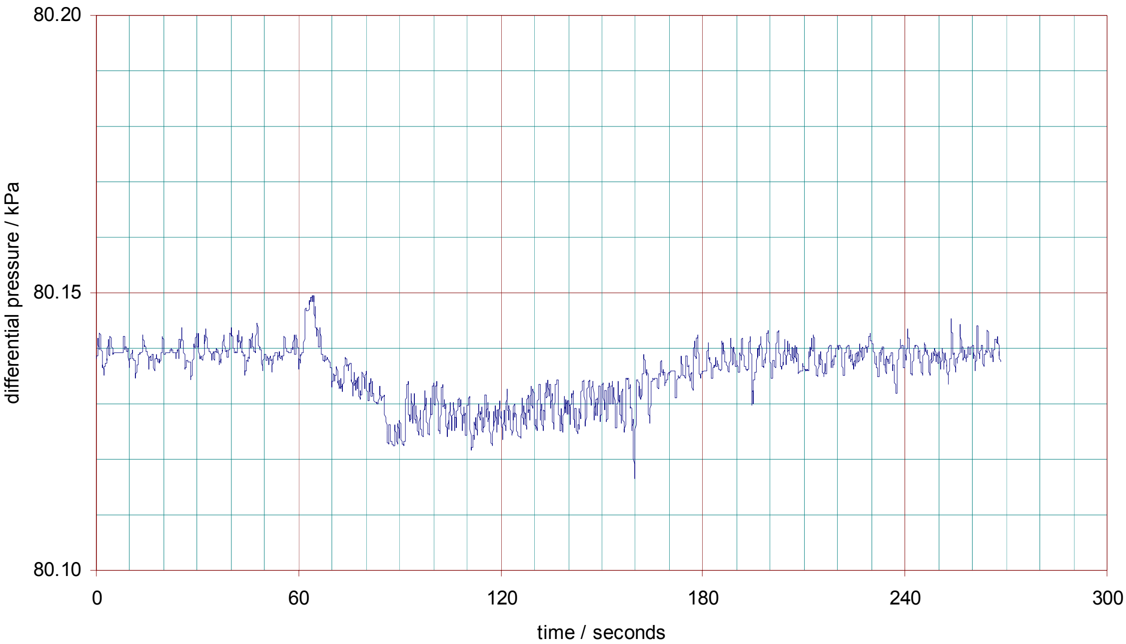

Figure 32 Divider: alternative example of 'glitch'

It was found that the glitches occurred more frequently during the first few hours following start-up of the divider – broadly the period required to reach thermal equilibrium. The real-time graphical software enabled the glitches to be observed and therefore avoided during measurements.

The glitches were similar to ones described by a user of another divider. One theory considered was the intermittent non-concentric rotation of a piston – possibly caused by horizontal frictional forces in the piston-connecting mechanisms. The effective area of a piston-cylinder will change if the axis of the piston moves with respect to that of the cylinder (the piston 'falls over'). The magnitude of the glitch in Figure 31, however, is about 20 Pa; it is superimposed on a differential pressure of 40 kPa and therefore corresponds to a change in effective area of one of the divider's piston-cylinders of around 5 parts in 10^4, or 500 ppm. – implausibly large – and the theory did not, therefore explain the observed effect.

[Since reading a draft of this Report the manufacturer has acknowledged the phenomenon. They suggest that it may be caused by a discontinuous lubricating film and that a solution is to ensure that, for several hours before use, the instrument be left with the upper (high) pressure chamber pressurised and the lower (low) pressure chamber opened to ambient pressure, and with the pistons floating and rotating.]

10.3.2 Motor-drive effect (hydraulic pressure balance)

Superimposed on the divider's differential pressure waveform, Figure 33 shows two pressure pulses which coincided with the drive motor nudging the piston of the hydraulic pressure balance, their amplitudes presumed to be substantially attenuated by the divider. Although clear in this Figure, it should be noted that the pulses occurred in-phase with the rotating-assembly-induced oscillations; when the hydraulic pressure balance's motor-drive nudged out of phase, the effect was barely noticeable. Most times, of course, there were varying degrees of phase-shift. Figure 30 and Figure 31 show similar pulses.

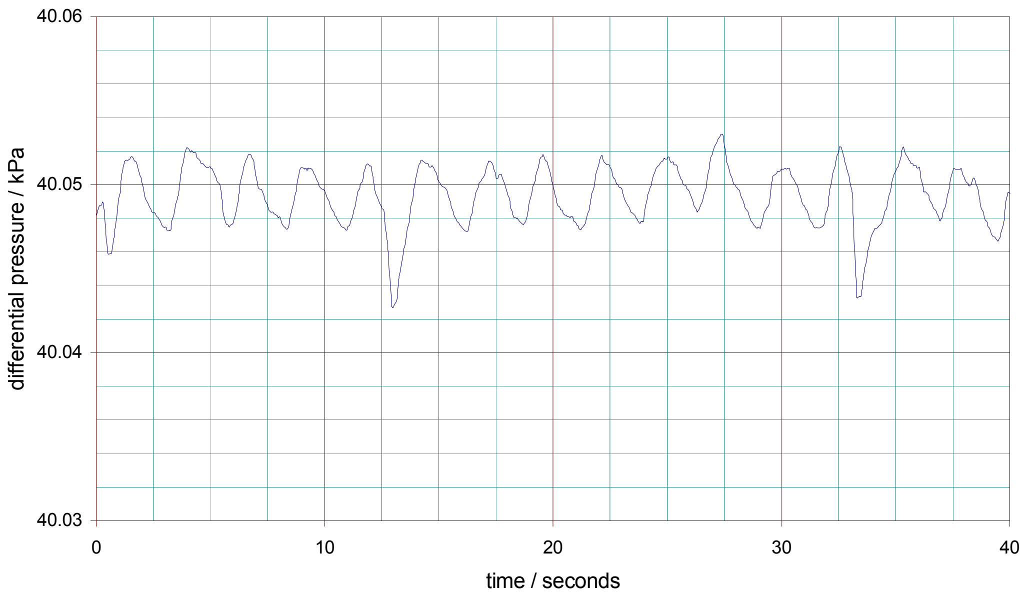

Figure 33 Divider: effects of the motor-drive

10.3.3 Pipe-work configuration

The *normal* pipework configuration included approximately 1 metre of '¼ inch' pipe (each side of the pressure system) of internal diameter approximately 4.5 mm to connect together the manifolds of the three differential pressure transmitters mounted on the transmitter assembly. The assembly was connected to the generator via 1 metre flexible hoses with a nominal internal diameter of 6.4 mm.

To examine the potential effect that differences in the dimensions of the pressure system could have on the dynamic characteristics of the generator, additional pipes and tanks were fitted such that they could readily be valved-in or out, thus changing the length and volume of pipework between the generator and the transmitters (see Figure 10).

A comparison was made between (i) results recorded using the normal pipework configuration, (ii) those recorded after increasing the normal configuration by 4 metres of '¼ inch' pipework (on each side) and (iii) those recorded after increasing the normal pipework by including a 300 ml tank (on each side).

It was found that the changes in pipe configuration did not have a significant effect on the dynamic characteristics of the system.

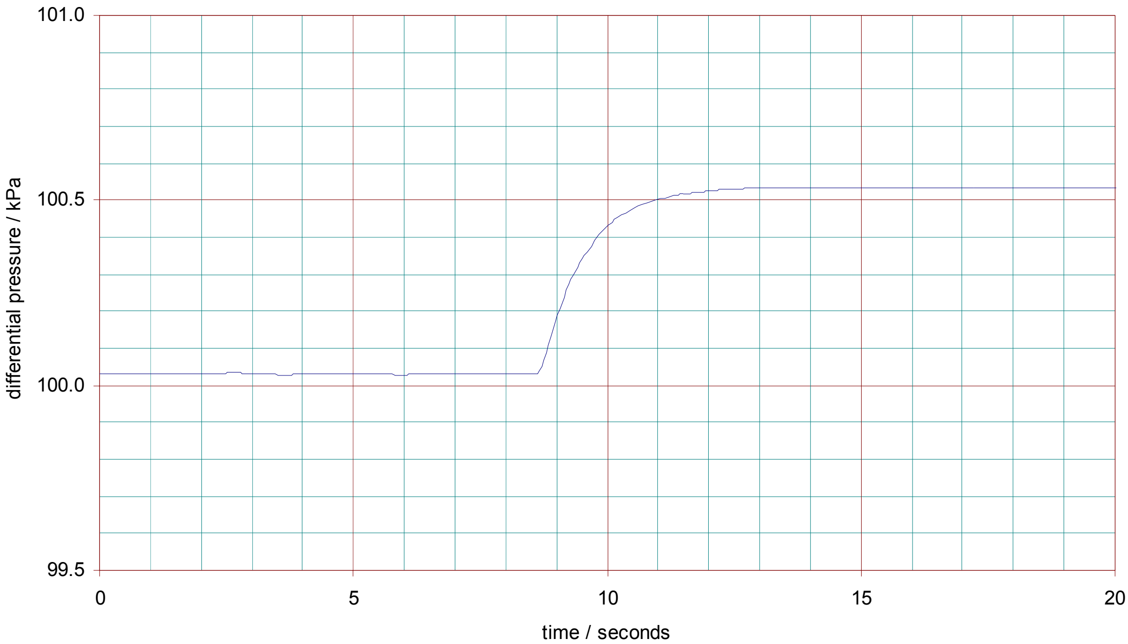

Figure 34 Divider: response to a step increase in applied mass – normal pressure circuit

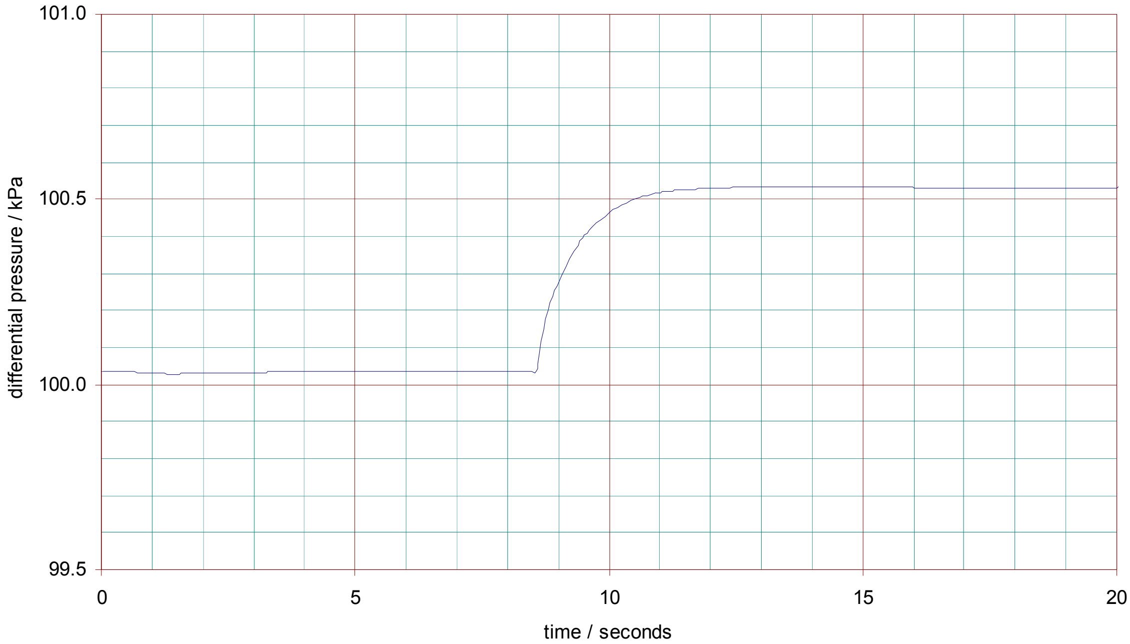

Figure 35 Divider: response to a step increase in applied mass – extra pipe

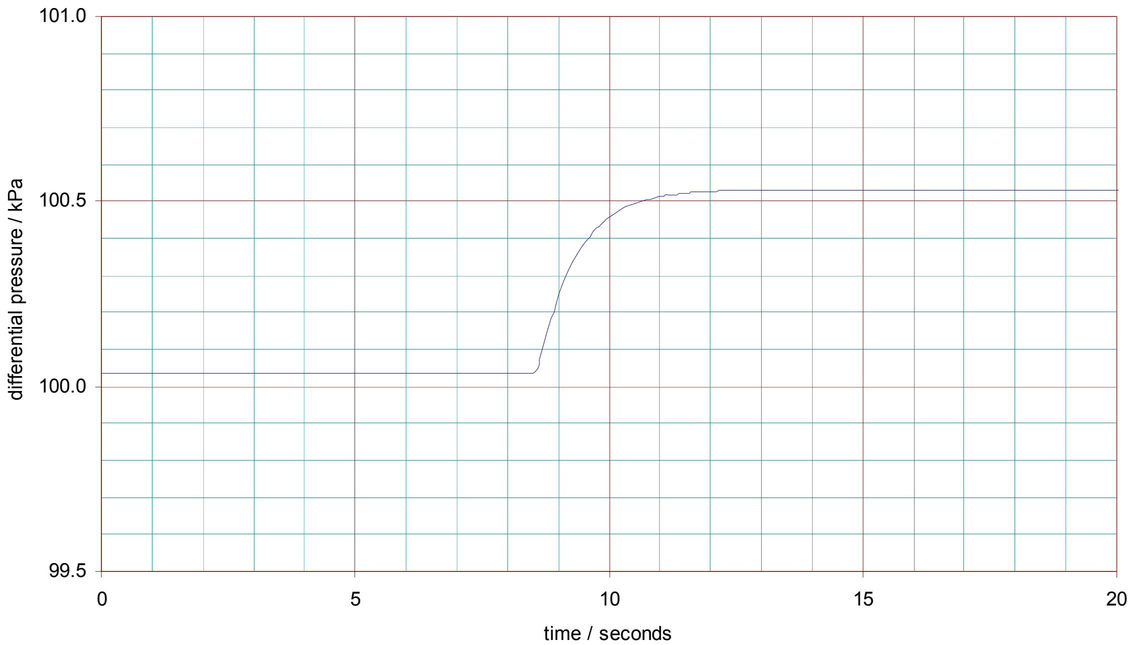

Figure 36 Divider: response to a step increase in applied mass – extra tank

10.4 DIVIDING RATIO

10.4.1 Method of determination

The divider's dividing ratio was determined at various line and differential pressures by comparison with the oil-lubricated twin-post device. The technique – which enabled direct comparison rather than indirect comparison via a transfer device – demanded a highly dextrous procedure to keep four piston-cylinder assemblies in proper state simultaneously. The oil-lubricated twin-post instrument was chosen for the work, rather than the gas-lubricated one, because its reduced inclination to 'bounce' and its lower fall-rate enabled equilibrium to be sustained for a longer period.

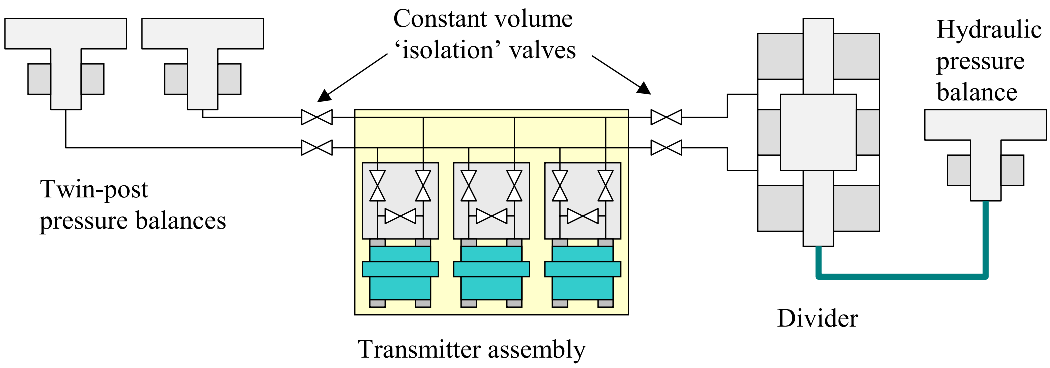

Figure 37 Determination of dividing ratio

The high- and low-pressure ports of the divider were connected to the twin-post pressure balances via an assembly containing differential pressure transmitters – used as an aid to establishing equilibrium – and constant volume valves to enable the divider and twin-post pressure balances to be isolated without introducing significant pressure changes (see Figure 37).

Before each calibration both generators were pressurised to the nominal line pressure and given sufficient time (>12 hours) to stabilise with motor-drive mechanisms running.

At the start of a calibration the twin-post pressure balances were isolated from the divider and cross-floated at the nominated line pressure; all the isolation valves were then opened and 'volumes adjusted' to re-establish correct piston height. The twin-post isolation valves were then closed and the mass on the hydraulic pressure balance adjusted to achieve a cross-float with the divider's rotating assembly. This process was repeated until all pistons (two twin-post, one hydraulic and the divider's rotating assembly) were falling at their correct rates, irrespective of the positions of the isolation valves.

The divider was isolated, mass applied to the twin-post *high* piston to generate differential pressure and the output of the differential pressure transmitter recorded. The twin-post piston-cylinders were then isolated, the divider's isolation valves opened and mass applied to the hydraulic pressure balance until the output of the transmitter equalled that recorded when connected to the twin-post. The isolation valves between generators were opened and final adjustments to volumes and masses made to ensure that all pistons were floating at their correct reference levels. The dividing ratio was then calculated by dividing the increase in the hydraulic pressure by the differential pressure calculated from the twin-post device. This process was repeated at a number of line and differential pressures.

10.4.2 Line and differential pressure dependency

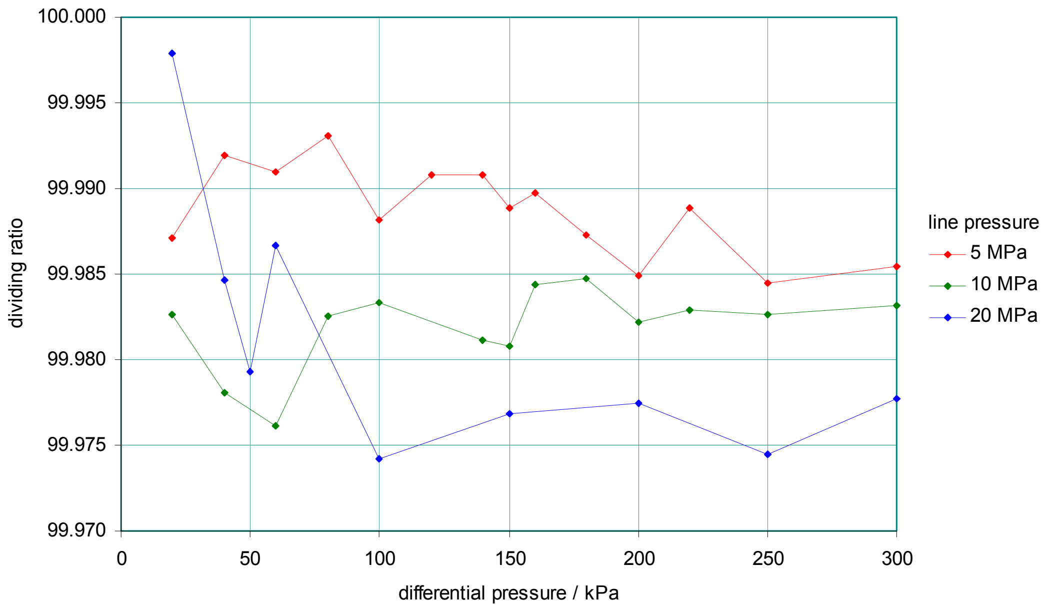

Figure 38 Variation in dividing ratio with line and differential pressure

Figure 38 shows the dividing ratio determined from measurements made over a range of line and differential pressures and how it varied with both. At low differential pressures the variations were small compared with the associated uncertainties but at higher differential pressures the systematic differences had some significance.

Figure 39 shows the residual errors in differential pressure which would result from using a single (mean) value for the dividing ratio.

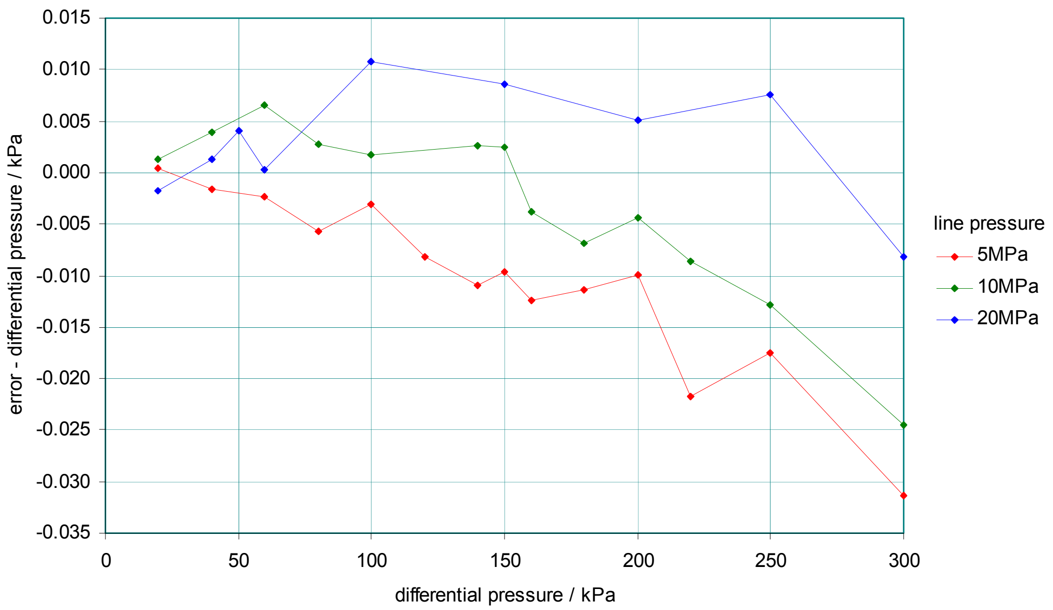

Figure 39 Residual errors in differential pressure from using a single dividing ratio

Applying corrections for the effect of line and differential pressure significantly reduced the errors. Assuming, from Figure 38 and to a first-order approximation, the dividing ratio to vary linearly with both line and differential pressure, it was expressed in the form:

$$R_D = R_o(1+\alpha\ dp)\ (1+\beta\ lp) \tag{42}$$

where R_D is the dividing ratio at a given line and differential pressure

R_o is the dividing ratio at zero line and differential pressure

α is a differential pressure dependent term

dp is the differential pressure

β is a line pressure dependent term

lp is the line pressure

Using an iterative process, residuals were minimised by incrementally varying values of R_o α and β from *arbitrary* initial values estimated from Figure 38. The final values, for this instrument, minimised the computed variation between measured and calculated values of differential pressure and were: R_o = *99.9945*, α = -1.5×10^{-7} kPa^{-1} and β = -7×10^{-6} MPa^{-1}, leading to the residuals shown in Figure 40.

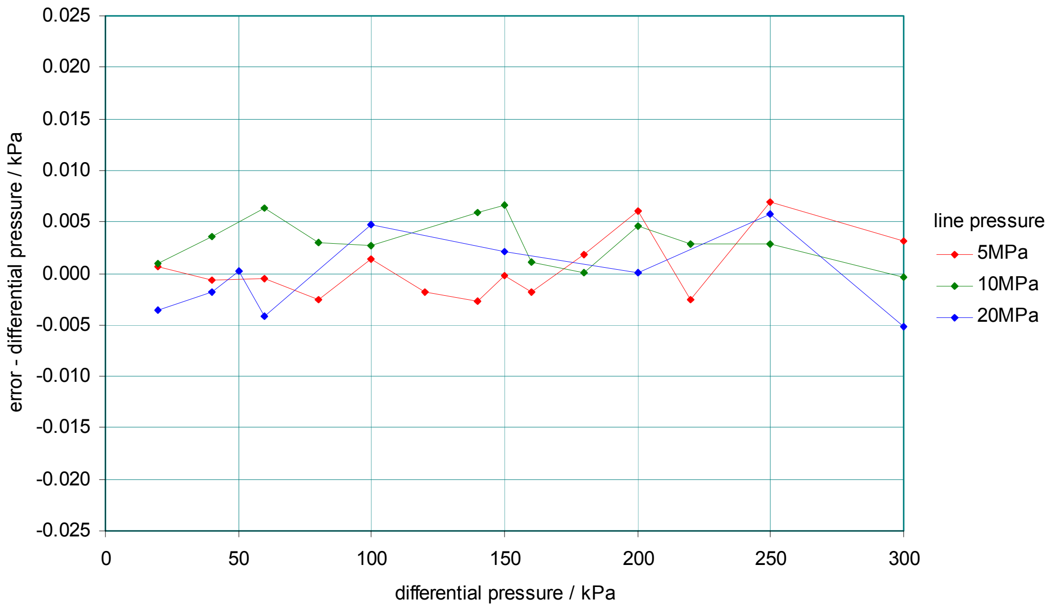

Figure 40 Residual errors after applying line and differential pressure corrections

10.4.3 Finite element analysis

Finite element techniques use knowledge of piston-cylinder design, geometry, clamping arrangements, dimensional data, the elastic properties of the materials and details of the pressure medium to iteratively compute flow and pressure gradients along the engagement length, changes in piston-cylinder gap profile, piston fall-rate and hence changes in effective area with pressure.

The empirically derived data in Figure 38 showed that, whilst the line and differential pressure effects on dividing ratio were significant, they were sufficiently small to question the potential benefits of using finite element techniques for further analysis; an attempt was made, however.

Using bespoke NPL software and data supplied by the manufacturer the variation in dividing ratio with line and differential pressure was computed. Figure 41 shows a dividing ratio broadly equivalent to the mean empirical value in Figure 38 although the line pressure effect is significantly less pronounced. Figure 42, however, shows that the computed dividing ratio changed significantly, consistent with simple geometry, when the assumed clearance of the divider's lower piston *C* (see Figure 3) was reduced from the upper to the lower bound suggested by the manufacturer (0.4 µm to 0.2 µm). This illustrated that the best data available was still inadequate to enable the line pressure dependency to be modelled sufficiently well.

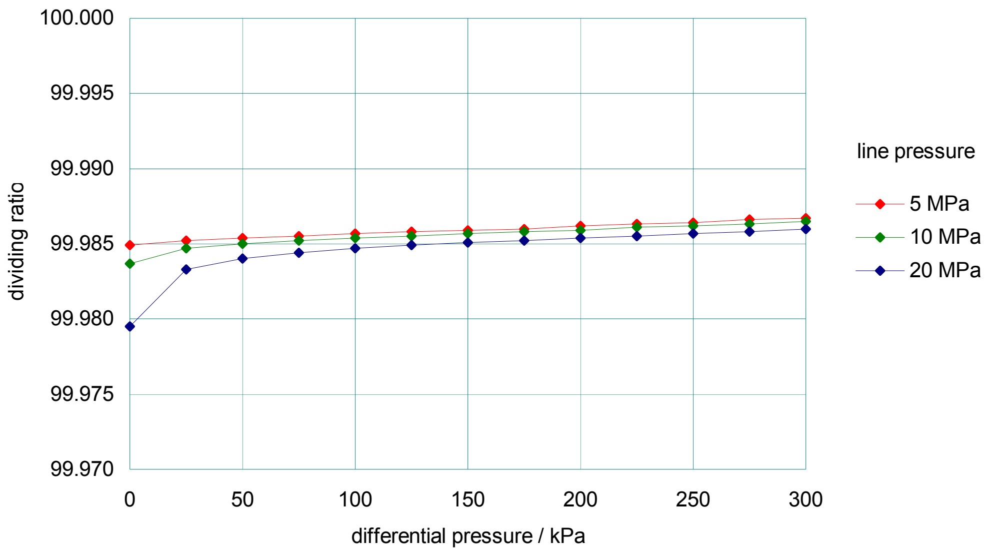

Figure 41 Dividing ratio computed using FEA

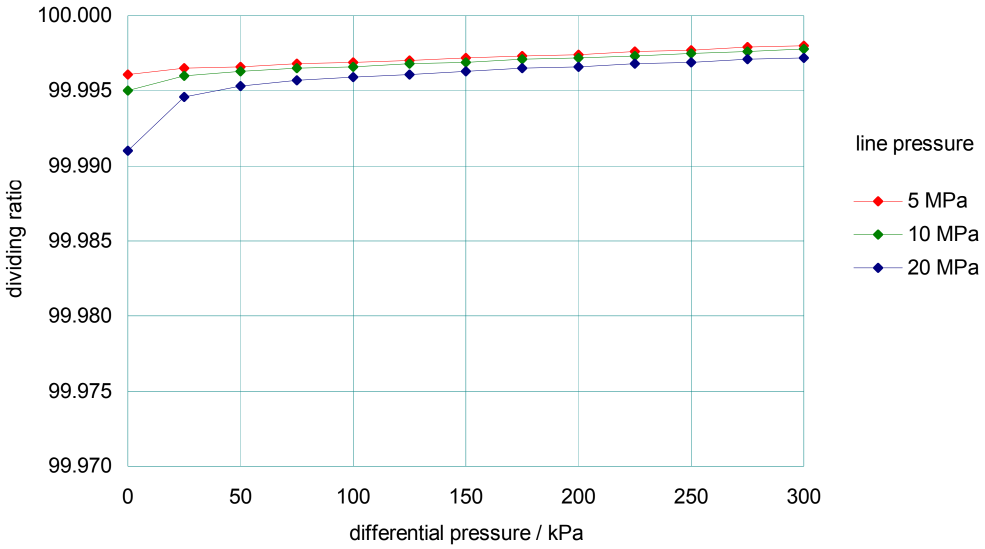

Figure 42 Dividing ratio computed with FEA – alternative piston-cylinder clearance

FEA is a powerful tool, and particularly good at predicting the effects of design changes, but the validity of its results depend very much on the precision and accuracy of the model used. The results shown in Figure 41 and Figure 42 had to be based on a number of approximations. For example the values used for Young's modulus and Poisson's ratio of the piston and cylinder materials could only be nominal – figures based on artefacts are generally not available – and the values used for the clearances between components were based on the manufacturers' tolerances rather than 'real' dimensional data.

To develop the divider's FEA model further, account would have to be taken of additional factors such as the elastic properties of the piston-linking mechanisms and the real geometric shape of the piston and cylinder. Whilst this could be done, the complexity of the model required to observe the comparatively subtle effects detected empirically was not considered to have significant potential benefit to the project – the empirical data certainly did not suggest a design weakness.

10.4.4 Temperature dependency

Unlike the twin-post devices, the divider does not come supplied with a value of temperature distortion coefficient which can be used to correct the generated differential pressure for changes in temperature.

To investigate temperature dependency, several thermometer probes were attached to the divider at locations which enabled the measurement of temperature as close as possible to the rotating assembly. The divider was placed in a temperature controlled housing and set to generate a differential pressure of 100 kPa and a line pressure of 10 MPa, leaving the hydraulic pressure balance and pressure transmitters outside the housing. Where pipework passed from one thermal environment to the other, it was kept horizontal to minimise temperature induced fluid head instability.

Figure 43 shows the temperature recorded over a five hour period during which the temperature of the enclosure, shown in black, was varied between 15°C and 25°C. The green lines show the corresponding temperatures of the divider; the higher temperatures were recorded by the thermometer probes mounted closest to the motor-drive. Figure 44 shows the change in generated differential pressure, measured with two transmitters, during the same period.

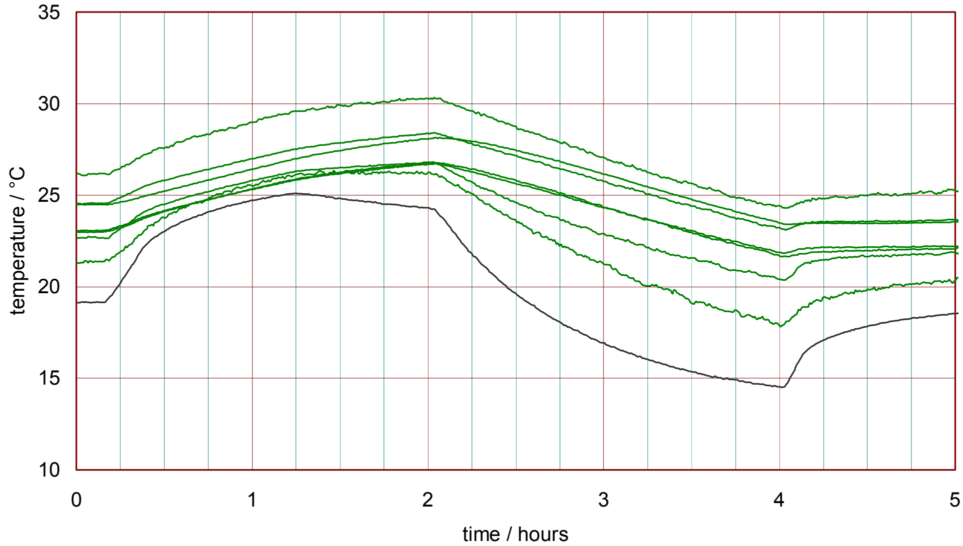

Figure 43 Divider temperature measurements

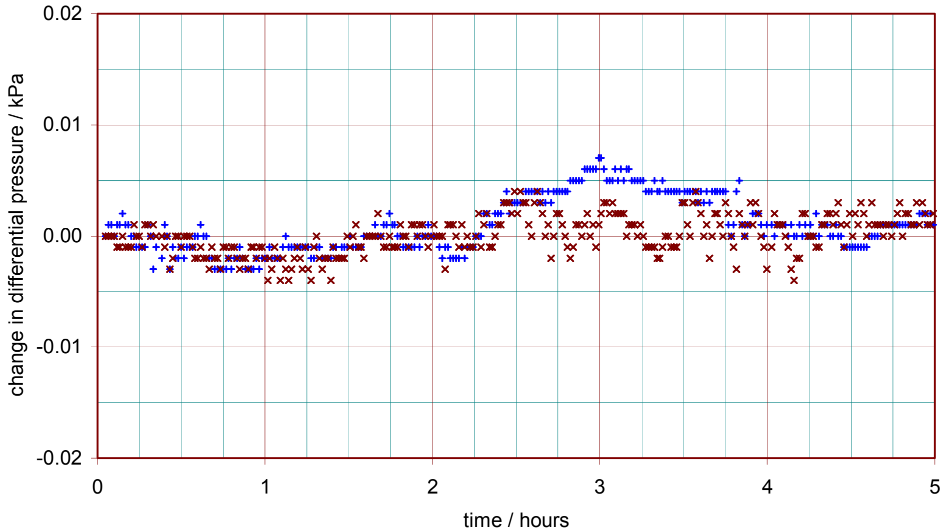

Figure 44 Differential pressure generated at different divider temperatures

When subjected to temperature changes of up to 10 °C the differential pressure changed by less than ±10 Pa and mostly less than ±5 Pa. (The difference between the outputs of the two transmitters was presumed to be caused by drift in one transmitter.). This represented a very small temperature coefficient and under normal laboratory conditions (typically 20°C ±1°C) would be quite insignificant.

10.4.5 Reproducibility of 'zero' differential pressure

When operating twin-post pressure balances, changes in the temperature differential between the piston-cylinders during a calibration results in a change in the 'zero' differential pressure generated between the start and end of a calibration run. The temperatures of the piston-cylinders are measured and a correction applied using the thermal expansion coefficient λ.

In the case of the divider, no corrections are made for factors which may potentially result in changes in the generation of 'zero differential pressure'. The zero differential pressure can, however, be checked at the beginning and end of each calibration run to confirm that a change has not occurred.

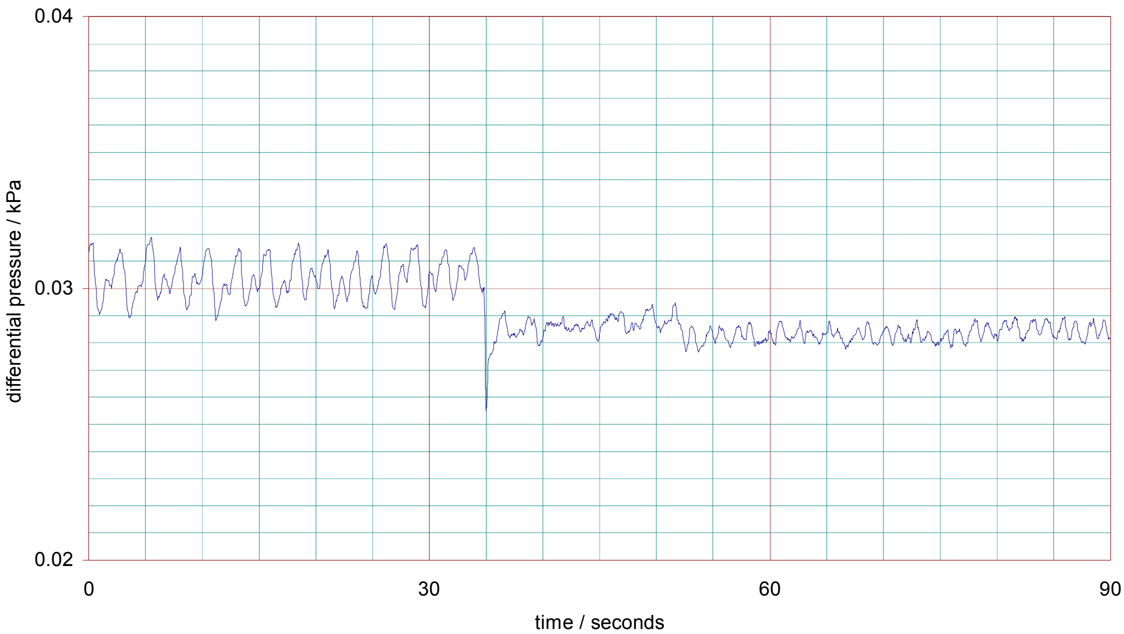

Figure 45 Plot illustrating the repeatability of the initial equilibrium

Figure 45 shows the result of the equalising valves being opened at the end of a typical calibration run which took 2½ hours, during which time the differential pressure was taken from 0 kPa up to 100 kPa and back in increments of 20 kPa. The plot shows a typical change in balance between the start and end of a calibration run – approximately 2 Pa.

11 UNCERTAINTY BUDGET – TWIN-POST

11.1 GENERAL

This section outlines the method used to estimate the measurement uncertainty associated with the generation of differential pressure using twin-post pressure balances. It lists *Type A* components of measurement uncertainty – those amenable to evaluation by statistical analysis of a series of observations – such as repeatability, and *Type B* components – those evaluated by other means – such as piston-cylinder effective area, acceleration due to gravity, air density etcetera. The magnitude of some components is clearly insignificant but they have been included, as it cannot be assumed that they will remain insignificant under different operational conditions.

The listing does *not* include all the factors which should be considered when calculating the *uncertainty in the measurement* associated with the calibration of an artefact using a generator (see Section 15).

11.2 ‘TYPE A’ COMPONENTS OF UNCERTAINTY

11.2.1 General

Differential pressure is an inherently analogue quantity; when generated using twin-post pressure balances the signal continually changes with the piston float-positions and also contains cyclic components at different frequencies due to the rotation of the pistons, piston bounce etcetera.

11.2.2 Differential pressure readings

The method chosen to observe generated differential pressure has a significant impact when estimating type A uncertainties. From the Figures in Sections 8.2 and 9.3 it can be seen that making a measurement by capturing a single ‘instantaneous’ data point is unlikely to be representative of the mean value of differential pressure, due to its oscillatory nature.

Closer agreement between readings was achieved when measurements were obtained by calculating the *mean* of successive ‘instantaneous’ values of differential pressure, sampled at a frequency of about 10 Hz - 20 Hz and over an interval greater than that of the oscillatory period. The repeatability of measurements was, obviously, highly dependent upon the stability of the differential pressure generator but also the tolerances adopted for its operation, such as piston float-position and angular velocity.

Maximum repeatability was obtained when measurements were taken with the pistons as close as possible to their reference levels and rotating close to prescribed angular velocities. Where necessary, piston bounce was allowed time to decay and measurements were avoided when any spurious pulses – for example caused by the action of the motor-drive – were evident. The time period over which a measurement was recorded was chosen to be at least twice as long as the lowest frequency component observed.

Observing the output of a differential pressure transmitter using the digital display of a voltmeter did not give sufficient resolution as the oscillations in pressure caused the least significant digits to change too rapidly to be of use.

11.2.3 Real-time graphical display and data capture

The real-time graphical display and data capture system (see Section 3.2.5), plotting differential pressure vs time, was used to determine the best moment to capture a representative set of data to include all frequency components. The sensitivity of the display was high, enabling subtle changes in generated differential pressure to be observed in the presence of signal oscillations and noise – effects that would be lost in a digital display.

11.2.4 'Type A' evaluation of standard uncertainty

To estimate the uncertainty the mean of the individual readings of differential pressure q was first calculated:

$$\bar{q} = \frac{1}{n}\sum_{j=1}^{n} q_j \tag{43}$$

From the sample of measurements an estimate was made of the standard deviation of the whole population:

$$s(q_j) = \sqrt{\frac{1}{(n-1)}\sum_{j=1}^{n}(q_j - \bar{q})^2} \tag{44}$$

The estimated standard deviation of the *uncorrected* mean was then calculated by:

$$s(\bar{q}) = \frac{s(q_j)}{\sqrt{n}} \tag{45}$$

By observing the output of transmitters graphically and in real-time, and only taking measurements when good pressure stability coincided with both pistons being at their correct float-position, it was possible to achieve a value of less than a few pascals. This required tolerances in float-position to be set at a much tighter level (±0.05 mm) than would be practicable during a calibration however, demanding an unrealistic number of attempts. In normal (good) calibration practice a tolerance of ±0.25 mm is considered to be realistic.

11.3 'TYPE B' COMPONENTS OF UNCERTAINTY

11.3.1 Mass applied to generate differential pressure – *dpm*

The uncertainties associated with the determination of mass values are predominantly systematic in nature. Thus the uncertainty in the applied mass was calculated by taking the arithmetic sum of the uncertainty of each individual weight rather than by quadrature summation.

A calibration certificate for a mass set will typically show uncertainties between about ±3 ppm and ±10 ppm of the mass value (at coverage factor $k = 2$) and probably higher for denominations less than 1 g. Best likely uncertainty in masses due to drift is about ±2 ppm of the mass value per year but masses used to generate differential pressure are generally subjected to relatively harsh treatment – frequently being placed on, and removed from, rotating mass stacks and occasionally dropped on the bench, floor or even oily surfaces. Historical data can be used to estimate the value of drift but it is likely to be considerably more than ±2 ppm of mass value and setting both the upper and lower limits at ±10 ppm is more realistic.

In calculating the standard uncertainty a normal distribution was assumed for the calibration data and a rectangular distribution for the drift in mass value.

11.3.2 Density of air – ρ_a

The density of air is generally calculated from knowledge of ambient atmospheric pressure, temperature and relative humidity using an equation which inevitably makes a number of assumptions (for example it is not generally practical to measure the air's composition).

The value for the air density used was assumed to be constant for the duration of a calibration (see Section 5.2) and the uncertainty estimated was ±0.05 kg m^{-3}. This equates to an uncertainty in differential pressure of approximately ±4 ppm. This was assumed to represent the limits of a rectangular distribution and a divisor of √3 was therefore used to calculate the standard uncertainty.

11.3.3 Density of the mass applied to generate differential pressure – ρ_m

This value is used in the calculation of the correction factor ϕ which compensates for differences between the density of the material and an assumed density of 8000 kg m^{-3} (see Section 5.2).

Without having the density of the masses determined, a typical value for the uncertainty in the density of a stainless steel mass is approximately ±200 kg m^{-3}. This was assumed to represent the limits of a rectangular distribution and a divisor of √3 was therefore used to calculate the standard uncertainty which equates to less than ±1 ppm of differential pressure.

11.3.4 Acceleration due to gravity – g

The uncertainty in the value of gravitational acceleration will depend upon the method used for its determination. A pressure calibration laboratory will generally have its local value determined by a geological institution, in which case a typical value for uncertainty would be $\pm 2 \times 10^{-5}$ m s^{-2} ($k = 2$).

11.3.5 Effective area of the '*high*' piston-cylinder – A_{oh}

The uncertainty in the effective area of the *high* piston-cylinder is obtained by calibration and will depend upon where the piston-cylinder was calibrated, against which standard and how it performed during the calibration. Typical values will range from around ± 25 ppm to ±100 ppm of effective area ($k = 2$). The drift in effective area was estimated to be typically 6 ppm per year.

In calculating the standard uncertainty a normal distribution was assumed for the calibration data and a rectangular distribution for the drift in effective area.

11.3.6 Pressure dependent term for the '*high*' piston-cylinder area – α_{oh}

The uncertainty in the pressure dependent term is given on the calibration certificate along with the effective area (see Section 11.3.5). Typical values will be about $\pm 0.3 \times 10^{-6}$ MPa^{-1} ($k = 2$).

11.3.7 Line pressure at which the initial cross-float is achieved – P_{ho}

A separate uncertainty budget is required to estimate the uncertainty in the pressure at which the initial cross-float is achieved. A large uncertainty (100s of parts per million) will have negligible effect on the overall uncertainty in generated differential pressure however, so there is little point in producing a comprehensive work.

11.3.8 Nominal value of differential pressure used in the calculation of area – *dp*

The calculation of differential pressure is, to a small degree, recursive. This demands either an iterative approach or the use of a nominal value. Whilst the latter attracts a higher uncertainty than the former, even the higher uncertainty it is negligible. This is because, in the differential pressure equation, the differential pressure value is multiplied by the pressure dependent term, which is typically only 1×10^{-6} MPa^{-1}.

11.3.9 Temperature coefficient of the piston-cylinders – λ

An uncertainty value of $\pm 0.5 \times 10^{-6}$ °C^{-1} was supplied, by the manufacturers, for the temperature coefficient of the tungsten carbide. This corresponds to an uncertainty of $\pm 0.7 \times 10^{-6}$ °C^{-1} in the value of λ, the temperature coefficient of the piston-cylinder combination. As with most such values, they are not based on measurements of pistons or cylinders but alternatively-shaped specimens made specifically for determining such characteristics. The uncertainty in λ for a piston-cylinder is therefore likely to be larger than suggested and a value of $\pm 1 \times 10^{-6}$ °C^{-1} was assumed.

Figure 46 gives additional empirical evidence that the value of temperature coefficient assumed is reasonable. The generated differential pressure was measured whilst the temperature of one piston-cylinder was changed, and the graph shows the change in differential pressure as a function of temperature change. The gradient of this line is equivalent to the temperature coefficient and was calculated to be 9.12×10^{-6} °C^{-1} – close to the assumed value of 9×10^{-6} °C^{-1}.

The apparent hysteresis is thought to be due to the piston-cylinder units responding to changes in ambient temperature faster than the thermometers supposedly measuring their temperatures (see Section 11.3.10).

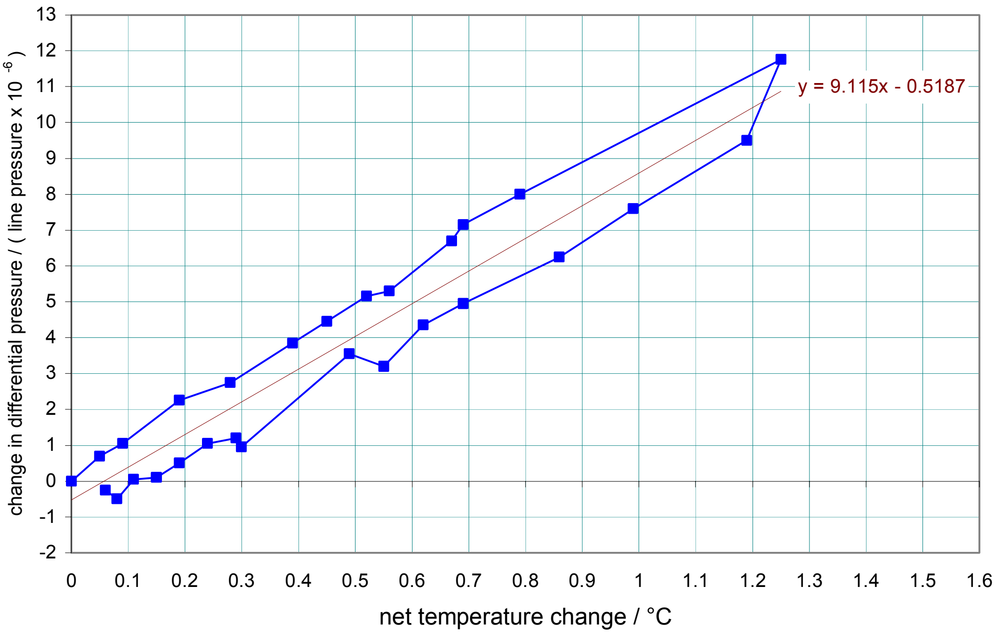

Figure 46 Empirical determination of temperature coefficient

11.3.10 Piston-cylinder temperatures – t_h, t_l, Δt_h and Δt_l

It is felt that the uncertainty in the measurement of piston-cylinder temperatures (t_h and t_l) can at best be estimated to within ±0.1 °C (assuming that the uncertainty in the thermometer readings is much less). This presumes good environmental conditions but appreciates that the positions at which the temperatures are measured are not necessarily in very close proximity to the piston-cylinders and also that a single thermometer cannot provide a properly integrated value of a piston-cylinder temperature. It also assumes that systems have reached general thermal equilibrium, for example after switching on a motor-drive (this can take at least one working day and elevate temperatures by up to about 3 °C).

It can be argued that the uncertainty in temperature *changes* (Δt_h and Δt_l) – that is differences between temperatures recorded during the initial cross-float and those recorded during the pressure measurement – may be a fraction less through systematic errors cancelling out. Any such reduction in uncertainty, however, will be insignificant alongside the temperature integration problems described above and in practice the uncertainty in the estimation of temperature change will closely equal the uncertainty in a single measurement.

It has been suggested that the relative change in piston-cylinder temperatures can be inferred by measuring the temperature of just one 'measuring post' (into which the cylinder is fitted) and the difference in balance between the start and end of a calibration run (eg from necessary changes in trim masses or observed transmitter output). Similarly, it has been argued that 'perfect' reproduction of the initial cross-float gives confidence that the temperature difference has not changed during the calibration. This argument is sometimes used to compute temperature changes with uncertainties lower than likely from practical temperature measurements of the system. It does, however, represent a simplistic model, which effectively assumes that at no stage did temperatures lie outside the bounds of the two measurements – an assumption which is undoubtedly not always valid.

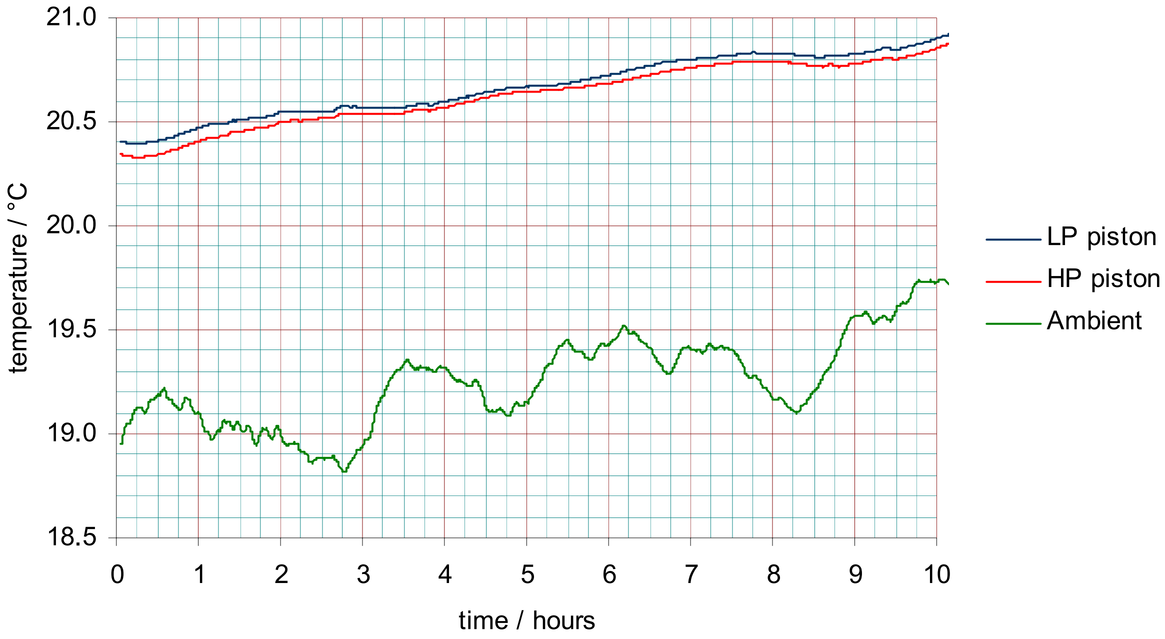

Figure 47 Thermometers measuring piston-cylinder and ambient temperatures

Figure 47 shows the output from three thermometers – one in each of the measuring posts on the oil-lubricated twin-post device and the other in air level with the piston-cylinders. The drive motor was in operation and had been switched on the previous day to ensure thermal equilibrium. As is normal practice with these devices, it was used with its back removed to allow motor heat to escape – to limit temperature gradients. All three thermometers had a thermal time constant of just a couple of seconds and the one measuring ambient air temperature therefore shows significantly more detail than normally seen on conventional thermographs (which have a time constant greater than 1 hour).

Over the 10 hour period shown, it can be seen that the mean room temperature increased by about 0.5 °C and in a fashion not untypical of the air in a well temperature controlled laboratory. The increase was closely mirrored by the thermometers in the measuring posts, keeping the motor-induced difference in temperature to about 1.5 °C. The pressure (nominally 10 MPa line and 0 kPa differential) was not changed during the temperature measurement period.

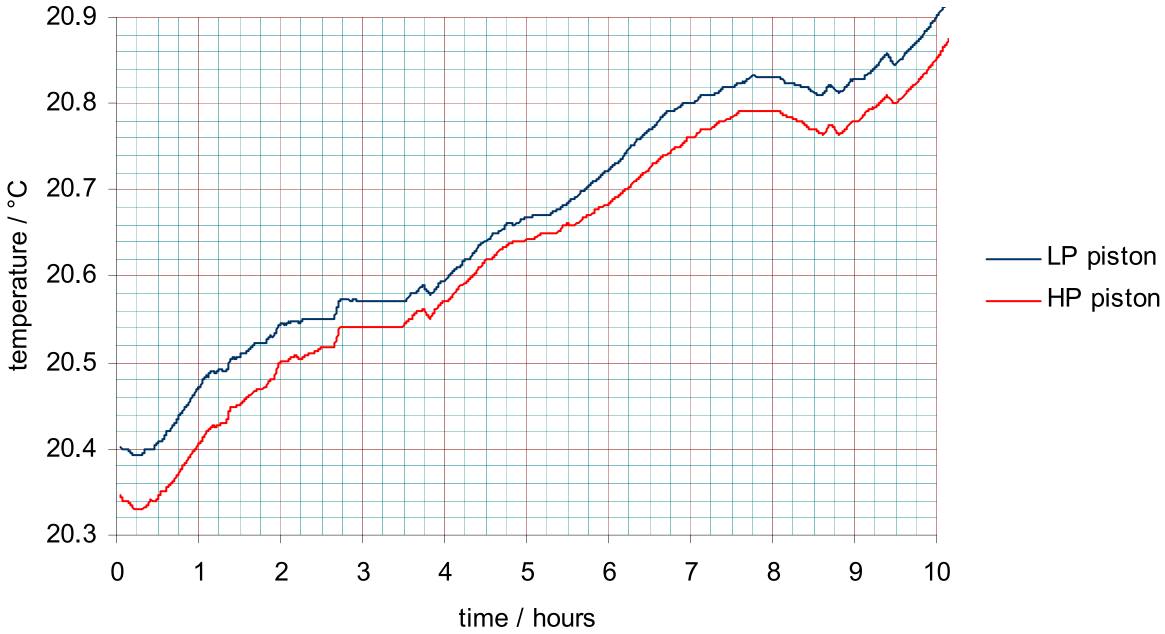

Figure 48 Expanded view of piston-cylinder temperatures

Figure 48 shows the measuring post traces with increased sensitivity on the vertical scale, highlighting that the *difference* between the measuring post temperatures *changed* by 0.05 °C. When in normal use, with pressures being altered and staff standing close by, the real changes in the piston-cylinder temperature differences could easily approach double this value, that is 0.1 °C.

As mentioned before, part of the reason for this is that a single thermometer, no matter how accurate, cannot properly integrate piston-cylinder temperature across its dimensional extremities. Also the time taken for a piston-cylinder to respond to changes in ambient temperature will be different to that of the thermometer – which is mounted some distance away. As ambient temperature changes, the relationship between piston-cylinder and thermometer temperature will vary.

To illustrate this, an experiment was conducted using the oil-lubricated twin-post device – with thermometers positioned in the piston mounting posts as described in Section 9.1 – whilst balanced at a line pressure of 10 MPa. A small heat source (about 60 W) was directed at the weight stack of the low pressure piston-cylinder until its temperature was about 1 °C greater than that of the high pressure piston-cylinder. The heat source was then switched off and the low-pressure piston-cylinder allowed to return to ambient temperature.

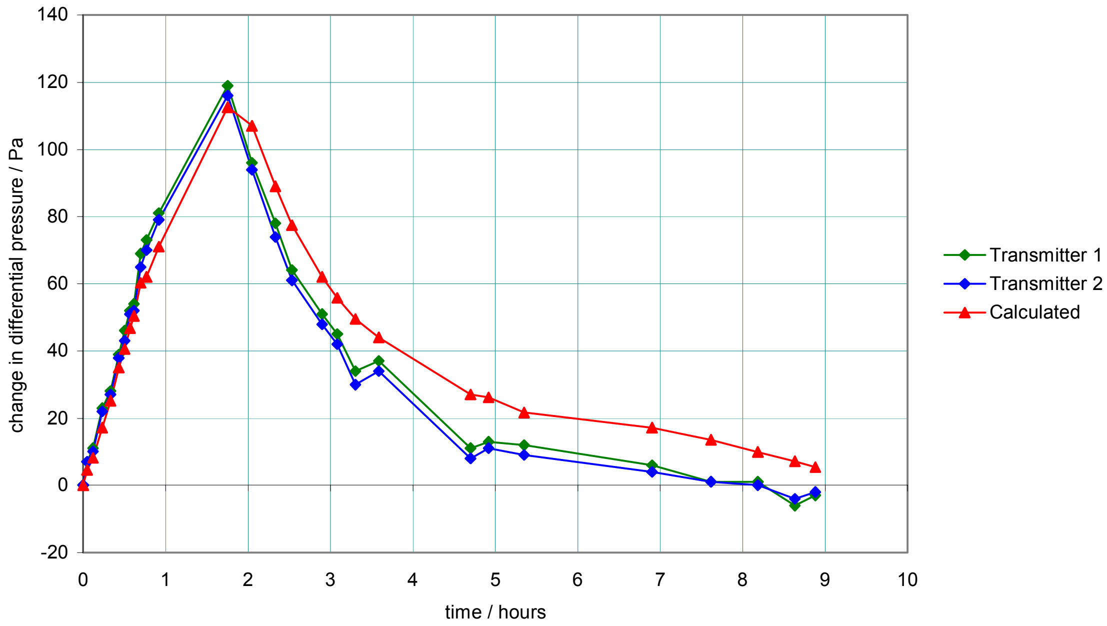

Figure 49 Measured and calculated effect of changes in piston-cylinder temperature

During the experiment the generated differential pressure was measured with two transmitters and the temperatures of the thermometers in the piston mounting posts were recorded. Figure 49 shows the differences between the measured differential pressure and those calculated by taking piston-cylinder temperature changes into account.

The phase shifts between the empirical and calculated differential pressures show that, in this particular design, the piston-cylinder units respond to changes in ambient temperature faster than the thermometers supposedly measuring their temperatures.

Similar measurements were not made on the gas-lubricated twin-post device but the effect should be expected to be comparable or potentially greater because the thermometers were further away still from the piston cylinder. This would also be the general case where two single gas-lubricated gas-operated pressure balances are used in tandem.

In a separate experiment to establish relative thermal time constants, several thermometers were attached at various locations to the oil-lubricated twin-post (including the piston-cylinder measuring points). The device was placed in a temperature controlled enclosure and held at nominally 15 °C; the controlled temperature was then adjusted to 19 °C. Temperature measurements made throughout the transition are shown in Figure 50.

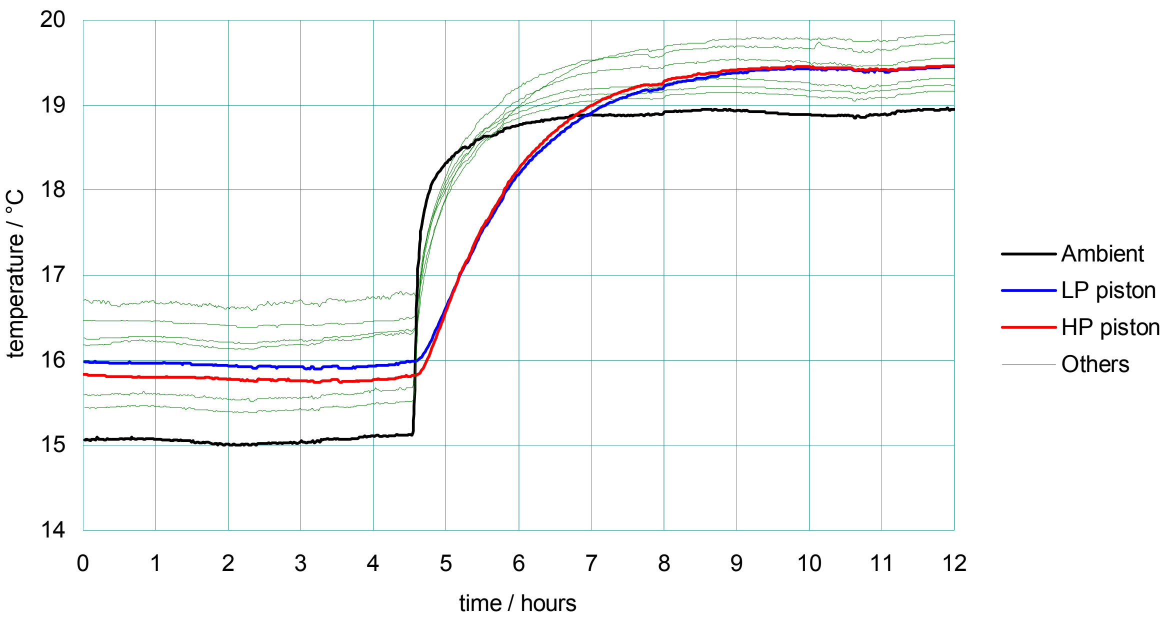

Figure 50 Response to an increase in temperature

As might be assumed for more massive items, the temperatures measured in the piston mounting posts changed at a slower rate than at other locations. The red and blue lines represent mounting post temperatures and suggest a time constant of around 1.5 hours. If such a device is exposed to a significant temperature change it will take up to about 5 hours at the new temperature before the most precise measurements can be made.

Similar measurements were not made on the gas-lubricated twin-post device but the effect should be expected to be less because its thermal mass was less.

11.3.11 Tilt

The devices were levelled, using their adjustable feet, to ensure the axis of the piston-cylinder was vertical. This was achieved on the oil-lubricated pressure balance by placing a spirit level on top of the weight stack and making measurements at several intervals throughout a 360° rotation of the piston. The top surface of the cylinder was used to level the gas-lubricated device (presuming the top surface to be adequately perpendicular to the piston-cylinder axis).

If the piston axis is inclined at an angle θ to the vertical, then the downward force acting along the piston axis will be:

$$W \cos \theta \tag{46}$$

where W is the vertical downward force.

It is estimated that, when using a good spirit level, a piston can typically be levelled to within 5 minutes of arc. This corresponds to a maximum error due to tilt of approximately 1 ppm of differential pressure. Strictly, this uncertainty has a one-sided (asymmetric) distribution; an offset of -0.5 ppm of differential pressure was applied (half the maximum error due to tilt) and an uncertainty of ±0.5 ppm of differential pressure adopted, with a rectangular distribution.

Whilst the magnitude of the uncertainty, when the instrument is levelled to this degree, is insignificant, the point is made to illustrate the nature of the calculation required should the tilt be greater than in this example.

11.3.12 Fluid head

The equation used to calculate differential pressure assumes that both pistons are *floating* at their correct reference levels. To accommodate non-perfect simultaneous convergence of pistons and reference levels however, and also to allow sufficient time to make differential pressure measurements, tolerances in the piston float-positions need to be established (see Sections 8.2.6 and 9.3.7)

The pressure due to this tolerance-dependent fluid head (H) for each piston may be calculated from:

$$H = h\left(\rho_f - \rho_a\right) g \tag{47}$$

where h is the height above the reference level

ρ_f is the density of the pressure generating fluid

ρ_a is the density of air

g is the acceleration due to gravity

The density of the fluid (see Section 7) can be calculated by:

$$\rho_2 = \frac{T_1\ \rho_1\ P_2}{T_2\ P_1} \tag{48}$$

By combining equations (47) and (48) it can be estimated that a change in piston height will result in a change in pressure of approximately 120×10^{-6} m^{-1}. If the float-positions for each of the two pistons is repeated to within a tolerance of ±0.25 mm, the total uncertainty in differential pressure due to fluid head will be approximately ±0.04 ppm of line pressure.

11.3.13 Piston taper

Sections 8.2.7 and 9.3.8 discuss changes in generated differential pressure with vertical displacement of a piston of around 1 ppm of line pressure per millimetre. The uncertainty resulting from this will depend upon the tolerance limits set for piston float-positions and the degree of piston taper. To obtain a realistic uncertainty value it is therefore necessary to make quantitative measurements of piston taper for both *high* and *low* piston-cylinders. The maximum possible change in differential pressure can then be estimated using the tolerances set for the piston float-positions during a calibration.

If the float-position for each piston is within ±0.25 mm of the reference level and the effect of piston taper is taken to be 1 ppm of line pressure per millimetre (on each piston-cylinder), the uncertainty in differential pressure due to piston taper will be approximately ±0.35 ppm of line pressure.

11.3.14 Difference in height between transmitter and generator

Section 7 shows that the additional differential pressure due to mounting the instrument being calibrated at a height other than the reference of the differential pressure generator is approximately 0.1 ppm of differential pressure per millimetre. There is no clear convention for ascribing a datum level to a transmitter and generally they are not physically marked. An uncertainty of ±50 mm is therefore appropriate when adjusting the transmitters height to the datum level of the generator; this corresponds to ±5 ppm of the differential pressure – of marginal significance.

11.3.15 Angular velocity

Section 9.3.3 (oil-lubricated twin-post) shows that variations in angular velocity can cause significant changes in differential pressure – in this case very approximately 0.1 ppm of line pressure per revolution per minute. When calculating uncertainties it is thus necessary to define the angular velocity range within which measurements will be taken and hence the corresponding uncertainty. If a motor-drive is used, the range will be insignificantly small; if a motor-drive is not used the range will depend on the operating time allowed to make pressure measurements and also the users ability to estimate angular velocity values. If they are estimated by eye, the range will probably be around 10 rpm. During this project it was shown that non-motor-drive measurements could be made within an angular velocity tolerance of about ±1 rpm by using a laser tachometer.

11.3.16 Resolution of cross-float

The resolution in the cross-floating process depends, to a certain extent, upon the criteria used to judge hydrostatic equilibrium. During this project hydrostatic equilibrium was taken to be when the operation of a constant volume valve between the two pressure balances made no difference to the fall-rates of the pistons. In cases where the fall-rate was negligible equilibrium was confirmed by a reversal of fall-rates.

As an aid to achieving hydrostatic equilibrium a differential pressure transmitter, set to give a high resolution (<0.1 Pa), was used as a null indicator. The mass on one piston was adjusted until the transmitter output with the equalising valve closed was similar to that with the equalising valve open. The equalising valves were then opened and the fall-rates measured to confirm hydrostatic equilibrium.

It should be noted that use of the transmitter was to speed the process of achieving proper cross-floating conditions; it did *not* provide a higher cross-float resolution; the transmitter cannot, for example, differentiate between ‘perfect’ cross-float conditions and exactly compensating piston height and temperature errors.

With the use of capacitive sensors and associated graphical software for measuring piston fall-rates, cross-floats were achieved with a resolution of <5Pa. Without the use of similar ancillary apparatus the expected resolution would be poorer.

11.3.17 Repeatability of cross-float

At the end of a calibration run (when the masses are as they were for the initial cross-float) the equalising valves between the twin pressure balances are opened and a check made to determine the degree to which hydrostatic equilibrium still exists. A component has to be added to the uncertainty budget to take into account the deviations from the initial equilibrium after correcting for piston-cylinder temperature changes.

This component is estimated from repeated cross-floats, using the differential pressure equation (25) to calculate the deviations from the initial cross-float equilibrium, taking required mass changes and the latest temperatures into account. The deviations allow the component uncertainty to be calculated and also a tolerance within which subsequent repeat cross-floats should fall. As it is not possible to determine when the change in balance occurred, or the rate at which the change occurred, a rectangular distribution is assumed.

It was found that when a calibration was conducted under stable conditions the cross-float could often be repeated to within a few pascals. If conditions were not stable, however – for example if insufficient time was allowed for temperature stabilisation – changes of tens of pascals were recorded.

11.4 COMBINED STANDARD UNCERTAINTY

The differential pressure equation derived in Section 5.7 of this report shows the functional relationship between the input quantities and the generated differential pressure.

$$dp = \frac{dpm\left[1-(\rho_a-1.2)\left(\frac{1}{\rho_m}-\frac{1}{8000}\right)\right]\left(1-\frac{\rho_a}{8000}\right)g}{A_{oh}\left(1+\alpha_h\,(p_{ho}+dp)\right)\left(1+\lambda\,(t_h-20)\right)} + p_{ho}\left[\frac{(1+\alpha_h p_{ho})\left(1+\lambda\,(t_{ho}-20)\right)}{\left(1+\alpha_h(p_{ho}+dp)\right)\left(1+\lambda\,(t_{ho}+\Delta t_h-20)\right)}-\frac{\left(1+\lambda\,(t_{lo}-20)\right)}{\left(1+\lambda\,(t_{lo}+\Delta t_l-20)\right)}\right] \tag{49}$$

This can be expressed as:

$$dp = dpa + dpb \tag{50}$$

where *dpa* is the 'differential pressure proportional' part of the equation:

$$dpa = \frac{dpm\left[1-(\rho_a-1.2)\left(\frac{1}{\rho_m}-\frac{1}{8000}\right)\right]\left(1-\frac{\rho_a}{8000}\right)g}{A_{oh}\left(1+\alpha_h\,(p_{ho}+dp)\right)\left(1+\lambda\,(t_h-20)\right)} \tag{51}$$

and *dpb* is the 'line pressure proportional' part of the equation:

$$dpb = p_{ho}\left[\frac{(1+\alpha_h p_{ho})\left(1+\lambda\,(t_{ho}-20)\right)}{\left(1+\alpha_h(p_{ho}+dp)\right)\left(1+\lambda\,(t_{ho}+\Delta t_h-20)\right)}-\frac{\left(1+\lambda\,(t_{lo}-20)\right)}{\left(1+\lambda\,(t_{lo}+\Delta t_l-20)\right)}\right] \tag{52}$$

Calculating the uncertainty in 'line pressure proportional' and 'differential pressure proportional' terms separately results in an uncertainty statement valid for the entire range of differential and line pressure.

11.4.1 Sensitivity coefficients

Once the standard uncertainties of the input quantities have been found the combined standard uncertainty of the output quantity can be calculated using the equation:

$$u_c(y) = \sqrt{\sum_{i=1}^{N} {c_i}^2 u^2(x_i)} \qquad (53)$$

where c_i , the sensitivity coefficient, is the partial derivative $\partial f / \partial x_i$

11.4.2 Symbolic representation of the partial derivatives of *dpa*

11.4.2.1 Mass applied to generate the differential pressure – *dpm*

$$\frac{\partial\ dpa}{\partial\ dpm} = \left[1-(\rho_a - 1.2)\left(\frac{1}{\rho_m} - \frac{1}{8000}\right)\right]\left(1 - \frac{1}{8000}\ \rho_a\right)\frac{g}{A_{oh}\left(1+\alpha_h\ (p_{ho}+dp)\right)\left(1+\lambda\ (t_h - 20)\right)} \qquad (54)$$

11.4.2.2 Density of air – ρ_a

$$\frac{\partial\ dpa}{\partial\ \rho_a} = \frac{-1}{8000}\ dpm\left[1-(\rho_a - 1.2)\left(\frac{1}{\rho_m} - \frac{1}{8000}\right)\right]\ \frac{g}{A_{oh}\left(1+\alpha_h\ (p_{ho}+dp)\right)\left(1+\lambda\ (t_h - 20)\right)} \qquad (55)$$

11.4.2.3 Density of the mass applied to generate differential pressure – ρ_m

$$\frac{\partial\ dpa}{\partial\ \rho_m} = dpm\ \frac{(\rho_a - 1.2)}{{\rho_m}^2}\left(1 - \frac{1}{8000}\ \rho_a\right)\frac{g}{A_{oh}\left(1+\alpha_h\ (p_{ho}+dp)\right)\left(1+\lambda\ (t_h - 20)\right)} \qquad (56)$$

11.4.2.4 Acceleration due to gravity – *g*

$$\frac{\partial\ dpa}{\partial\ g} = dpm\ \left[1-(\rho_a - 1.2)\left(\frac{1}{\rho_m} - \frac{1}{8000}\right)\right]\ \frac{\left(1 - \frac{1}{8000}\ \rho_a\right)}{A_{oh}\left(1+\alpha_h\ (p_{ho}+dp)\right)\left(1+\lambda\ (t_h - 20)\right)} \qquad (57)$$

11.4.2.5 Effective area of the high piston-cylinder – A_{oh}

$$\frac{\partial\ dpa}{\partial\ A_{oh}} = -dpm\left[1-(\rho_a-1.2)\left(\frac{1}{\rho_m}-\frac{1}{8000}\right)\right]\left(1-\frac{1}{8000}\ \rho_a\right)\frac{g}{A_{oh}{}^2\big(1+\alpha_h\ (p_{ho}+dp)\big)\ \big(1+\lambda\ (t_h-20)\big)} \tag{58}$$

11.4.2.6 Pressure dependent term for the high piston-cylinder – α_h

$$\frac{\partial\ dpa}{\partial\ \alpha_h} = -dpm\left[1-(\rho_a-1.2)\left(\frac{1}{\rho_m}-\frac{1}{8000}\right)\right]\left(1-\frac{1}{8000}\ \rho_a\right)\ \frac{g}{A_{oh}\big(1+\alpha_h\ (p_{ho}+dp)\big)^2\big(1+\lambda\ (t_h-20)\big)}\ (p_{ho}+dp) \tag{59}$$

11.4.2.7 Temperature of the high piston-cylinder – t_h

$$\frac{\partial\ dpa}{\partial\ t_h} = -dpm\left[1-(\rho_a-1.2)\left(\frac{1}{\rho_m}-\frac{1}{8000}\right)\right]\left(1-\frac{1}{8000}\ \rho_a\right)\ \frac{g}{A_{oh}\big(1+\alpha_h\ (p_{ho}+dp)\big)\ \big(1+\lambda\ (t_h-20)\big)^2}\ \lambda \tag{60}$$

11.4.2.8 Line pressure at which the initial cross-float is achieved – P_{ho}

$$\frac{\partial\ dpa}{\partial\ P_{ho}} = -dpm\left[1-(\rho_a-1.2)\left(\frac{1}{\rho_m}-\frac{1}{8000}\right)\right]\left(1-\frac{1}{8000}\ \rho_a\right)\ \frac{g}{A_{oh}\big(1+\alpha_h\ (p_{ho}+dp)\big)^2\big(1+\lambda\ (t_h-20)\big)}\ \alpha_h \tag{61}$$

11.4.2.9 Nominal value of differential pressure used in the calculation of area – dp

$$\frac{\partial\ dpa}{\partial\ dp} = -dpm\left[1-(\rho_a-1.2)\left(\frac{1}{\rho_m}-\frac{1}{8000}\right)\right]\left(1-\frac{1}{8000}\ \rho_a\right)\ \frac{g}{A_{oh}\big(1+\alpha_h\ (p_{ho}+dp)\big)^2\big(1+\lambda\ (t_h-20)\big)}\ \alpha_h \tag{62}$$

11.4.2.10 Temperature coefficient of the piston-cylinders – λ

$$\frac{\partial\ dpa}{\partial\ \lambda} = -dpm\left[1-(\rho_a-1.2)\left(\frac{1}{\rho_m}-\frac{1}{8000}\right)\right]\left(1-\frac{1}{8000}\ \rho_a\right)\ \frac{g}{A_{oh}\big(1+\alpha_h\ (p_{ho}+dp)\big)\ \big(1+\lambda\ (t_h-20)\big)^2}\ (t_h-20) \tag{63}$$

11.4.3 Symbolic representation of the partial derivatives of *dpb*

11.4.3.1 Line pressure at which the initial cross-float is achieved – P_{ho}

$$\frac{\partial\ dpb}{\partial\ p_{ho}} = \left(1+\alpha\ \ p_{ho}\right)\cdot\frac{\left(1+\lambda\ \left(t_{ho}-20\right)\right)}{\left(1+\alpha_h\ \left(p_{ho}+dp\right)\right)\left(1+\lambda\ \left(t_{ho}+\Delta t_h-20\right)\right)} - \frac{1+\lambda\ \left(t_{lo}-20\right)}{1+\lambda\ \left(t_{lo}+\Delta t_l-20\right)}$$
$$+p_{ho}\left[\alpha_h\ \frac{\left(1+\lambda\ \left(t_{ho}-20\right)\right)}{\left(1+\alpha_h\ \left(p_{ho}+dp\right)\right)\left(1+\lambda\ \left(t_{ho}+\Delta t_h-20\right)\right)} - \left(1+\alpha_h\ p_{ho}\right)\frac{\left(1+\lambda\ \left(t_{ho}-20\right)\right)}{\left(1+\alpha_h\ \left(p_{ho}+dp\right)\right)^2\left(1+\lambda\ \left(t_{ho}+\Delta t_h-20\right)\right)}\ \alpha_h\right] \tag{64}$$

11.4.3.2 Nominal value of differential pressure used in the calculation of area – *dp*

$$\frac{\partial\ dpb}{\partial\ dp} = -p_{ho}\ \left(1+\alpha_h\ p_{ho}\right)\frac{1+\lambda\ \left(t_{ho}-20\right)}{\left(1+\alpha_h\ \left(p_{ho}+dp\right)\right)^2\left(1+\lambda\ \left(t_{ho}+\Delta t_h-20\right)\right)}\ \alpha_h \tag{65}$$

11.4.3.3 Temperature coefficient of the piston-cylinders – λ

$$\frac{\partial\ dpb}{\partial\ \lambda} = p_{ho}\left[\begin{array}{l}\left(1+\alpha_h\ p_{ho}\right)\ \dfrac{t_{ho}-20}{\left(1+\alpha_h\ \left(p_{ho}+dp\right)\right)\left(1+\lambda\ \left(t_{ho}+\Delta t_h-20\right)\right)} \\ -\left(1+\alpha_h\ p_{ho}\right)\ \dfrac{1+\lambda\ \left(t_{ho}-20\right)}{\left(1+\alpha_h\ \left(p_{ho}+dp\right)\right)\left(1+\lambda\ \left(t_{ho}+\Delta t_h-20\right)\right)^2}\ \left(t_{ho}+\Delta t_h-20\right) \\ -\dfrac{t_{lo}-20}{\left(1+\lambda\ \left(t_{lo}+\Delta t_l-20\right)\right)} + \dfrac{1+\lambda\ \left(t_{lo}-20\right)}{\left(1+\lambda\ \left(t_{lo}+\Delta t_l-20\right)\right)^2}\left(t_{lo}+\Delta t_l-20\right)\end{array}\right] \tag{66}$$

11.4.3.4 Initial temperature of the high piston-cylinder – t_{ho}

$$\frac{\partial\ dpb}{\partial\ t_{ho}} = p_{ho}\ \left(1+\alpha_h\ p_{ho}\right)\ \lambda^2\ \frac{\Delta t_h}{\left(1+\alpha_h\ \left(p_{ho}+dp\right)\right)\left(1+\lambda\ \left(t_{ho}+\Delta t_h-20\right)\right)^2} \tag{67}$$

11.4.3.5 Change in temperature of the high piston-cylinder – Δt_h

$$\frac{\partial\ dpb}{\partial\ \Delta t_h} = -p_{ho}\ \left(1+\alpha_h\ p_{ho}\right)\ \frac{1+\lambda\ \left(t_{ho}-20\right)}{\left(1+\alpha_h\ \left(p_{ho}+dp\right)\right)\left(1+\lambda\ \left(t_{ho}+\Delta t_h-20\right)\right)^2}\ \lambda \tag{68}$$

11.4.3.6 Initial temperature of the low piston-cylinder – t_{lo}

$$\frac{\partial \ dpb}{\partial \ t_{lo}} = -p_{ho} \ \lambda^2 \ \frac{\Delta t_l}{\left(1 + \lambda \ \left(t_{lo} + \Delta t_l - 20\right)\right)^2} \tag{69}$$

11.4.3.7 Change in temperature of the low piston-cylinder – Δt_l

$$\frac{\partial \ dpb}{\partial \ \Delta t_h} = p_{ho} \ \frac{1 + \lambda \ \left(t_{lo} - 20\right)}{\left(1 + \lambda \ \left(t_{lo} + \Delta t_l - 20\right)\right)^2} \ \lambda \tag{70}$$

11.4.4 Uncertainty estimate using typical input quantity values

Table 1 shows a sample calculation of the estimated uncertainty in generated differential pressure – at 10 MPa line pressure and 100 kPa differential pressure:

Differential pressure proportional terms

Source of uncertainty/unit	Symbol	Value/unit	Uncertainty/ unit	Probability distribution	Divisor	C_i	U_i/Pa
Mass applied to generate dp /kg	*dpm*	2×10^{-1}	1×10^{-6}	Normal	2	5.003×10^{5}	0.250
Drift in above mass /kg	*dpm*	2×10^{-1}	2×10^{-6}	Rectangular	√3	5.003×10^{5}	0.578
Density of air /kg m^{-3}	ρ_a	1.21	5×10^{-2}	Rectangular	√3	1.251×10^{1}	0.361
Density of mass /kg m^{-3}	ρ_m	7.8×10^{3}	2×10^{2}	Rectangular	√3	1.645×10^{-5}	0.002
Acceleration due to gravity/m s^{-2}	g	9.81181	2×10^{-5}	Normal	2	1.020×10^{4}	0.102
Effective area of '*high*' p-c / m^{2}	A_{oh}	1.96×10^{-5}	4.90×10^{-10}	Normal	2	5.102×10^{9}	1.251
Drift in above area / m^{2}	A_{oh}	1.96×10^{-5}	1.96×10^{-10}	Rectangular	√3	5.102×10^{9}	0.578
Pressure term for '*high*' p-c × Pa	α_h	-2.2×10^{-12}	3×10^{-13}	Normal	2	1.011×10^{12}	0.152
Line pressure / Pa	P_h	1×10^{7}	2×10^{3}	Normal	2	2.201×10^{-7}	0.000
Nominal dp / Pa	dp	1×10^{5}	1×10^{2}	Normal	2	1.011×10^{12}	0.000
Temperature coefficient × °C	λ	9×10^{-6}	1×10^{-6}	Normal	2	6.403×10^{4}	0.032
Temperature of '*high*' p-c / °C	t_h	20.64	0.1	Rectangular	√3	9.005×10^{-1}	0.052
Effect of tilt/Pa			1×10^{-1}	Rectangular	√3	1	0.058
Effect of transmitter height / Pa			5×10^{-1}	Rectangular	√3	1	0.289
	Combined standard uncertainty			Normal			1.596
	Expanded uncertainty			Normal			3.193

Thus the differential pressure proportional expanded uncertainty (k = 2) = 32×10^{-6} × differential pressure

Line pressure proportional terms

Source of uncertainty/unit	Symbol	Value	Uncertainty	Probability distribution	Divisor	C_i	U_i/Pa
Line pressure / Pa	P_h	1×10^{7}	2×10^{3}	Normal	2	2.200×10^{-7}	0.000
Temperature coefficient × °C	λ	9×10^{-6}	1×10^{-6}	Normal	2	6.320×10^{-1}	0.100
Initial temp. of '*low*' p-c / °C	t_l	20.50	0.1	Rectangular	√3	3.240×10^{-5}	0.000
Temp. increase of '*low*' p-c / °C	Δt_l	0.04	0.1	Rectangular	√3	9.000×10^{1}	5.196
Initial temp. of '*high*' p-c / °C	t_h	20.6	0.1	Rectangular	√3	3.240×10^{-5}	0.000
Temp. increase of '*high*' p-c / °C	Δt_h	0.04	0.1	Rectangular	√3	9.000×10^{1}	5.196
Pressure term for p-cs × Pa	α	-2.2×10^{-12}	3×10^{-13}	Normal	2	8.389×10^{1}	0.152
Effect of piston taper / Pa			3.5	Rectangular	√3	1	2.021
Effect of fluid head / Pa			0.4	Rectangular	√3	1	0.231
Effect of angular velocity / Pa			2.5	Rectangular	√3	1	1.443
	Combined standard uncertainty			Normal			7.760
	Expanded uncertainty			Normal			15.520

Thus the line pressure proportional expanded uncertainty (k = 2) = 1.6 × 10^{-6} × line pressure

Fixed pressure terms

Source of uncertainty/unit	Symbol	Value	Uncertainty	Probability distribution	Divisor	C_i	U_i/Pa
Measurement repeatability /Pa			5	Normal	2	1	2.500
Cross-float repeatability /Pa			5	Normal	2	1	2.500
Resolution of cross-float /Pa			5	Rectangular	√3	1	2.887
	Combined standard uncertainty			Normal			4.564
	Expanded uncertainty			Normal			9.129

Thus the fixed pressure expanded uncertainty (k = 2) = 9 Pa

Table 1 Twin-post pressure balance uncertainty calculation

The calculation was repeated to estimate uncertainty for values throughout the full range of line and differential pressures. The results of the calculations showed that the 'line pressure proportional' and the 'fixed pressure' terms remained constant throughout the operating range whilst the 'differential pressure proportional' term changed very slightly with line and differential pressure – due to the uncertainty in the pressure dependent term α.

In this example, the uncertainty across the full range of line and differential pressures may therefore be expressed by the combination of the three terms:

differential pressure proportional term :	33×10^{-6} × differential pressure
line pressure proportional term :	1.6×10^{-6} × line pressure
fixed pressure term :	9 Pa

The 'line pressure proportional' and the 'fixed pressure' terms are independent of each other and may be added in quadrature, resulting in a combined expression of uncertainty of:

$$\pm\left[33\times10^{-6}\times dp+\sqrt{\left(1.6\times10^{-6}\times lp\right)^2+9^2}\right]\ Pa \tag{71}$$

where *dp* and *lp* are the differential and line pressures respectively (expressed in pascal).

This expression is represented graphically in Figure 51.

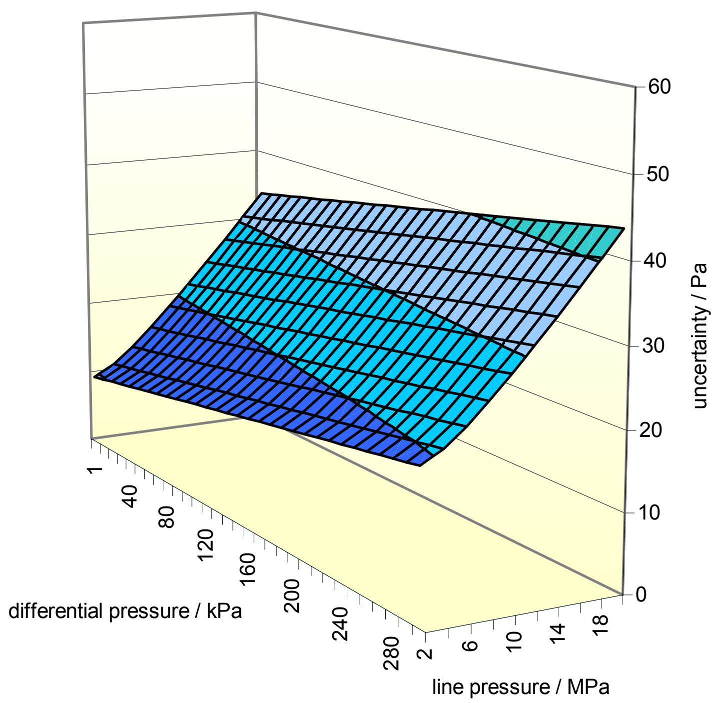

Figure 51 Twin-post uncertainty

11.4.5 Comment

Uncertainties for differential pressure measurements are presented in a number of different ways – as mathematical expressions showing one, two or three terms combined linearly, in quadrature or both. When interpreting and comparing such expressions it is important to ensure that the methods which were used are fully appreciated and that no terms are inadvertently ignored – for example by erroneously presuming that a component is insignificantly small.

It is interesting to compare the uncertainty estimate in Section 11.4.4 with the best measurement capabilities adopted by accredited laboratories.

The ‘fixed pressure’ term is comparable with typical values claimed elsewhere whereas the ‘differential pressure proportional’ term equates broadly with the best values claimed. The ‘line pressure proportional’ term, however, is about twice as large as typically claimed in other laboratories and at higher line pressures this represents a significant discrepancy. The dominant terms contributing to this figure come from the estimates of piston-cylinder temperature and, as discussed in Section 11.3.10, it is considered too optimistic to claim uncertainties in the changes in piston-cylinder temperature beyond those suggested.

Large differences in values of measurement uncertainty effectively hinge on hair-splitingly different arguments about estimation of temperature. At high line pressures uncertainties reduce by around one third by shaving just 50 mK off temperature uncertainties – a less-than-robust situation which itself indicates unjustified metrological optimism.

In this report the values of uncertainty shown represent those which are thought to be achievable using good quality equipment in a suitable environment and where the procedural tolerances used are consistent with working in an economically viable time frame. They do not represent what might be called the *momentarily best achievable* uncertainty, nor do they represent the *uncertainty in measurement* which should include dynamic effects, repeatability, resolution of the instrument being calibrated, etcetera. (see Section 15).

12 UNCERTAINTY BUDGET – DIVIDER

12.1 GENERAL

This section outlines the method used to estimate the measurement uncertainty associated with the generation of differential pressure using a divider. It lists *Type A* components of measurement uncertainty – those amenable to evaluation by statistical analysis of a series of observations – such as repeatability*,* and *Type B* components – those evaluated by other means – such as hydraulic piston-cylinder effective area, acceleration due to gravity, air density etcetera. The magnitude of some components is clearly insignificant but they have been included as it cannot be assumed that they will remain insignificant under different operational conditions.

The listing does *not* include all the factors which should be considered when calculating the *uncertainty in the measurement* associated with the calibration of an artefact using a generator (see Section 15).

Some practitioners provide traceability to the SI by calibrating dividers at zero line pressure only, against a single pressure balance, and using a theoretical model to argue that the line pressure effects are negligible. At the low level of uncertainty in question, however, the authors believes that the best theoretical models are insufficiently accurate to make this assumption and that measurements at line pressure are necessary. The uncertainty budget below is therefore based on the presumption that such data will be available.

12.2 ‘TYPE A’ COMPONENTS OF UNCERTAINTY

12.2.1 General

Differential pressure, when generated using a pressure divider, contains cyclic components – at a frequency equal to the rotation of the divider’s rotating assembly – oscillating around a relatively constant mean value.

12.2.2 Differential pressure readings

As the generated differential pressure is relatively stable, capturing a single ‘instantaneous’ data point is likely to be close to the mean value of differential pressure.

Closer agreement between readings was achieved when measurements were obtained by calculating the *mean* of successive ‘instantaneous’ values of differential pressure, sampled at a frequency of about 10 Hz - 20 Hz and over a few seconds – an interval greater than that of the oscillatory period.

12.2.3 Real-time graphical display and data capture

The real-time graphical display and data capture system (see Section 3.2.5), plotting differential pressure vs time, was used to determine the best moment to capture a representative set of data to include all frequency components. The sensitivity of the display was high, enabling subtle changes in generated differential pressure to be observed in the presence of signal oscillations and noise – effects that would be lost in a digital display.

To ensure that a measurement was taken at a time which avoided spurious measurements due to 'glitches' (see Figure 31 and Figure 32) the output of the divider was observed for a period of several minutes (>5) prior to making a measurement.

12.2.4 'Type A' evaluation of standard uncertainty

The 'Type A' uncertainty in differential pressure generated by the divider was estimated using the same procedure as used for the twin-post pressure balances.

To estimate the uncertainty the mean of the individual readings of differential pressure q was first calculated:

$$\bar{q} = \frac{1}{n}\sum_{j=1}^{n} q_j \tag{72}$$

From the sample of measurements an estimate was made of the standard deviation of the whole population:

$$s(q_j) = \sqrt{\frac{1}{(n-1)}\sum_{j=1}^{n}(q_j - \bar{q})^2} \tag{73}$$

The estimated standard deviation of the *uncorrected* mean was then calculated by:

$$s(\bar{q}) = \frac{s(q_j)}{\sqrt{n}} \tag{74}$$

By observing the output of transmitters graphically and in real-time, it was possible to achieve a value of less than a few pascals by taking measurements over a time period several times greater than that of the rotation of the divider and avoiding spurious glitches and pulses caused by the motor-drive.

Due to the inherent stability of the divider, the difference between the 'best achievable' uncertainty (see Section 12.5.4) and the uncertainty which would typically be obtained is minimal.

12.3 'TYPE B' COMPONENTS OF UNCERTAINTY IN 'HYDRAULIC' PRESSURE

12.3.1 General

A number of Type B uncertainty components are common to both twin-post devices and the hydraulic pressure balance used in conjunction with dividers but, for clarity and completeness, they have been included in both sections.

12.3.2 Mass applied to the hydraulic pressure balance to generate differential pressure – *dpm*

The uncertainties associated with the determination of mass values are predominantly systematic in nature. Thus the uncertainty in the total applied mass was calculated by taking the arithmetic sum of the uncertainty of each individual weight rather than by quadrature summation.

A calibration certificate for a mass set will typically show uncertainties between about ±3 ppm and ±10 ppm of the mass value (at a coverage factor $k = 2$). The best likely uncertainty in masses due to drift will be about ±2 ppm of the mass value per year but in practice ±5 ppm per year is more realistic. In calculating the standard uncertainty a normal distribution was assumed for the calibration data and a rectangular distribution for the drift.

12.3.3 Density of air – ρ_a

The density of air is generally calculated from knowledge of ambient atmospheric pressure, temperature and relative humidity using an equation which inevitably makes a number of assumptions (for example it is not generally practical to measure the air's composition).

The value for the air density used was assumed to be constant for the duration of a calibration and the uncertainty estimated was ±0.05 kg m^{-3}. This was assumed to represent the limits of a rectangular distribution and a divisor of √3 was therefore used to calculate the standard uncertainty.

12.3.4 Density of the mass applied to generate hydraulic pressure – ρ_m

This value is used in the calculation of correction factor ϕ which compensates for differences between the density of the material and an assumed density of 8000 kg m^{-3}.

Without having the density of the masses determined, a typical value for the uncertainty in the density of a stainless steel mass is approximately ±200 kg m^{-3}. This was assumed to represent the limits of a rectangular distribution and a divisor of √3 was therefore used to calculate the standard uncertainty – which equates to less than ±1 ppm of pressure.

12.3.5 Acceleration due to gravity – g

The uncertainty in the value of gravitational acceleration will depend upon the method used for its determination. A pressure calibration laboratory will generally have its local value determined by a geological institution, in which case a typical value for uncertainty would be $\pm 2 \times 10^{-5}$ m s^{-2} ($k = 2$).

12.3.6 Effective area of the hydraulic piston-cylinder – A_o

The uncertainty in the effective area of the hydraulic piston-cylinder is obtained by calibration and will depend upon where the piston-cylinder was calibrated, against which standard and how it performed during the calibration. Typical values will range from around ±25 ppm to ±100 ppm of effective area ($k = 2$). The drift in effective area was estimated to be typically 6 ppm per year.

In calculating the standard uncertainty a normal distribution was assumed for the calibration data and a rectangular distribution for the drift in effective area.

12.3.7 Pressure dependent term for the piston-cylinder area – α

The uncertainty in the pressure dependent term is usually given on the calibration certificate along with the effective area (see Section 12.3.6). Typical values will be about $\pm 0.3 \times 10^{-6}$ MPa^{-1} ($k = 2$).

12.3.8 Hydraulic pressure generated during the initial balance – p_{oil}

A separate uncertainty budget is required to estimate the uncertainty in the hydraulic pressure at which the initial cross-float is achieved but, as a relatively large uncertainty (100s of parts per million) will have negligible effect on the overall uncertainty in generated differential pressure, a comprehensive work is generally not needed.

12.3.9 Nominal value of incremental hydraulic pressure used in the calculation of area – Δp_{oil}

The calculation of the increase in hydraulic pressure is, to a small degree, recursive. This demands either an iterative approach or the use of a nominal value. Whilst the latter attracts a higher uncertainty than the former, even the higher uncertainty is negligible. This is because, in the calculation, the hydraulic pressure value is multiplied by the pressure dependent term, which is typically around 1×10^{-6} MPa^{-1}.

12.3.10 Temperature coefficient of the oil piston-cylinder – λ

An uncertainty value of $\pm 0.5 \times 10^{-6}$ °C^{-1} was supplied, by the manufacturers, for the temperature coefficient of the tungsten carbide. This corresponds to an uncertainty of $\pm 0.7 \times 10^{-6}$ °C^{-1} in the value of λ, the temperature coefficient of the piston-cylinder combination. As with most such values, they are not based on measurements of pistons or cylinders but alternatively-shaped specimens made specifically for determining such characteristics. The uncertainty in λ for a piston-cylinder is therefore likely to be larger than suggested and a value of $\pm 1 \times 10^{-6}$ °C^{-1} was assumed ($k = 2$).

12.3.11 Piston-cylinder temperature – t

It is felt that the uncertainty in the measurement of piston-cylinder temperature can at best be estimated to within ±0.1 °C (assuming that the uncertainty in the thermometer reading is much less). This presumes good environmental conditions but appreciates that the positions at which the temperatures are measured are not necessarily in very close proximity to the piston-cylinders and also that a single thermometer cannot provide a properly integrated value of a piston-cylinder temperature. It also assumes that systems have reached general thermal equilibrium, for example after switching on a motor-drive (this can take at least one working day and elevate temperatures by up to about 3 °C).

12.3.12 Tilt

The device was levelled, using its adjustable feet, to ensure the axis of the piston-cylinder was vertical. This was achieved by placing a spirit level on top of the weight stack and making measurements at several intervals throughout a 360° rotation of the piston. If the piston axis is inclined at an angle θ to the vertical, then the downward force acting along the piston axis will be:

$$W \cos \theta \tag{75}$$

where W is the vertical downward force.

It is estimated that, when using a good spirit level, a piston can typically be levelled to within 5 minutes of arc. This corresponds to a maximum error due to tilt of approximately 1 ppm of pressure. Strictly, this uncertainty has a one-sided (asymmetric) distribution; an offset of -0.5 ppm of pressure was applied (half the maximum error due to tilt) and an uncertainty of ±0.5 ppm of pressure adopted, with a rectangular distribution.

Whilst the magnitude of the uncertainty, when the instrument is levelled to this degree, is insignificant, the point is made to illustrate the nature of the calculation required should the tilt be greater than in this example.

12.3.13 Piston taper

It was estimated, from measurements made using piston-cylinders of a similar design, that changes in generated pressure of around 1 ppm per millimetre vertical displacement of the piston may be expected. The maximum possible change in differential pressure can then be estimated using the tolerances allowed for the piston float-position during a calibration.

If the float-position for the piston is repeated to within a tolerance of ±0.25 mm and the effect of piston taper is taken to be 1 ppm of pressure per millimetre, the total uncertainty in differential pressure due to piston taper will be approximately ±0.25 ppm of pressure – of little significance.

12.4 'TYPE B' COMPONENTS OF UNCERTAINTY IN DIFFERENTIAL PRESSURE

12.4.1 Calibration of divider

The uncertainty in generated differential pressure, when using the dividing ratio obtained by calibration, will depend upon the uncertainty of the twin-post standard against which it was calibrated and how it performed during the calibration. The best uncertainty achievable in the calibration of a divider, calibrated against a good twin-post device, over its line and differential pressure range is estimated to be approximately:

$$\pm\,(50\times10^{-6}\times\text{differential pressure} + 1.5\times10^{-6}\times\text{line pressure} + 5\ \text{Pa})$$

These figures take into account the Type A and Type B uncertainties associated with the twin-post device against which it was calibrated, the hydraulic pressure balance and the calibration process.

12.4.2 Drift

At present there is insufficient data upon which to accurately estimate the uncertainty due to drift in dividing ratio. More calibrations are required, at elevated line pressures, over a longer period of time (years) before a robust statistical analysis can be performed.

12.4.3 Difference in height between transmitter and generator

Section 7 shows that the additional differential pressure due to mounting the instrument being calibrated at a height other than the reference of the differential pressure generator is approximately 0.1 ppm of differential pressure per millimetre. There is no clear convention for ascribing a datum level to a transmitter and generally they are not physically marked, an uncertainty of ±50 mm is therefore appropriate when adjusting the transmitters height to the datum level of the generator; this corresponds to ±5 ppm of the differential pressure – of marginal significance.

12.4.4 Resolution of cross-float

The resolution in cross-floating the hydraulic pressure balance against the dividers rotating assembly depends, to a certain extent, upon the criteria used to judge hydrostatic equilibrium. During this project hydrostatic equilibrium was determined by a reversal of fall-rates.

As an aid to achieving hydrostatic equilibrium a differential pressure transmitter, set to give a high resolution (<0.1 Pa), was used as a null indicator. The mass on the hydraulic pressure balance was adjusted until the transmitter output with the divider's equalising valve closed was similar to that with the equalising valve open. The equalising valves were then opened and the fall-rates measured to confirm hydrostatic equilibrium.

It should be noted that use of the transmitter was to speed the process of achieving proper cross-floating conditions; it did *not* provide a higher cross-float resolution; the transmitter cannot, for example, differentiate between 'perfect' cross-float conditions and exactly compensating piston height and temperature errors.

With the use of capacitive sensors and associated graphical software for measuring piston fall-rates, cross-floats were achieved with a resolution of <5Pa. Without the use of similar ancillary apparatus the expected resolution would be poorer.

12.4.5 Repeatability of cross-float

At the end of a calibration run (when the masses are as they were for the initial cross-float) the equalising valves are opened and a check made to determine the degree to which hydrostatic equilibrium still exists. A component has to be added to the uncertainty budget to take into account the deviations from the initial equilibrium after correcting for piston-cylinder temperature changes.

As it is not possible to determine when the change in balance occurred, or the rate at which the change occurred, a rectangular distribution is assumed. It was found that the cross-float could generally be repeated to within a few pascals.

12.5 COMBINED STANDARD UNCERTAINTY

The hydraulic pressure equation derived in Section 6.2 of this report shows the functional relationship between the input quantities and the generated hydraulic pressure.

$$\Delta P_{oil} = \frac{dpm\left[1-(\rho_a-1.2)\left(\frac{1}{\rho_m}-\frac{1}{8000}\right)\right]\left(1-\frac{\rho_a}{8000}\right)g}{A_o\left(1+\alpha\left(P_{oil}+\Delta P_{oil}\right)\right)\left(1+\lambda\left(t-20\right)\right)} + P_{oil}\left(\frac{\left(1+\alpha P_{oil}\right)\left(1+\lambda\left(t_o-20\right)\right)}{\left(1+\alpha\left(P_{oil}+\Delta P_{oil}\right)\right)\left(1+\lambda\left(t-20\right)\right)}-1\right) \tag{76}$$

12.5.1 Sensitivity Coefficients

Once the standard uncertainties of the input quantities have been quantified the combined standard uncertainty of the output quantity can be calculated using the equation:

$$u_c(y) = \sqrt{\sum_{i=1}^{N} c_i^{\,2} u^2(x_i)} \tag{77}$$

where c_i , the sensitivity coefficient, is the partial derivative $\partial f/\partial x_I$

12.5.2 Symbolic representation of the partial derivatives of Δp_{oil}

12.5.2.1 Mass applied to generate the differential pressure – *dpm*

$$\frac{\partial\ \Delta p_{oil}}{\partial\ dpm} = \left[1-(\rho_a - 1.2)\left(\frac{1}{\rho_m} - \frac{1}{8000}\right)\right]\left(1 - \frac{1}{8000}\ \rho_a\right)\frac{g}{A_o\left(1+\alpha\ \left(p_{oil}+\Delta p_{oil}\right)\right)\left(1+\lambda\ \left(t_o+\Delta t-20\right)\right)} \tag{78}$$

12.5.2.2 Density of air – ρ_a

$$\frac{\partial\ \Delta p_{oil}}{\partial\ \rho_a} = -6.25\times10^{-9}\ dpm\ g\ \frac{160024000 - 40000\ \rho_a - 3\ \rho_m + 5\ \rho_a\ \rho_m}{\rho_m\ A_o\left(1+\alpha\ \left(p_{oil}+\Delta p_{oil}\right)\right)\left(1+\lambda\ \left(t_o+\Delta t-20\right)\right)} \tag{79}$$

12.5.2.3 Density of the mass applied to generate differential pressure – ρ_m

$$\frac{\partial\ \Delta p_{oil}}{\partial\ \rho_m} = dpm\ \frac{(\rho_a - 1.2)}{\rho_m^{\ 2}}\left(1 - \frac{1}{8000}\ \rho_a\right)\frac{g}{A_o\left(1+\alpha\ \left(p_{oil}+\Delta p_{oil}\right)\right)\left(1+\lambda\ \left(t_o+\Delta t-20\right)\right)} \tag{80}$$

12.5.2.4 Acceleration due to gravity – *g*

$$\frac{\partial\ \Delta p_{oil}}{\partial\ g} = dpm\ \left[1-(\rho_a - 1.2)\left(\frac{1}{\rho_m} - \frac{1}{8000}\right)\right]\frac{\left(1 - \frac{1}{8000}\ \rho_a\right)}{A_o\left(1+\alpha\ \left(p_{oil}+\Delta p_{oil}\right)\right)\left(1+\lambda\ \left(t_o+\Delta t-20\right)\right)} \tag{81}$$

12.5.2.5 Effective area of the piston-cylinder – A_o

$$\frac{\partial\ \Delta p_{oil}}{\partial\ A_o} = -dpm\ \left[1-(\rho_a - 1.2)\left(\frac{1}{\rho_m} - \frac{1}{8000}\right)\right]\left(1 - \frac{1}{8000}\ \rho_a\right)\frac{g}{A_o^{\,2}\left(1+\alpha\ \left(p_{oil}+\Delta p_{oil}\right)\right)\left(1+\lambda\ \left(t_o+\Delta t-20\right)\right)} \tag{82}$$

12.5.2.6 Pressure dependent term for the piston-cylinder – α

$$\frac{\partial\,\Delta p_{oil}}{\partial\,\alpha} = -dpm\left[1-(\rho_a-1.2)\left(\frac{1}{\rho_m}-\frac{1}{8000}\right)\right]\left(1-\frac{1}{8000}\,\rho_a\right)\frac{g}{A_o\left(1+\alpha_h\,(p_{oil}+\Delta p_{oil})\right)^2\left(1+\lambda\,(t_o+\Delta t-20)\right)}\,(p_{oil}+\Delta p_{oil})$$
$$+\,p_{oil}\left[p_{oil}\frac{1+\lambda\,(t_o-20)}{\left(1+\alpha_h\,(p_{oil}+\Delta p_{oil})\right)\left(1+\lambda\,(t_o+\Delta t-20)\right)}-(1+\alpha\,p_{oil})\frac{1+\lambda\,(t_o-20)}{\left(1+\alpha_h\,(p_{oil}+\Delta p_{oil})\right)^2\left(1+\lambda\,(t_o+\Delta t-20)\right)}\,(p_{oil}+\Delta p_{oil})\right] \tag{83}$$

12.5.2.7 Hydraulic pressure at which the initial cross-float is achieved – P_{oil}

$$\frac{\partial\,\Delta p_{oil}}{\partial\,P_{oil}} = -dpm\left[1-(\rho_a-1.2)\left(\frac{1}{\rho_m}-\frac{1}{8000}\right)\right]\left(1-\frac{1}{8000}\,\rho_a\right)\frac{g}{A_o\left(1+\alpha\,(p_{oil}+\Delta p_{oil})\right)^2\left(1+\lambda\,(t_o+\Delta t-20)\right)}\,\alpha$$
$$+(1+\alpha\,p_{oil})\frac{1+\lambda\,(t_o-20)}{\left(1+\alpha\,(p_{oil}+\Delta p_{oil})\right)\left(1+\lambda\,(t_o+\Delta t-20)\right)}-1$$
$$+\,p_{oil}\left[\alpha\,\frac{1+\lambda\,(t_o-20)}{\left(1+\alpha\,(p_{oil}+\Delta p_{oil})\right)\left(1+\lambda\,(t_o+\Delta t-20)\right)}-(1+\alpha\,p_{oil})\frac{1+\lambda\,(t_o-20)}{\left(1+\alpha\,(p_{oil}+\Delta p_{oil})\right)^2\left(1+\lambda\,(t_o+\Delta t-20)\right)}\,\alpha\right] \tag{84}$$

12.5.2.8 Nominal value of incremental hydraulic pressure used in the calculation of area – *Δp_{oil}*

$$\frac{\partial\,\Delta p_{oil}}{\partial\,\Delta p_{oil}} = -dpm\left[1-(\rho_a-1.2)\left(\frac{1}{\rho_m}-\frac{1}{8000}\right)\right]\left(1-\frac{1}{8000}\,\rho_a\right)\frac{g}{A_o\left(1+\alpha\,(p_{oil}+\Delta p_{oil})\right)^2\left(1+\lambda\,(t_o+\Delta t-20)\right)}\,\alpha$$
$$-\,p_{oil}\,(1+\alpha\,p_{oil})\frac{\left(1+\lambda\,(t_o-20)\right)}{\left(1+\alpha\,(p_{oil}+\Delta p_{oil})\right)^2\left(1+\lambda\,(t_o+\Delta t-20)\right)}\,\alpha \tag{85}$$

12.5.2.9 Temperature coefficient of the piston-cylinder – λ

$$\frac{\partial\,\Delta p_{oil}}{\partial\,\lambda} = -dpm\left[1-(\rho_a-1.2)\left(\frac{1}{\rho_m}-\frac{1}{8000}\right)\right]\left(1-\frac{1}{8000}\,\rho_a\right)\frac{g}{A_o\left(1+\alpha\,(p_{oil}+\Delta p_{oil})\right)\left(1+\lambda\,(t_o+\Delta t-20)\right)^2}\,(t_o+\Delta t-20)$$
$$+\,p_{oil}\left[\begin{array}{l}(1+\alpha\,p_{oil})\dfrac{t_o-20}{\left(1+\alpha\,(p_{oil}+\Delta p_{oil})\right)\left(1+\lambda\,(t_o+\Delta t-20)\right)}\\ -(1+\alpha\,p_{oil})\dfrac{\left(1+\lambda\,(t_o-20)\right)}{\left(1+\alpha\,(p_{oil}+\Delta p_{oil})\right)\left(1+\lambda\,(t_o+\Delta t-20)\right)^2}\,(t_o+\Delta t-20)\end{array}\right] \tag{86}$$

12.5.2.10 Initial temperature of the piston-cylinder – t_o

$$\frac{\partial\,\Delta p_{oil}}{\partial\,t_o} = -dpm\left[1-(\rho_a-1.2)\left(\frac{1}{\rho_m}-\frac{1}{8000}\right)\right]\left(1-\frac{1}{8000}\,\rho_a\right)\frac{g}{A_o\left(1+\alpha\,(p_{oil}+\Delta p_{oil})\right)\left(1+\lambda\,(t_o+\Delta t-20)\right)^2}\,\lambda$$
$$+\,p_{oil}\left[(1+\alpha\,p_{oil})\frac{\lambda}{\left(1+\alpha\,(p_{oil}+\Delta p_{oil})\right)\left(1+\lambda\,(t_o+\Delta t-20)\right)}-(1+\alpha\,p_{oil})\frac{\left(1+\lambda\,(t_o-20)\right)}{\left(1+\alpha\,(p_{oil}+\Delta p_{oil})\right)\left(1+\lambda\,(t_o+\Delta t-20)\right)^2}\,\lambda\right] \tag{87}$$

12.5.2.11 Change in temperature of the piston-cylinder – Δt

$$\frac{\partial\ \Delta p_{oil}}{\partial\ \Delta t} = -dpm\left[1-\left(\rho_a-1.2\right)\left(\frac{1}{\rho_m}-\frac{1}{8000}\right)\right]\left(1-\frac{1}{8000}\ \rho_a\right)\frac{g}{A_o\left(1+\alpha\ \left(p_{oil}+\Delta p_{oil}\right)\right)\left(1+\lambda\ \left(t_o+\Delta t-20\right)\right)^2}\ \lambda$$
$$-\ p_{oil}\ \left(1+\alpha\ p_{oil}\right)\frac{\left(1+\lambda\ \left(t_o-20\right)\right)}{\left(1+\alpha\ \left(p_{oil}+\Delta p_{oil}\right)\right)\left(1+\lambda\ \left(t_o+\Delta t-20\right)\right)^2}\ \lambda \tag{88}$$

12.5.3 Uncertainty estimate using typical input quantity values

Table 2 shows a sample calculation of the estimated uncertainty in the hydraulic pressure Δp_{oil} – at 10 MPa.

Uncertainty in hydraulic pressure							
Source of uncertainty/unit	Symbol	Value/unit	Uncertainty/ unit	Probability distribution	Divisor	C_i	U_i/Pa
Mass applied to generate dp /kg	*dpm*	1×10^{1}	3×10^{-5}	Normal	2	9.994×10^{5}	15
Drift in above mass /kg	*dpm*	1×10^{1}	2×10^{-5}	Normal	2	9.994×10^{5}	12
Density of air /kg m^{-3}	ρ_a	1.21	5×10^{-2}	Rectangular	√3	1.262×10^{3}	36
Density of mass /kg m^{-3}	ρ_m	7.92×10^{3}	1×10^{2}	Rectangular	√3	1.593×10^{-3}	0
Acceleration due to gravity/m s^{-2}	g	9.81181	2×10^{-5}	Normal	2	1.018×10^{6}	3
Effective area of p-c / m^{2}	A_o	9.816×10^{-6}	2.5×10^{-10}	Normal	2	1.018×10^{12}	127
Drift in above area / m^{2}	A_o	9.816×10^{-6}	9.8×10^{-11}	Rectangular	√3	1.018×10^{12}	58
Pressure term for p-c × Pa	α	8.3×10^{-13}	3×10^{-13}	Normal	2	1.199×10^{14}	18
Nominal balance pressure / Pa	P_{oil}	1×10^{6}	3×10^{1}	Normal	2	6.159×10^{-5}	0
Nominal increase in P_{oil} / Pa	ΔP_{oil}	1×10^{7}	3×10^{2}	Normal	2	9.125×10^{-6}	0
Temperature coefficient × °C	λ	9×10^{-6}	1×10^{-6}	Normal	2	5.497×10^{7}	27
Temperature of p-c / °C	t	20.00	1×10^{-1}	Rectangular	√3	8.993×10^{-1}	5
Change in temp. p-c / °C	Δt	1.00	1×10^{-1}	Rectangular	√3	9.894×10^{-1}	6
Effect of tilt/Pa			2×10^{-1}	Rectangular	√3	1	12
	Combined standard uncertainty			Normal			150
	Expanded uncertainty			Normal			300
Thus the expanded uncertainty ($k = 2$) = 30×10^{-6} × hydraulic pressure							

Table 2 Uncertainty in hydraulic pressure

The calculation was repeated to estimate values of uncertainty in the hydraulic pressure throughout the full range of the device. The results of the calculations (plotted in Figure 52) show, as might be obvious, that as the value of hydraulic pressure Δp_{oil} approaches zero there is a sharp increase in the relative uncertainty.

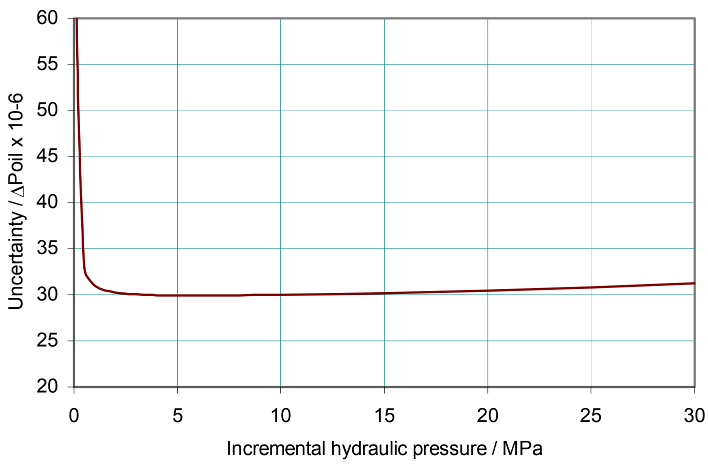

Figure 52 Uncertainty in hydraulic pressure

By including a small 'fixed pressure' term, the estimated uncertainty in hydraulic pressure can be expressed using a single expression to cover the full range of the device.

$$\pm\,(33\times10^{-6} \times \text{hydraulic pressure} + 5\ \text{Pa})$$

Table 3 shows an example calculation of the estimated uncertainty in generated differential pressure – at 10 MPa line pressure and 100 kPa differential pressure:

Differential pressure proportional terms							
Source of uncertainty/unit	Symbol	Value/unit	Uncertainty/ unit	Probability distribution	Divisor	C_i	U_i/Pa
Incremental hydraulic pressure / Pa	Δp_{oil}	1×10^7	3.3×10^2	Normal	2	0.01	1.65
Differential pressure proportional term (from divider calibration)/ Pa			5	Normal	2	1	2.5
Effect of transmitter height / Pa			5×10^{-1}	Rectangular	√3	1	0.289
	Combined standard uncertainty			Normal			3.01
	Expanded uncertainty			Normal			6.02
Thus the differential pressure proportional expanded uncertainty (*k* = *2*) = 61×10^{-6} × differential pressure							
Line pressure proportional terms							
Source of uncertainty/unit	Symbol	Value	Uncertainty	Probability distribution	Divisor	C_i	U_i/Pa
Line pressure proportional term (from divider calibration)/ Pa			15	Normal	2	1	7.5
	Combined standard uncertainty			Normal			7.5
	Expanded uncertainty			Normal			15
Thus the line pressure proportional expanded uncertainty (*k* = *2*) = 1.5 × 10^{-6} × line pressure							
Fixed pressure terms							
Source of uncertainty/unit	Symbol	Value	Uncertainty	Probability distribution	Divisor	C_i	U_i/Pa
Incremental hydraulic pressure / Pa	Δp_{oil}		10	Normal	2	0.01	0.1
Fixed pressure term (from divider calibration)/ Pa			6	Normal	2	1	3
Measurement repeatability /Pa			5	Normal	2	1	2.5
Cross-float repeatability /Pa			5	Normal	2	1	2.5
Resolution of cross-float /Pa			5	Rectangular	√3	1	2.887
	Combined standard uncertainty			Normal			5.46
	Expanded uncertainty			Normal			11
Thus the fixed pressure expanded uncertainty (*k* = *2*) = 11 Pa							

Table 3 Divider uncertainty calculation

The calculation was repeated to estimate measurement uncertainty throughout the full range of line and differential pressures. The results of the calculations showed that the 'line pressure proportional' and the 'fixed pressure' terms remained constant throughout the operating range whilst the 'differential pressure proportional' term changed very slightly with line and differential pressure – due to the uncertainty in the pressure dependant term α.

In this example, the uncertainty across the full range of line and differential pressures may therefore be expressed by the combination of the three terms:

differential pressure proportional term :	$61\times10^{-6} \times$ differential pressure
line pressure proportional term :	$1.5\times10^{-6} \times$ line pressure
fixed pressure term :	11 Pa

The 'line pressure proportional' and the 'fixed pressure' terms are independent of each other and may be combined in quadrature, resulting in a combined expression of uncertainty of:

$$\pm\left[61\times10^{-6}\times dp+\sqrt{\left(1.5\times10^{-6}\times lp\right)^2+11^2}\right]\ Pa \tag{89}$$

where dp and lp are the differential and line pressures respectively (expressed in pascal).

This expression is represented graphically in Figure 53.

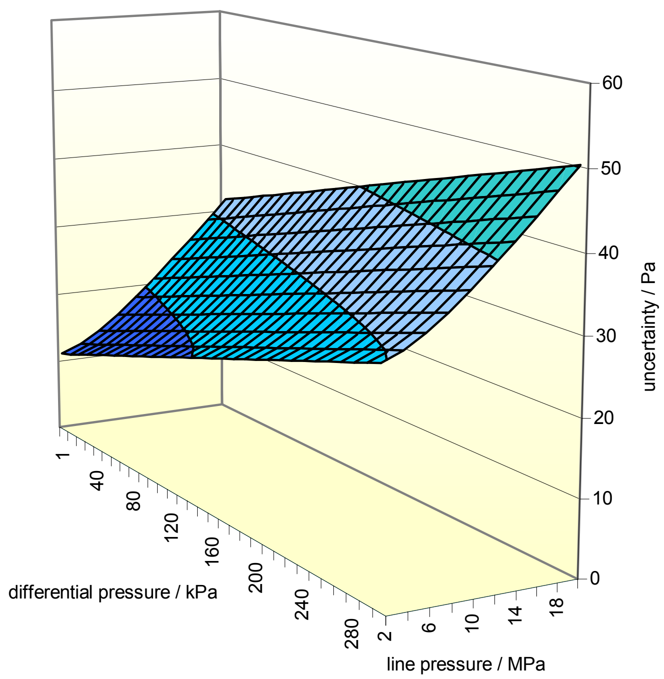

Figure 53 Divider uncertainty

12.5.4 Comment

The values shown represent uncertainties which are thought to be achievable using good quality equipment in a suitable environment. They do not represent the *uncertainty in measurement* which should include dynamic effects, repeatability and resolution of the instrument being calibrated (see Section 15).

Assuming that the divider's calibration against the twin-post pressure balance is undertaken in a good environment, uncertainties only marginally higher than that of the calibrating twin-post can be achieved. If the two devices are subsequently used under poorer operating conditions, perhaps environmental or where less time is available, it is possible - particularly at lower differential pressures - for the calculated uncertainty associated with the divider to be slightly lower than that of the twin-post.

13 EMPIRICAL COMPARISON OF THREE DEVICES

The results of the comparison between the divider and the oil-lubricated twin-post device are recorded in Section 10.4.2 where the divider's dividing ratio was determined by calibration against the oil-lubricated twin-post pressure balance. It can be seen, from the residuals plotted in Figure 40 (also in Section 10.4.2), that close agreement was achieved between the divider and the twin-post pressure balance when the dividing ratio was corrected for line and differential pressure dependency.

A comparison was made between the gas- and oil-lubricated twin-post pressure balances. Following a similar procedure to that for the comparison between the divider and the oil-lubricated twin-post, both twin-posts were set to generate the nominated line and differential pressure, and transmitters were used to obtain an approximate equilibrium. All equalising valves between the devices were then opened and the mass on the '*high*' piston of the oil-lubricated pressure balance adjusted until both *high* and *low* pistons were in equilibrium. The generated differential pressure was then calculated independently for both the oil- and gas-lubricated devices using equation (25). The difference between the differential pressure calculated for each device is plotted in Figure 54.

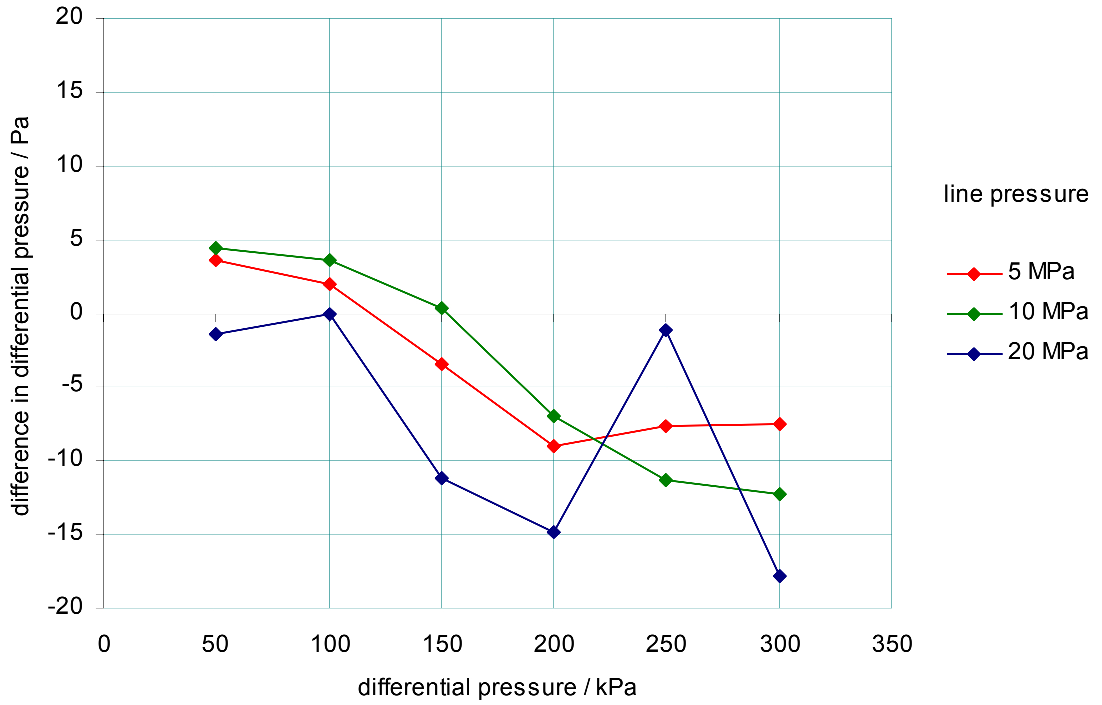

Figure 54 Differences between oil- and gas-lubricated twin-post devices

The E_N *Ratios* plotted in Figure 55 were calculated by dividing the differences measured between the two devices (as shown in Figure 54) by the quadratic summation of their expanded uncertainties (at the coverage factor $k = 2$). The chart shows that the differences between the differential pressures calculated for each device are less than the combined uncertainty of the two systems.

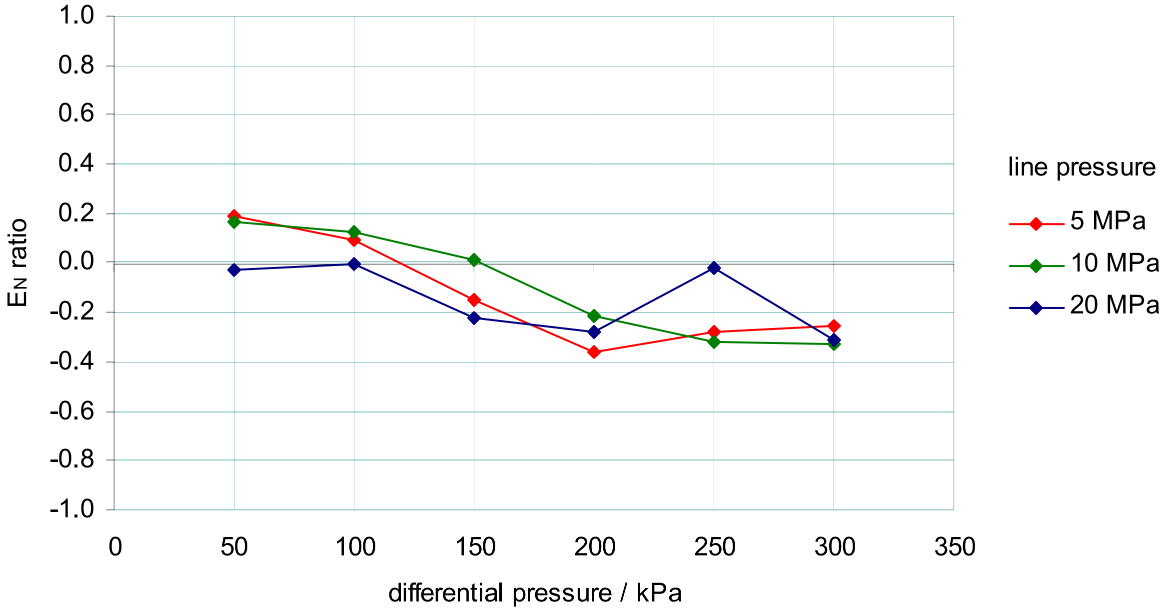

Figure 55 Agreement between oil- and gas-lubricated devices

When quantified as discussed, there is clearly a high level of agreement between the oil- and gas-lubricated twin-post devices and hence good *closure* between them and the NPL standard against which they were calibrated.

14 SUMMARY AND CONCLUSIONS

The main objective of this project was to investigate potential discrepancies between three methods of generating differential pressure at high line pressures; the strategy entailed comparing the instruments practically and developing comprehensive mathematical models together with the corresponding uncertainty budgets.

Three differential pressure *generators* were purchased, together with a number of differential pressure transmitters and ancillary equipment. A software package was developed which allowed real-time graphical displays of the electrical outputs from the transmitters – a facility which gave invaluable and unprecedented insight into otherwise hidden instrumental characteristics.

Meetings were held with representatives of organisations working in the field, to tap their knowledge and seek their views, and visits were made to a number of laboratories. Much information was collated including some which, whilst not strictly within the scope of the project, has been included in Section 15 for completeness.

Detailed models of the three generators were developed in an iterative process of measurement, analysis and model-enhancement. A number of characteristics that had been observed previously but whose cause had remained speculative were pin-pointed. For example, seemingly random fluctuations in differential pressure were traced to piston taper and fall-rate issues, and the pressure divider was found to have a measurable line pressure dependency which, if ignored, would leave its uncertainty budget too optimistic. Also, assumptions sometimes made – for example that changes in piston heights on a twin-post device will cancel each other out – were found to be incorrect. It was also shown that large differences in values of measurement uncertainty can effectively hinge on hair-splitingly different arguments about estimation of temperature – in some cases uncertainties reduce by around one third by shaving just 50 mK off temperature uncertainties – a less-than-robust situation which itself indicates unjustified metrological optimism.

Extensive uncertainty budgets were developed for each instrument and suggestions made for typical values of input quantities. When evaluated in this way, and used in accordance with the procedures developed, the agreement between the instruments was within their combined uncertainties.

The conclusion is that there are significant measurement discrepancies between the various methods of generating differential pressure when over-simplistic models are used to describe their characteristics or over-optimistic estimates of uncertainty are made. Furthermore, and for the same reason, discrepancies are just as likely between devices of similar design.

15 ADDITIONAL SOURCES OF MEASUREMENT DISCREPANCY

This project has essentially quantified and compared the performance of differential pressure generators in a calibration laboratory environment. When differential pressure measurements are made 'in the field' – including use of additional apparatus – there are other potential sources of discrepancy. Whilst not strictly within the project's scope, it was thought appropriate to list them, so that they may be taken into account where appropriate.

15.1 DIFFERENTIAL PRESSURE TRANSMITTERS

15.1.1 General

The characteristics of differential pressure transmitters under test may have a significant influence on the uncertainty in measurement both during calibration and subsequent use.

15.1.2 Resolution

The resolution of transmitters can result in significant *quantization* errors (see Section 3.2.2) and must be taken into account. When observing the output of analogue transmitters using a digital voltmeter it is difficult to accurately establish the resolution in the presence of differential pressure 'noise' – digits flicker too quickly to enable the quantization error to be measured.

The resolution of the transmitter should be included in the uncertainty budget with a rectangular distribution.

15.1.3 Interpolation

Laboratories are commonly asked to provide calibration certificates with results corresponding to cardinal pressure values and to do this some interpolation is generally required. Errors can be introduced during this process if proper account is not taken of the transmitter's resolution, hysteresis and non-linearity.

15.1.4 Transmitter orientation

Differential pressure transmitters are normally mounted with both pressure connection ports at the same height. When used on a system measuring gas, it is good practice to mount transmitters with their pressure ports pointing downwards to enable any liquid present to drain – a build up of liquid on transmitters' diaphragms can result in erroneous readings. On a liquid system, transmitters are normally mounted with the pressure connections uppermost to prevent gas in the system from becoming trapped.

Significant errors may arise if a transmitter is not calibrated in the same orientation as it is used. The most significant changes in transmitter output with orientation occur when a transmitter is rotated in the plane adjacent to its diaphragm.

15.1.5 Clamping effects

Most differential pressure transmitters have *process flanges* by which they may be attached to a standard manifold. It has been reported that the action of bolting a flange to a manifold can cause mechanical stress on the transmitter's diaphragm resulting in changes to its characteristics.

15.2 ELECTRICAL MEASUREMENTS

15.2.1 General

The 4 mA - 20 mA output from transmitters is generally calculated by dividing the voltage measured across a standard resistor (in series with the transmitters wiring *loop*) by the value of the standard resistor. Both of these measurements are subject to measurement uncertainty. The uncertainty in the resistance may be calculated from calibration data and an estimate of drift. It is also necessary to account for the resistor's temperature coefficient – it heats up due to the power being dissipated. The uncertainty in the voltage measurement is calculated from the uncertainty in calibration data and an estimate of drift.

15.2.2 Method of observing output and data capture

The potential for spurious measurements during a calibration is increased if the output of a differential pressure transmitter is not monitored in real-time using a system similar to that described in Section 3.2.5. The effect of not using such a system will be an increase the 'type A' uncertainty as the data used for the statistical analysis will contain both spurious measurements due to 'glitches' and motor-drive induced 'pulses'. The scatter in the results will be greater as it will not be possible to select a measurement period which includes a proper sample of the differential pressure waveform (as described in Sections 11.2.3 and 12.2.3).

Also, an oscillating signal is momentarily more stable at its extremities and changes most rapidly at the mean value; there is thus a tendency, when reading a digital display by eye, to take measurements at inappropriate moments.

15.3 VARIATION IN LINE PRESSURE

Changes in line pressure may affect the output of differential pressure transmitters. The span of traditional analogue transmitters changes with line pressure (often a linear relationship with a predetermined correction factor) and the output of modern digital devices is *characterised* to correct for changes in line pressure. A potential for discrepancy therefore occurs when a transmitter is used for measurements at a line pressure different to that of the calibration.

The line pressure of a flow measurement system is normally expressed in absolute pressure units. It may therefore be prudent to seek clarification on calibration parameters and state the barometric pressure recorded during the calibration.

15.4 PRESSURE UNITS

Differential pressure measurements are commonly made using so called 'manometric' units, particularly inches of water, which express pressure in terms of the height of a column of liquid. Such units depend on assumed values for liquid density and the acceleration due to gravity - assumptions which inherently limit their validity as no national measurement institutes establish pressure standards in this way. Instead they use the internationally agreed SI unit for pressure - the *pascal* - and it is *impossible* to ascribe an *exact* conversion factor between the pascal and any manomeric unit; the definitions are simply not compatible and cannot be made so.

Further, confusion and large errors abound through use of differing ‘manometric’ definitions and there are many stories of this leading to major mistakes in pressure measurement. It should also be appreciated that many digital transmitters have built-in unit conversion software and the conversion factors used may conflict with those used during calibration or use.

ACKNOWLEDGEMENTS

This work was funded by the National Measurements System Policy Unit of the UK Department of Trade and Industry.

The authors would like to acknowledge the contributions made by colleagues in the NPL Pressure and Vacuum Section, including Bernard Waller for his practical help, Pauline Leggat for discussing many aspects of the project, and Ade Idowu for undertaking the Finite Element modelling and calculations.

REFERENCES

[1] International Organization for Standardization. *International Vocabulary of Basic and General Terms in Metrology*, ISO, 1995.

[2] International Organization for Standardization, *Guide to the Expression of Uncertainty in Measurement*, ISO, 1993.

[3] BS 5233: 1986 British Standard, *Glossary of terms used in metrology*.

[4] Institute of Measurement and Control, *Guide to the Measurement of Pressure and Vacuum*, 1998

[5] SIMPSON, D. I., Computerized Techniques for Calibrating Pressure Balances, *Metrologia*, 1993/94, **30**, 655-658.

[6] LEWIS, S. L. and PEGGS, G. N. *The Pressure Balance: A practical guide to its use*. London, HMSO, 1992 (Second Edition).